PNNL-13143
UC-900

Final Report

CRADA with Air Products Corporation and Pacific Northwest National Laboratory (PNL-088):

Air Products Tape Development

J.W. Stevenson and T.R. Armstrong

January 2000

Prepared for the U.S. Department of Energy
under Contract DE-ACO6-76RLO 1830

Pacific Northwest National Laboratory
Operated for the U.S. Department of Energy
by Battelle

DISCLAIMER

PACIFIC NORTHWEST NATIONAL LABORATORY
operated by
BATTELLE
for the
UNITED STATES DEPARTMENT OF ENERGY
under Contract DE-AC05-76RL01830

Printed in the United States of America

Available to DOE and DOE contractors from the Office of Scientific and Technical Information,
P.O. Box 62, Oak Ridge, TN 37831-0062
www.osti.gov
ph: (865) 576-8401
fax: (865) 576-5728
email: reports@osti.gov

Available to the public from the National Technical Information Service
5301 Shawnee Rd., Alexandria, VA 22312
ph: (800) 553-NTIS (6847)
or (703) 605-6000
email: info@ntis.gov
Online ordering: http://www.ntis.gov

[redacted]

Introduction

The purpose of this project was to develop fabrication techniques for the manufacture of oxygen separation membranes based on sintered mixed-conducting oxides. This required fabrication of a thin, dense active membrane on a porous substrate which provided mechanical strength without preventing gas transport to the surface of the active membrane. The approach in this project was to utilize tape calendering techniques to prepare polymer tapes loaded with oxide powders which could be laminated and sintered to yield the desired asymmetric membrane structure.

Experimental Procedure

The mixed-conducting powders were supplied by Air Products. Three different batches of powder were received and investigated. The first batch received was designated B2B; the second batch was designated B2, and the final batch received was designated B2(2).

The particle size distribution of the powders was characterized using a Microtrac FRA particle size analyzer. As required, the powders were calcined in air in electric furnaces, ball-milled in HDPE jars using zirconia media and 2-propanol, and sieved using stainless steel sieves.

The precursor batches for the calendered tapes were prepared by mixing the required ingredients (e.g., mixed-conducting powder, pore forming agents, binder, plasticizer) in a high shear mixer (30 rpm, 115°C) for 20 minutes. The volumetric ratio of binder (polyvinyl butyral, PVB 98) to plasticizer (butyl benzyl phthalate, BBP) was 1:18. The volume of the precursor batches was 47 cc. The resulting mixtures were then calendered using a two roll mill (stainless steel rollers, 15 rpm, 33°C). The nip between the rolls was progressively reduced as the tape was repeatedly calendered, until the final desired green (i.e., unsintered) thickness was achieved. Asymmetric tapes were prepared by laminating two tapes together and then rolling the resulting tape down to the desired green thickness.

Disk-shaped specimens (1.5" green diameter) of the tapes were sintered in air on porous zirconia substrates in electric furnaces using the following schedule:

20 - 150°C	2°C/min	1 hour dwell
150 - 500	0.5°C/min	1 hour dwell
500 - 800	0.5°C/min	

800 - Sintering Temp	3°C/min	1 hour dwell
Sintering Temp – 20°C	3°C/min	

Polished specimens of the sintered tapes were examined by optical microscopy and scanning electron microscopy (SEM). The sintered densities of the tapes were measured by the Archimedes method using ethanol.

Results and Discussion

1. Tapes Based on B2B Powder

1A. Calendered Mixed Conductor Tapes, Dense

The as-received B2B powder had a median particle size of 1.8-2.3 μm (as measured by Air Products). This powder was calcined at 1000°C for 1 hour and then sieved to –60 mesh. The particle size analysis for this powder is shown in Figure 1. Calendered tapes were prepared using solids loading of 52.5, 55, and 57.5 vol.% (Tapes B2B-D-1, B2B-D-2, and B2B-D-3, respectively). (In this report, the term "solids loading" refers to the volume fraction of ingredients other than binder and plasticizer in the total batch.) A batch having a solids loading of 60 vol.% was prepared, but it could not be calendered successfully. Tape specimens were sintered in air at 1050°C for 1 h. Table I summarizes the properties of these tapes. The reported radial shrinkages are highly approximate due to the tendency of the discs to warp during sintering. (Warping of the tapes during sintering was reduced in later sintering runs (after 12/16/96) by placing zirconia cover plates above the tape specimens during sintering). The relative densities (i.e., % of theoretical density) were calculated using a theoretical density of 5.7 g/cc (as provided by Air Products). SEM micrographs of sintered fracture surfaces are shown in Figures 2-4.

1B. Calendered Mixed Conductor Tapes, Porous

A. Tapes using –60 Mesh B2B Powder

Calendered tapes were prepared (using B2B powder which had been calcined at 1000°C for 1 hour and then sieved to –60 mesh) in which rice starch was added as a pore-forming agent. Specimens of the first tapes (#B2B-P-1, #B2B-P-2, and #B2B-P-3) sintered to undesirably high densities at 1050°C, even though they contained high levels of rice starch (30-40 vol.% of solids). Table II summarizes the properties of these tapes. SEM micrographs of sintered fracture surfaces are shown in Figures 5-7.

In the next set of tapes, ceria (Ceramatec CC810) was added as a sintering inhibitor. The particle size distribution of this ceria powder is shown in Figure 8; the particles are mostly sub-micron in size. The properties of these tapes are summarized in Tables II and III (for sintering temperatures of 1050 and 1075°C, respectively). The sintering behavior was strongly affected by the presence of ceria. While some tapes were prepared containing relatively large amounts of ceria (Tapes #B2B-P-4 (20 vol.% of solids), #B2B-P-5 (15 vol.% of solids), #B2B-P-6 (10 vol.% of solids), and #B2B-P-7 (7 vol.% of solids)), it was found that only small additions (1-3 vol.% of solids) of ceria were required to maintain substantial porosity in the sintered tapes (see Tapes #B2B-P-8 through #B2B-P-19 in Table II).

SEM micrographs of fracture surfaces of the high-ceria content sintered tapes are shown in Figures 9-12. SEM micrographs of fracture surfaces of the low-ceria content sintered tapes are shown in Figures 13-24. XRD analysis on a sintered tape (#B2B-P-10) did not find evidence of any significant reaction between the perovskite and ceria to form additional phases.

B. Tapes using Spray Dried or Wet Milled B2B Powder

It was apparent that the sintered porous tapes contained high density regions scattered within the more porous matrix. This was a consequence of using a relatively coarse powder (-60 mesh) as feedstock. Several powder processing routes were tested in order to increase the homogeneity of the calcined B2B powder, including spray drying the powder both with and without binder, and wet-milling in 2-propanol followed by sieving to –200 mesh. Properties of tapes utilizing these processed powders are summarized in Tables II and III (for sintering temperatures of 1050 and 1075°C, respectively). A tape batch containing B2B powder spray dried with Carbowax binder (included in the 2-propanol/water slurry) was very difficult to calender, but B2B spray dried without binder was successfully incorporated into a porous tape (#B2B-P-21) and a dense tape (#B2B-D-7). Figure 25 is an optical micrograph of a polished cross-section of sintered #B2B-P-21. Figure 26 shows a sintered tape (#B2B-P-22) utilizing –200 mesh B2B which had been wet milled in 2-propanol without dispersant. Both of these tapes showed improved microstructural homogeneity, but some dense regions were still evident in #B2B-P-22. In order to improve the microstructure of tapes utilizing wet milled B2B, a dispersant (1 wt.% of Darvan C dispersant) was added to the milling batch. The particle size analysis of the resulting powder is shown in Figure 27. Several tapes were made using this powder (see #B2B-P-23 through #B2B-P-27 in Table II); optical micrographs of polished cross-

sections are shown in Figures 28-32. The addition of the dispersant resulted in improved homogeneity of the porous microstructure of the sintered tapes.

Mercury porosimetry was performed on sintered specimens of several of the tapes. The results are shown in Figures 33-35. As shown in the figures, the values obtained for open porosity in these specimens agreed very well with the values obtained by the Archimedes density measurements.

Tensile strength tests were performed on several of the calendered tapes. The tests were performed in air at room temperature; the test rate was 2"/min, as recommended by ASTM. The results are shown in Table IV. Tapes containing rice starch and B2B were weaker than tapes containing only the B2B, but the addition of ceria as well as starch to the tapes appeared to minimize the decrease in tensile strength.

1C. Calendered Asymmetric Tapes

A. Asymmetric tapes using –60 Mesh Powder

Asymmetric tapes were prepared by co-calendering dense and porous green tapes. The green properties of these tapes (Asymmetric tapes #B2B-B-1 through #B2B-B-9) are summarized in Table V. Three different sintering temperatures were investigated: 1050°, 1075°, and 1100°C. The properties of the sintered Asymmetric tapes are summarized in Table VI. While the density and uniformity of the dense layers tended to increase with increasing sintering temperature, the porosity in the porous layers tended to decrease with increasing temperature; this decreased porosity was especially significant in specimens sintered at 1100°C.

SEM micrographs of fracture surfaces are shown in Figures 36-50. Optical micrographs of polished cross-sections of Asymmetric tape #B2B-B-5 sintered at 1050°C and 1075°C are shown in Figures 51 and 52, respectively. In the porous layers, the high density regions scattered within the more porous matrix are clearly visible.

Several asymmetric tapes were prepared with thicker dense layers (≈50-75 μm; #B2B-B-6 through #B2B-B-9) than the previous asymmetric tapes (which had dense layer thickness of ≈20-40 μm). SEM micrographs of polished cross-sections after sintering at 1075°C are shown in Figures 53-56.

B. Asymmetric Tapes using Spray Dried or Wet-Milled B2B Powder

Asymmetric tape #B2B-B-10 was prepared using B2B powder which had been spray dried with Carbowax binder; specimens of this tape cracked during sintering. Asymmetric tape #B2B-B-11 was prepared using B2B powder which had been spray dried without binder. SEM micrographs of polished cross sections after sintering at 1050, 1075,

and 1100°C are shown in Figures 57-59. Asymmetric tapes #B2B-B-12, #B2B-B-13, and #B2B-B-14 were prepared using B2B powder which had been wet-milled and sieved to –200 mesh. The sintered thickness of the dense layers of tapes #B2B-B-12 and #B2B-B-13 was ≈40 μm; the sintered thickness of the dense layer of tape #B2B-B-14 was ≈20 μm. The green and sintered properties of the asymmetric tapes are summarized in Table V and VI, respectively. Optical micrographs of polished cross sections after sintering are shown in Figures 60-65. As expected, the homogeneity of the microstructures of the porous layers was greatly improved by using spray dried or wet-milled powder.

2. Tapes Based on B2 Powder

2A. Calendered Mixed Conductor Tapes, Dense

The particle size analysis of the as-received B2 powder is shown in Figure 66. A dense tape was prepared using the as-received powder (Tape #B2-D-1). The vol.% solids loading was limited to 52.5%, indicating that the surface area of the powder was higher than desired. Calcination of the B2 powder at 900°C for 1 hour (particle size analysis shown in Figure 67) allowed the solid loading to be increased to 57.5%. Tape # B2-D-4 contained calcined B2 which had been sieved to –70 mesh. Tape # B2-D-3 contained B2 which had been sieved to –70 mesh, wet-milled for 8 hours, and then sieved to –200 mesh. Both tapes sintered to high density at 975°C; optical micrographs of polished cross sections after sintering are shown in Figures 68 and 69. The properties of the dense tapes are summarized in Table VII.

2B. Calendered Mixed Conductor Tapes, Porous

A porous tape was prepared using the as-received powder (Tape #B2-P-1). It was possible to achieve a solids loading of 57.5%, but the tape was somewhat stiffer than desired. The use of B2 powder which had been calcined and sieved to –200 mesh (as described in Section 2A) produced better tapes. Tape #B2-P-2 contained Ceramatec CC810 ceria as a sintering inhibitor. Other sintering inhibitors were also investigated: NexTech ceria (Tape #B2-P-3), Alfa/Aesar MgO (-325 mesh; particle size analysis shown in Figure 70; Tape #B2-P-4), and MgO synthesized by glycine/nitrate combustion synthesis (wet-milled 144h; -200 mesh; particle size analysis shown in Figure 71; Tape #B2-P-5). The properties of these tapes are summarized in Table VIII. Figure 72 gives a graphical summary of the temperature dependence of the open, closed, and total porosity in the tapes, as calculated from the Archimedes measurements. Overall, the Alfa/Aesar MgO appeared to be the best choice, in terms of effectiveness, cost, and availability. Optical

micrographs of polished cross sections of specimens sintered at 975°C are shown in Figures 73-76. The need for milling the B2 powder after calcination can be seen clearly in Figure 77, which shows the microstructure of a porous tape (#B2-P-6, sintered 975°C) prepared using powder which was calcined and sieved to –70 mesh, but not subsequently wet-milled and sieved to –200 mesh.

2C. Calendered Asymmetric Tapes

Asymmetric tapes were prepared using each of the four sintering inhibitors in the porous layer: Ceramatec ceria (Bilayer #B2-B-2), NexTech ceria (Bilayer #B2-B-1), Alfa/Aesar MgO (Bilayer #B2-B-3), and glycine/nitrate MgO (Bilayer #B2-B-4). The properties of the green and sintered asymmetric tapes are summarized in Tables IX and X. Some of the dense layers contained cracks (see asterisks in Table X). Sintering for only 0.5 hour appeared to cause more cracking than sintering for 1 hour, suggesting that the higher shrinkage occurring in the porous layers during the longer sintering time resulted in less stress being generated in the dense layer during cooling. Optical micrographs of polished cross sections after sintering at 975°C for 1 hour are shown in Figures 78-81. A section of asymmetric tape #B2-B-3 (designated #B2-B-3A) was calendered down to a reduced green thickness (180 μm). An optical micrograph of a polished cross-section is shown in Figure 82.

2D. Calendered Tapes Delivered to Air Products

Six asymmetric tapes of recipe #B2-B-3 were prepared and delivered to Air Products. The total area of these tapes was ≈2.75 sq.ft.; the green thickness of the asymmetric tapes was 200-220 μm. Eight dense tapes of recipe #B2-D-3 were prepared and delivered. The total area of these tapes was ≈2.85 sq.ft.; the green thickness was 190-220 μm. Also, six thicker dense tapes of recipe #B2-D-3 were prepared and delivered. The total area of these tapes was ≈3.90 sq.ft.; the green thickness was 490-510 μm.

Specimens of these tapes were retained at PNNL and sintered at 975°C for 1 hour. Figure 83 shows the sintered asymmetric tape; the total sintered thickness was 190 μm (dense layer, 30 μm; porous layer, 160 μm). Figure 84 shows the sintered thin, dense tape; the sintered thickness was 200 μm. Figure 85 shows the sintered thick, dense tape; the sintered thickness was 400 μm.

3. Tapes Based on B2(2) Powder

3A. Calendered Mixed Conductor Tapes, Dense

The particle size analysis of the as-received B2(2) powder is shown in Figure 86. A dense tape was prepared using the as-received powder (Tape #B2(2)-D-1). The sintering behavior of this tape was not satisfactory, so wet-milling was used to reduce the particle size of the powder. The particle size analysis of B2(2) (after wet-milling for 48 hours and then sieving to –200 mesh) is shown in Figure 87. Satisfactory sintering behavior was obtained with a tape utilizing this powder (Tape #B2(2)-D-2); 95% of theoretical density was obtained by sintering at 975°C for 1 hour (Table XI).

3B. Calendered Mixed Conductor Tapes, Porous

Two porous tapes were prepared using the as-received B2(2) powder (Tapes #B2(2)-P-1, #B2(2)-P-2), but subsequent tapes contained B2(2) which had been wet-milled for 48 hours and sieved to –200 mesh. All of these tapes used Alfa/Aesar MgO as the sintering inhibitor. The properties of the sintered tapes are summarized in Tables XII(A) and XII(B).

Tape #B2(2)-P-3 contained 25 vol.% rice starch as the pore-former. In an effort to create larger pores in the porous tape, 25 vol.% Sigma potato starch was introduced into Tape #B2(2)-P-4. The potato starch was considerably coarser than the rice starch, as shown in the particle size analyses of the two starches (Figures 88 and 89). Optical micrographs of polished cross sections after sintering at 975°C are shown in Figures 90 and 91. The large pores formed by the potato starch are clearly present in Figure 91.

Several tapes were prepared containing both rice starch and potato starch with a total starch content of 25 vol.% (Tapes #B2(2)-P-5, #B2(2)-P-6, #B2(2)-P-7). Tape ##B2(2)-P-8 contained 40 vol.% starch (20% rice, 20% potato); tape #B2(2)-P-9 contained 50 vol.% starch (25% rice, 25% potato). Optical micrographs of polished cross sections after sintering at 975°C are shown in Figures 92-96. Figures 97 and 98 provide a graphical summary of the temperature dependence of the open, closed, and total porosity in the tapes, as calculated from the Archimedes measurements.

3C. Calendered Asymmetric Tapes

Asymmetric tape #B2(2)-B-1 was prepared using a porous tape containing 25 vol.% of starch (12% rice, 13% potato). Asymmetric tape #B2(2)-B-2 was prepared using a porous tape containing 40 vol.% of starch (20% rice, 20% potato). Asymmetric tape #B2(2)-B-3 was prepared using a porous tape containing 50 vol.% of starch (25% rice,

25% potato). The properties of the green and sintered asymmetric tapes are summarized in Tables XIII and XIV. Optical micrographs of polished cross sections (sintered at 975°C for 1 hour) are shown in Figures 99-101; SEM micrographs are shown in Figures 102-103. These micrographs show the mixture of coarse and fine porosity in the porous layer, as well as the excellent bonding between the dense and porous layers.

Conclusions

Three different batches of mixed conducting powders were incorporated into calendered tapes. Both dense and porous tapes were prepared. In the porous tapes, the residual porosity after sintering was a result of the introduction of both fugitive pore-forming phases and non-fugitive sintering inhibitors. The amount and morphology of residual porosity was tailored by varying the types and amounts of pore-formers and inhibitors in the tapes. Asymmetric tapes (i.e., a dense membrane on a porous substrate) were prepared by laminating dense and porous tapes together, and then calendering the resulting tape down to the desired thickness. Sintered specimens of the asymmetric tapes exhibited high density in the membrane layer, high porosity in the substrate layer, and excellent bonding at the interface between the two layers. Approximately 9.5 sq.ft. of calendered asymmetric tape and dense tape were delivered to Air Products for testing.

Table I. Properties of Dense B2B Tapes

Tape ID #	Sintering Conditions	Solids Loading (vol%)	Powder Notes	Starch Content (vol%)	Approx. X-Y (Radial) Shrinkage	Approx. Z (Thickness) Shrinkage	Relative Density
B2B-D-1	1050°C,1 h	52.5	-60 Mesh	0	17%	27%	94%
B2B-D-2	1050°C,1 h	55.0	-60 Mesh	0	17%	27%	95%
B2B-D-3	1050°C,1 h	57.5	-60 Mesh	0	16%	31%	94%
B2B-D-4*	--	60	-60 Mesh	0	--	--	--
B2B-D-5	--	52.5	Spray Dried w/ Carbowax	0	--	--	--
B2B-D-6*	--	57.5	Spray Dried w/o binder	0	--	--	--
B2B-D-7	1050°C,1 h	52.5	Spray Dried w/o binder	0	15%	19%	89%

* Unable to calender

Table II. Properties of Porous B2B Tapes; Sintered 1050°C

Tape ID #	Sintering Conditions	Solids Loading (vol%)	Powder Notes	Starch Content (vol%)	Ceria Content (vol%)	Approx.X-Y (Radial) Shrinkage	Approx. Z (Thickness) Shrinkage	Relative Density
B2B-P-1	1050°C,1 h	55.0	-60 Mesh	30	0	22%	29%	87%
B2B-P-2	1050°C,1 h	57.5	-60 Mesh	30	0	22%	25%	91%
B2B-P-3	1050°C,1 h	57.5	-60 Mesh	40	0	24%	23%	87%
B2B-P-4	1050°C,1 h	57.5	-60 Mesh	30	20	13%	15%	68%
B2B-P-5	1050°C,1 h	57.5	-60 Mesh	30	15	14%	15%	63%
B2B-P-6	1050°C,1 h	57.5	-60 Mesh	30	10	12%	27%	67%
B2B-P-7	1050°C,1 h	57.5	-60 Mesh	30	7	14%	31%	66%
B2B-P-8	1050°C,1 h	57.5	-60 Mesh	30	3	15%	20%	67%
B2B-P-9	1050°C,1 h	57.5	-60 Mesh	25	3	17%	14%	77%
B2B-P-10	1050°C,1 h	57.5	-60 Mesh	20	3	16%	14%	77%
B2B-P-11	1050°C,1 h	55.0	-60 Mesh	20	3	12%	0%	67%
B2B-P-12	1050°C,1 h	57.5	-60 Mesh	35	2	14%	0%	64%
B2B-P-13	1050°C,1 h	57.5	-60 Mesh	40	2	16%	0%	63%
B2B-P-14	1050°C,1 h	57.5	-60 Mesh	35	1	16%	6%	67%
B2B-P-15	1050°C,1 h	57.5	-60 Mesh	40	1	20%	31%	77%
B2B-P-16	1050°C,1 h	57.5	-60 Mesh	40	1.5	18%	--	66%
B2B-P-17	1050°C,1 h	57.5	-60 Mesh	25	2	13%	6%	71%
B2B-P-18	1050°C,1 h	57.5	-60 Mesh	25	1	15%	12%	74%
B2B-P-19	1050°C,1 h	58.5	-60 Mesh	25	3	15%	6%	71%
B2B-P-20	--	57.5	Spray Dried w/ Carbowax	40	1.5	--	--	--
B2B-P-21	1050°C,1 h	57.5	Spray Dried w/o binder	25	3	14%	10%	69%
B2B-P-22	1050°C,1 h	57.5	Wet milled, -200 Mesh	25	3	15%	14%	68%
B2B-P-23	1050°C,1 h	57.5	Wet milled w/ Darvan, -200 Mesh	25	3	15%	10%	68%
B2B-P-24	1050°C,1 h	57.5	Wet milled w/ Darvan, -200 Mesh	30	15	11%	5%	61%
B2B-P-25	1050°C,1 h	57.5	Wet milled w/ Darvan, -200 Mesh	30	3	13%	8%	65%
B2B-P-26	1050°C,1 h	57.5	Wet milled w/ Darvan, -200 Mesh	35	2	16%	9%	65%
B2B-P-27	1050°C,1 h	57.5	Wet milled w/ Darvan, -200 Mesh	40	2	16%	18%	61%
B2B-P-21	1050°C,2 h	57.5	Spray Dried w/o binder	25	3	--	--	75%
B2B-P-24	1050°C,2 h	57.5	Wet milled w/ Darvan, -200 Mesh	30	15	--	--	63%
B2B-P-27	1050°C,2 h	57.5	Wet milled w/ Darvan, -200 Mesh	40	2	--	--	70%

Table III. Properties of Porous B2B Tapes; Sintered 1075°C / 1 hour

Tape ID #	Sintering Conditions	Solids Loading (vol%)	Powder Notes	Starch Content (vol%)	Ceria Content (vol%)	Approx. X-Y (Radial) Shrinkage	Approx. Z (Thickness) Shrinkage	Relative Density
B2B-P-9	1075°C,1 h	57.5	-60 Mesh	25	3	16%	11%	78%
B2B-P-10	1075°C,1 h	57.5	-60 Mesh	20	3	16%	13%	80%
B2B-P-16	1075°C,1 h	57.5	-60 Mesh	40	1.5	19%	6%	71%
B2B-P-21	1075°C,1 h	57.5	Spray Dried w/o binder	25	3	18%	18%	75%
B2B-P-22	1075°C,1 h	57.5	Wet milled, -200 Mesh	25	3	16%	14%	73%
B2B-P-23	1075°C,1 h	57.5	Wet milled w/ Darvan, -200 Mesh	25	3	16%	17%	77%
B2B-P-24	1075°C,1 h	57.5	Wet milled w/ Darvan, -200 Mesh	30	15	14%	12%	66%
B2B-P-25	1075°C,1 h	57.5	Wet milled w/ Darvan, -200 Mesh	30	3	17%	17%	74%
B2B-P-26	1075°C,1 h	57.5	Wet milled w/ Darvan, -200 Mesh	35	2	19%	19%	75%
B2B-P-27	1075°C,1 h	57.5	Wet milled w/ Darvan, -200 Mesh	40	2	19%	18%	70%

Table. IV. Results of tensile strength tests on green tapes.

Batch #	Solid loading (vol.%)	Starch content (vol.%)	Ceria content (vol.%)	Strength (Mpa)	St.dev. (Mpa)	St.dev. (%)	# of specimens tested
B2B-D-1	52.5	0	0	4.44	0.29	6.5	6
B2B-D-2	55.0	0	0	5.30	0.12	2.3	10
B2B-D-3	57.5	0	0	4.82	0.15	3.1	10
B2B-P-1	55.0	30	0	3.47	0.17	4.9	10
B2B-P-2	57.5	30	0	3.54	0.15	4.2	10
B2B-P-3	57.5	40	0	3.13	0.10	3.2	10
B2B-P-5	57.5	30	15	3.98	0.13	3.3	10
B2B-P-8	57.5	30	3	4.75	0.17	3.6	10

Table V. Green Properties of B2B Bilayer Membranes

Bilayer ID #	Dense Tape ID #	Initial thickness (μm)	Porous Tape ID #	Initial thickness (μm)	Thickness Ratio	Green bilayer thickness (μm)
B2B-B-1	B2B-D-3	400	B2B-P-10	5200	13	500
B2B-B-2	B2B-D-3	400	B2B-P-9	4800	12	320
B2B-B-3	B2B-D-3	400	B2B-P-16	5200	13	520
B2B-B-4	B2B-D-2	370	B2B-P-16	5700	15	500
B2B-B-5	B2B-D-1	390	B2B-P-16	5700	15	500
B2B-B-6	B2B-D-1	400	B2B-P-16	2000	5	500
B2B-B-7	B2B-D-1	400	B2B-P-16	3000	8	500
B2B-B-8	B2B-D-3	400	B2B-P-9	2000	5	530
B2B-B-9	B2B-D-3	400	B2B-P-9	3000	8	500
B2B-B-10	B2B-D-5	450	B2B-P-20	5200	12	500
B2B-B-11	B2B-D-7	500	B2B-P-21	5000	10	500
B2B-B-12	B2B-D-7	390	B2B-P-24	5500	14	500
B2B-B-13	B2B-D-7	390	B2B-P-27	5300	14	500
B2B-B-14	B2B-D-7	400	B2B-P-27	8400	21	360

Table VI. Sintered Properties of B2B Bilayer Membranes

Bilayer ID #	Sintering Temperature (°C)	Final porous layer thickness (μm)	Final dense layer thickness (μm)	Thickness Ratio
B2B-B-1	1050	380	35	11
	1075	370	25	15
	1100	340	40	9
B2B-B-2	1050	250	20	13
	1075	215	25	9
	1100	205	30	7
B2B-B-3	1050	355	30	12
	1075	330	30	11
	1100	280	30	9
B2B-B-4	1050	335	25	13
	1075	325	35	9
	1100	310	35	9
B2B-B-5	1050	390	30	13
	1075	350	30	12
	1100	335	35	10
B2B-B-6	1075	310	70	4.4
B2B-B-7	1075	310	55	5.6
B2B-B-8	1075	340	75	4.5
B2B-B-9	1075	355	55	6.5
B2B-B-10*	1075			
B2B-B-11	1050	370	45	8.2
	1075	370	50	7.4
	1100	350	50	7
B2B-B-12	1050	380	40	9.5
	1075	380	40	9.5
B2B-B-13	1050	360	40	9
	1075	355	35	10.1
B2B-B-14	1050	250	20	12.5
	1075	240	20	12

* cracked during sintering

Table VII. Properties of Dense B2 Tapes

Tape ID #	Sintering Conditions	Solids Loading (vol%)	Powder Notes	Starch Content (vol%)	Approx. X-Y (Radial) Shrinkage	Approx. Z (Thickness) Shrinkage	Relative Density
B2-D-1	975°C,1 h	52.5	As Received	0	18	27	93%
	1000°C,1 h	52.5	As Received	0	19	27	92%*
B2-D-2	950°C,1 h	52.5	Calcined 900°C, -200 Mesh	0	14	16	83%
	975°C,1 h	52.5	Calcined 900°C, -200 Mesh	0	19	19	95%
	1000°C,1 h	52.5	Calcined 900°C, -200 Mesh	0	19	19	95%
B2-D-3	950°C,1 h	57.5	Calcined 900°C, -200 Mesh	0	13	17	86%
	975°C,1 h	57.5	Calcined 900°C, -200 Mesh	0	15	22	95%
B2-D-4	950°C,1 h	57.5	Calcined 900°C, -70 Mesh	0	13	13	83%
	975°C,1 h	57.5	Calcined 900°C, -70 Mesh	0	16	13	95%

*cracked in half during sintering

Table VIII. Properties of Porous B2 Tapes

Tape ID #	Sintering Conditions	Solids Loading (vol%)	Powder Notes	Starch Content (vol%)	Ceria/MgO Content (vol%)	Approx.X-Y (Radial) Shrinkage	Approx. Z (Thickness) Shrinkage	Relative Density
B2-P-1	975°C, 1h	57.5	As Received	25	3*	15	26	73%
	1000°C, 1h	57.5	As Received	25	3*	17	26	75%
	1025°C, 1h	57.5	As Received	25	3*	18	26	80%
	1050°C, 1h	57.5	As Received	25	3*	19	26	81%
	1075°C, 1h	57.5	As Received	25	3*	19	26	82%
B2-P-2	975°C, 1h	57.5	Calcined 900°C, -200 Mesh	25	3*	11	5	59%
	1000°C, 1h	57.5	Calcined 900°C, -200 Mesh	25	3*	14	10	68%
	1050°C, 1h	57.5	Calcined 900°C, -200 Mesh	25	3*	15	15	73%
B2-P-3	950°C, 1h	57.5	Calcined 900°C, -200 Mesh	25	3**	12	18	62%
	975°C, 1h	57.5	Calcined 900°C, -200 Mesh	25	3**	14	18	65%
	1000°C, 1h	57.5	Calcined 900°C, -200 Mesh	25	3**	14	23	66%
B2-P-4	950°C, 1h	57.5	Calcined 900°C, -200 Mesh	25	3***	10	17	60%
	975°C, 1h	57.5	Calcined 900°C, -200 Mesh	25	3***	11	21	62%
	1000°C, 1h	57.5	Calcined 900°C, -200 Mesh	25	3***	13	25	67%
B2-P-5	950°C, 1h	57.5	Calcined 900°C, -200 Mesh	25	3****	11	24	61%
	975°C, 1h	57.5	Calcined 900°C, -200 Mesh	25	3****	13	24	66%
	1000°C, 1h	57.5	Calcined 900°C, -200 Mesh	25	3****	15	20	72%
B2-P-6	950°C, 1h	57.5	Calcined 900°C, -70 Mesh	25	3***	11	12	62%
	975°C, 1h	57.5	Calcined 900°C, -70 Mesh	25	3***	12	18	64%

*Ceramatec Ceria, CC810

**NexTech Ceria

***Alfa/Aesar MgO, -325 Mesh

****G/N MgO, -200 Mesh

Table IX. Green Properties of B2 Bilayer Membranes

Bilayer ID #	Dense Tape ID #	Initial thickness (μm)	Porous Tape ID #	Initial thickness (μm)	Thickness Ratio	Green bilayer thickness (μm)
B2-B-1	B2-D-2	420	B2-P-3	5000	11.9	430
B2-B-2	B2-D-2	420	B2-P-2	4800	11.4	440
B2-B-3	B2-D-3	440	B2-P-4	5000	11.4	450
B2-B-4	B2-D-3	440	B2-P-5	5000	11.4	450
B2-B-5	B2-D-4	430	B2-P-6	4800	11.2	480
B2-B-3A	B2-D-3	440	B2-P-4	5000	11.4	180

Table X. Sintered Properties of B2 Bilayer Membranes

Bilayer ID #	Sintering Conditions	Final porous layer thickness (μm)	Final dense layer thickness (μm)	Thickness Ratio	Sintered bilayer thickness (μm)	Z sintering shrinkage (%)
B2-B-1	975°C, 0.5h	330	35*	9.4	365	15.1
	975°C, 1h	330	30*	11	360	16.3
B2-B-2	975°C, 0.5h	370	35*	10.6	405	8.0
	975°C, 1h	350	30*	11.7	380	13.6
B2-B-3	950°C, 1h	370	35	10.6	405	10.0
	975°C, 0.5h	360	35*	10.3	395	12.2
	975°C, 1h	325	30	10.8	355	21.1
B2-B-4	950°C, 1h	345	35	9.9	380	15.6
	975°C, 0.5h	350	35*	10	385	14.4
	975°C, 1h	320	35	9.1	355	21.1
B2-B-5	975°C, 0.5h	395	35	11.3	430	10.4
	975°C, 1h	370	40	9.3	410	14.6
B2-B-3A	975°C, 1h	148	17	8.7	165	8.3

* cracks observed through dense layer.

Table XI. Properties of Dense B2(2) Tapes

Tape ID #	Sintering Conditions	Solids Loading (vol%)	Powder Notes	Approx. X-Y (Radial) Shrinkage	Approx. Z (Thickness) Shrinkage	Relative Density
B2(2)-D-1	975°C,1 h	57.5	As Received	8%	5.5%	75%
	1100°C,1 h	57.5	As Received	*	*	*
B2(2)-D-2	950°C,1 h	57.5	Wet-milled 48 h, -200 mesh	11%	10%	75%
	975°C,1 h	57.5	Wet-milled 48 h, -200 mesh	18%	15%	95%
	1000°C,1 h	57.5	Wet-milled 48 h, -200 mesh	18%	20%	95%

* cracked extensively, stuck to substrate

Table XII(A). Properties of Porous B2(2) Tapes

Tape ID #	Sintering Conditions	Solids Loading (vol%)	Powder Notes	Rice Starch Content (vol%)	Potato Starch Content (vol%)	MgO Content (vol%)	Approx.X-Y (Radial) Shrinkage	Approx. Z (Thickness) Shrinkage	Relative Density
B2(2)-P-1	975°C, 1h	57.5	As Received	25	-	3	3%	10.5%	54%
	1100°C, 1h	57.5	As Received	25	-	3	7%	6%	58%
B2(2)-P-2	1100°C, 1h	57.5	As Received	-	25	3	*	*	*
B2(2)-P-3	950°C, 1h	57.5	Milled 48 h, -200 Mesh	25	-	3	12%	5%	59%
	975°C, 1h	57.5	Milled 48 h, -200 Mesh	25	-	3	13%	14%	61%
	1000°C, 1h	57.5	Milled 48 h, -200 Mesh	25	-	3	13%	14%	62%
B2(2)-P-4	950°C, 1h	57.5	Milled 48 h, -200 Mesh	-	25	3	13%	6%	59%
	975°C, 1h	57.5	Milled 48 h, -200 Mesh	-	25	3	13%	6%	59%
	1000°C, 1h	57.5	Milled 48 h, -200 Mesh	-	25	3	13%	6%	62%
B2(2)-P-5	950°C, 1h	57.5	Milled 48 h, -200 Mesh	17	8	3	13%	17%	60%
	975°C, 1h	57.5	Milled 48 h, -200 Mesh	17	8	3	13%	17%	62%
	1000°C, 1h	57.5	Milled 48 h, -200 Mesh	17	8	3	13%	17%	64%
	1025°C, 1h	57.5	Milled 48 h, -200 Mesh	17	8	3	15%	21%	67%
	1050°C, 1h	57.5	Milled 48 h, -200 Mesh	17	8	3	17%	25%	70%
B2(2)-P-6	950°C, 1h	57.5	Milled 48 h, -200 Mesh	8	17	3	13%	5%	59%
	975°C, 1h	57.5	Milled 48 h, -200 Mesh	8	17	3	13%	29%	61%
	1000°C, 1h	57.5	Milled 48 h, -200 Mesh	8	17	3	13%	10%	63%
	1025°C, 1h	57.5	Milled 48 h, -200 Mesh	8	17	3	15%	21%	67%
	1050°C, 1h	57.5	Milled 48 h, -200 Mesh	8	17	3	17%	19%	70%

* cracked extensively, stuck to substrate

Table XII(B). Properties of Porous B2(2) Tapes

Tape ID #	Sintering Conditions	Solids Loading (vol%)	Powder Notes	Rice Starch Content (vol%)	Potato Starch Content (vol%)	MgO Content (vol%)	Approx.X-Y (Radial) Shrinkage	Approx. Z (Thickness) Shrinkage	Relative Density
B2(2)-P-7	950°C, 1h	57.5	Milled 48 h, -200 Mesh	12	13	3	13%	14%	56%
	975°C, 1h	57.5	Milled 48 h, -200 Mesh	12	13	3	13%	19%	59%
	1000°C, 1h	57.5	Milled 48 h, -200 Mesh	12	13	3	13%	19%	62%
	1025°C, 1h	57.5	Milled 48 h, -200 Mesh	12	13	3	15%	24%	63%
	1050°C, 1h	57.5	Milled 48 h, -200 Mesh	12	13	3	15%	24%	66%
B2(2)-P-8	950°C, 1h	57.5	Milled 48 h, -200 Mesh	20	20	3	13%	17%	51%
	975°C, 1h	57.5	Milled 48 h, -200 Mesh	20	20	3	13%	17%	54%
	1000°C, 1h	57.5	Milled 48 h, -200 Mesh	20	20	3	17%	22%	55%
	1025°C, 1h	57.5	Milled 48 h, -200 Mesh	20	20	3	17%	22%	57%
	1050°C, 1h	57.5	Milled 48 h, -200 Mesh	20	20	3	17%	26%	60%
B2(2)-P-9	950°C, 1h	57.5	Milled 48 h, -200 Mesh	25	25	3	14%	19%	47%
	975°C, 1h	57.5	Milled 48 h, -200 Mesh	25	25	3	15%	24%	48%
	1000°C, 1h	57.5	Milled 48 h, -200 Mesh	25	25	3	15%	24%	50%
	1025°C, 1h	57.5	Milled 48 h, -200 Mesh	25	25	3	17%	19%	50%
	1050°C, 1h	57.5	Milled 48 h, -200 Mesh	25	25	3	17%	19%	52%

Table XIII. Green Properties of B2(2) Bilayer Membranes

Bilayer ID #	Dense Tape ID #	Initial thickness (μm)	Porous Tape ID #	Initial thickness (μm)	Thickness Ratio	Green bilayer thickness (μm)
B2(2)-B-1	B2(2)-D-2	530	B2(2)-P-7	4900	9.2	490
B2(2)-B-2	B2(2)-D-2	530	B2(2)-P-8	5000	9.4	500
B2(2)-B-3	B2(2)-D-2	530	B2(2)-P-9	5000	9.4	500

Table XIV. Sintered Properties of B2(2) Bilayer Membranes

Bilayer ID #	Sintering Conditions	Final porous layer thickness (μm)	Final dense layer thickness (μm)	Thickness Ratio	Sintered bilayer thickness (μm)	Z direction sintering shrinkage (%)
B2(2)-B-1	950°C/1h	385	50	7.7	435	11%
	975°C/1h	385	50	7.7	435	11%
	1000°C/1h	385	50	7.7	435	11%
	1025°C/1h	375	50	7.5	425	13%
	1050°C/1h	370	50	7.4	420	14%
B2(2)-B-2	950°C/1h	405	60	6.8	465	7%
	975°C/1h	395	60	6.6	455	9%
	1000°C/1h	385	55	7.0	440	12%
	1025°C/1h	375	55	6.8	430	14%
	1050°C/1h	350	55	6.4	405	19%
B2(2)-B-3	950°C/1h	360	55	6.5	415	17%
	975°C/1h	360	55	6.5	415	17%
	1000°C/1h	365	50	7.3	415	17%
	1025°C/1h	355	50	7.1	405	19%
	1050°C/1h	340	50	6.8	390	22%

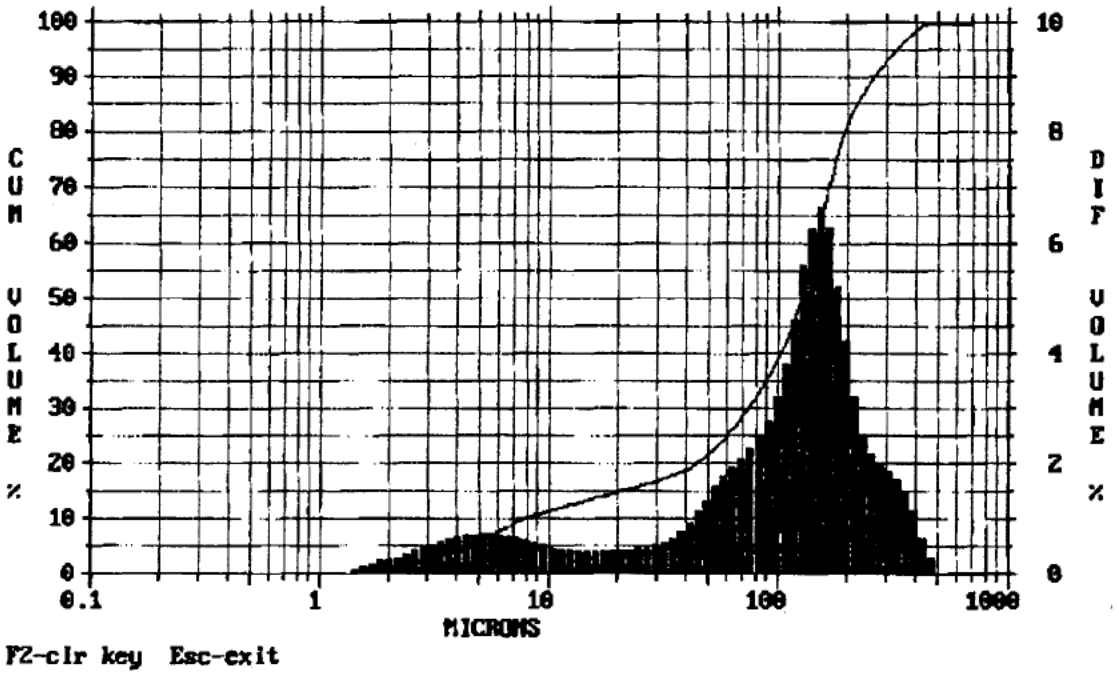

Fig. 1. Particle Size Analysis of B2B powder; calcined 1000°C/1h, sieved –60 mesh.

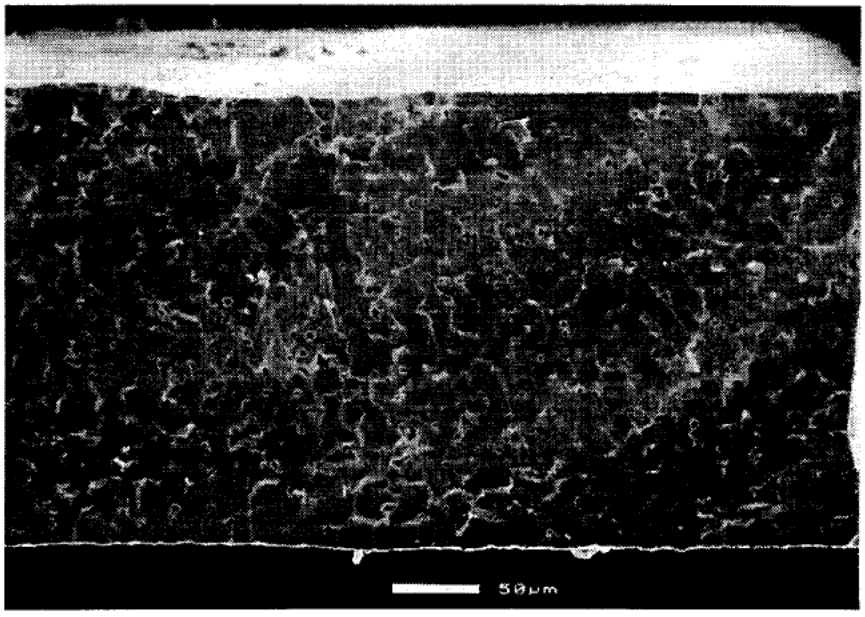

Fig. 2. Calendered Tape #B2B-D-1; sintered 1050°C/1h.

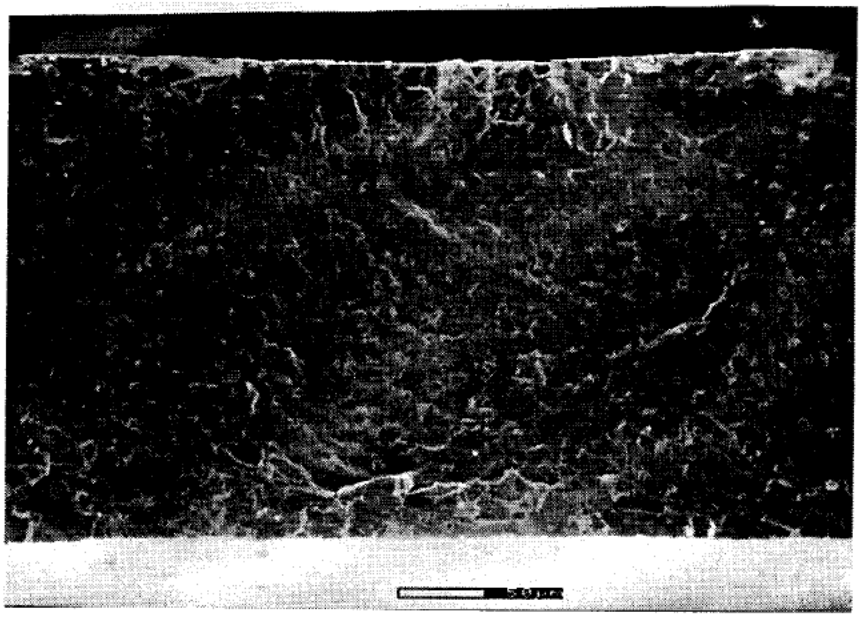

Fig. 3. Calendered Tape #B2B-D-2; sintered 1050°C/1h.

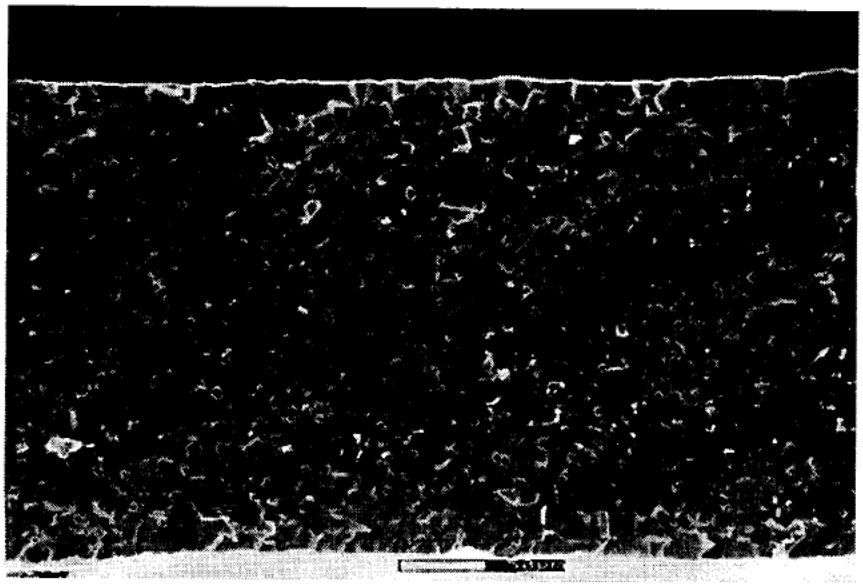

Fig. 4. Calendered Tape #B2B-D-3; sintered 1050°C/1h.

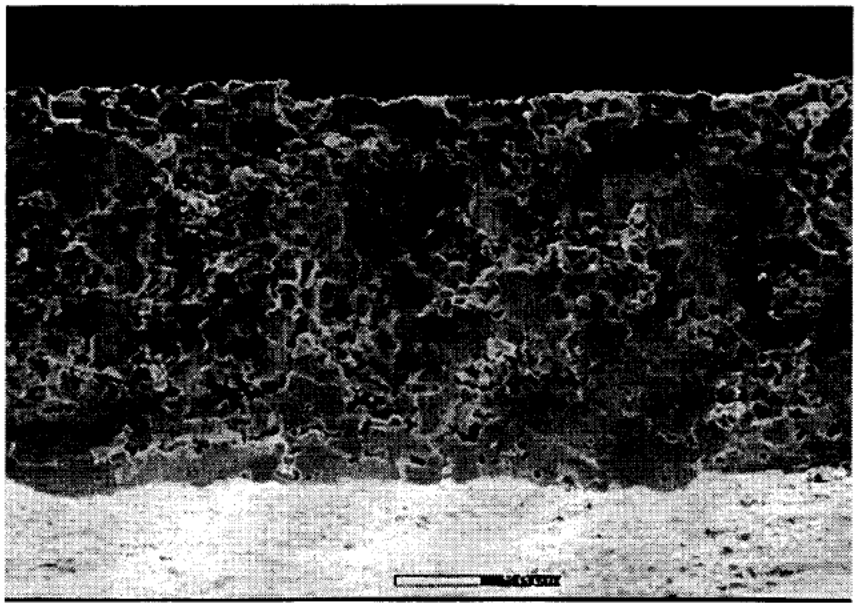

Fig. 5. Calendered Tape #B2B-P-1; sintered 1050°C/1h.

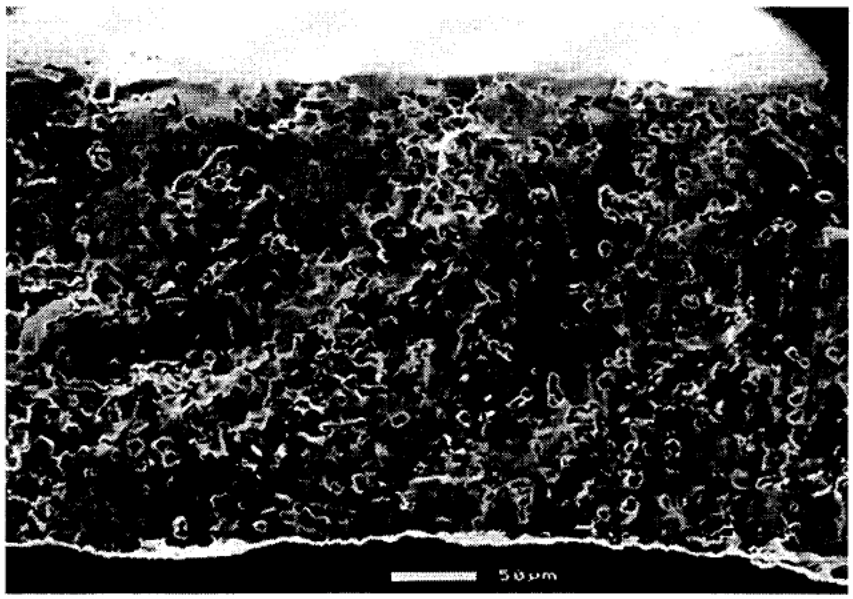

Fig.6. Calendered Tape #B2B-P-2; sintered 1050°C/1h.

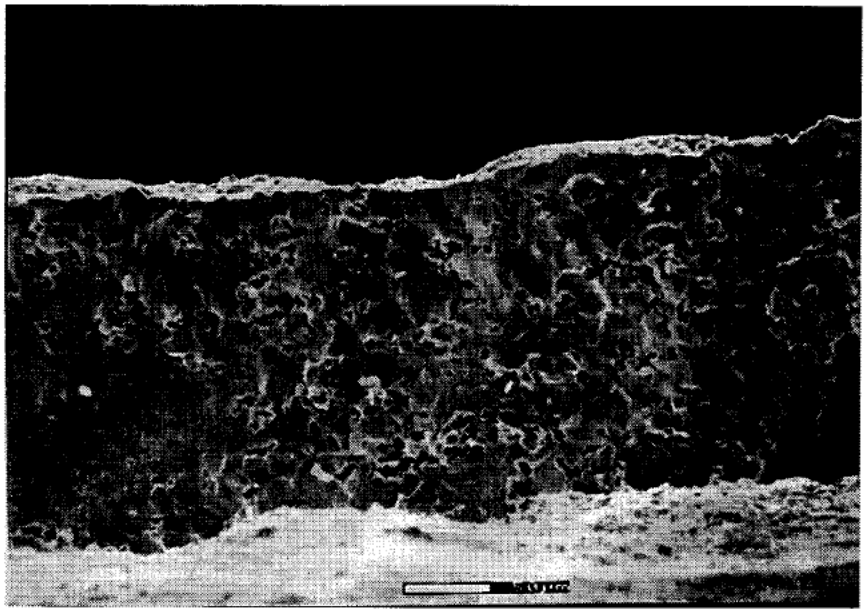

Fig. 7. Calendered Tape #B2B-P-3; sintered 1050°C/1h.

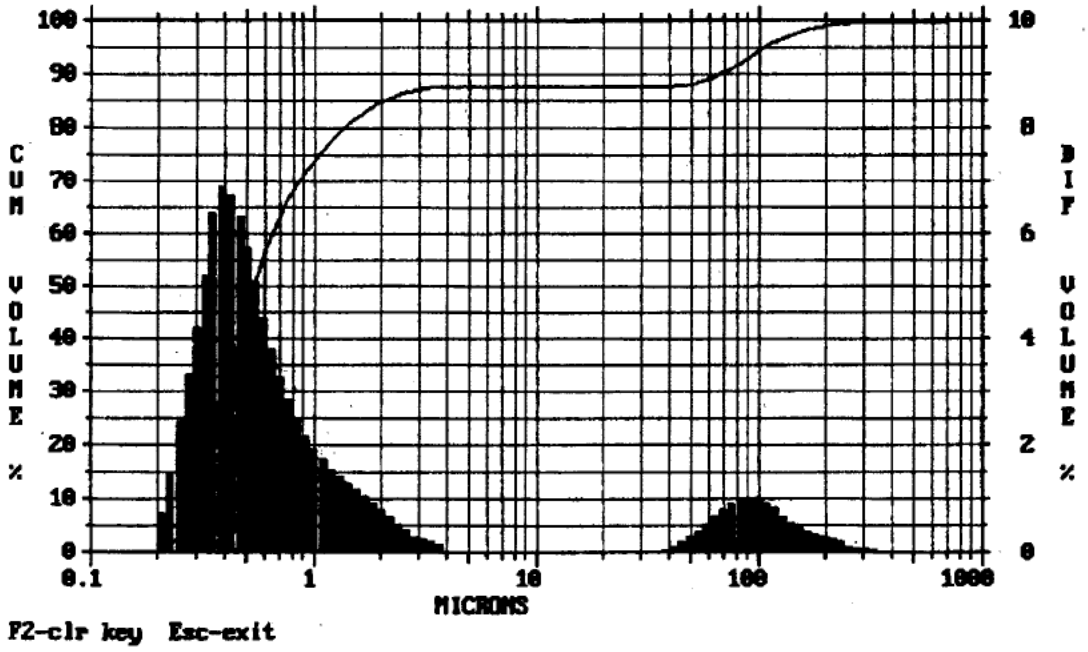

Figure 8. Particle Size Analysis of Ceria (CC810).

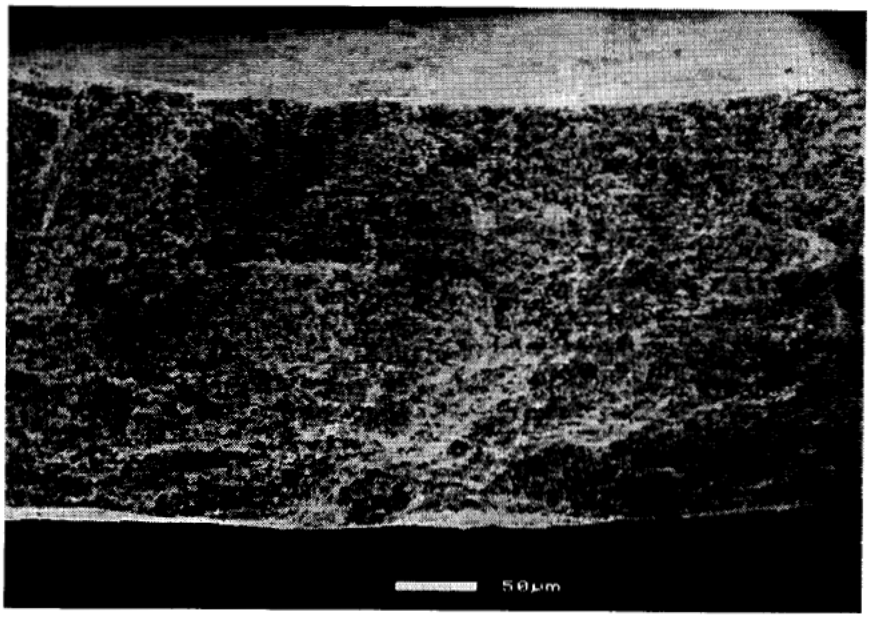

Fig. 9. Calendered Tape #B2B-P-4; sintered 1050°C/1h.

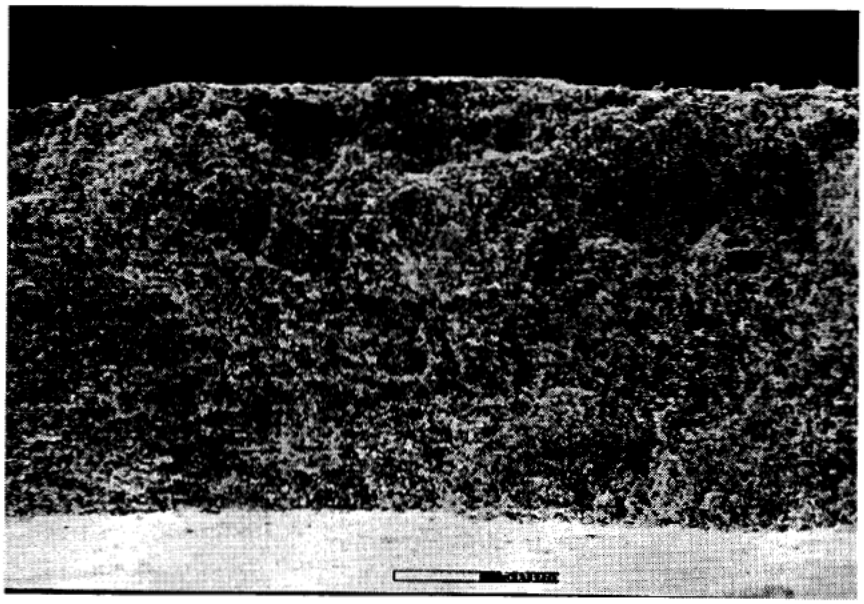

Fig. 10. Calendered Tape #B2B-P-5; sintered 1050°C/1h.

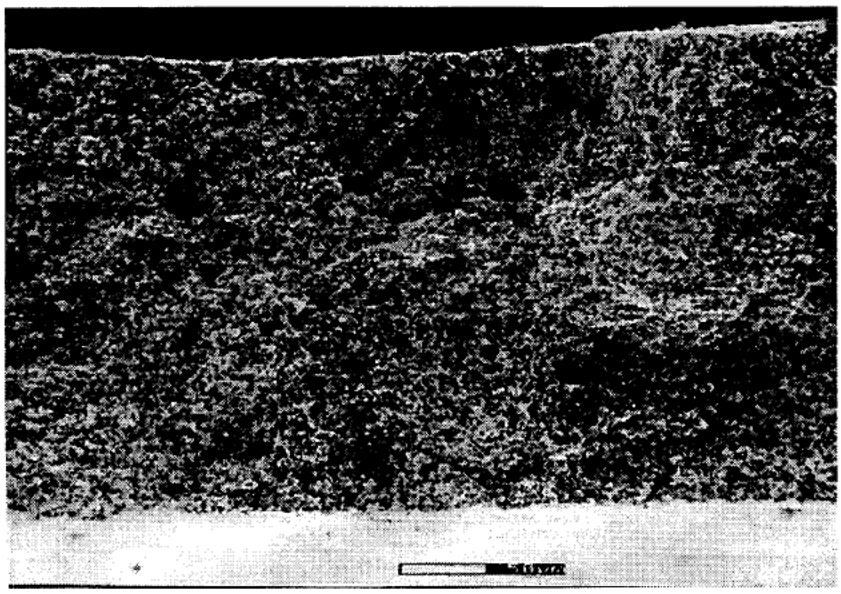

Fig. 11. Calendered Tape #B2B-P-6; sintered 1050°C/1h.

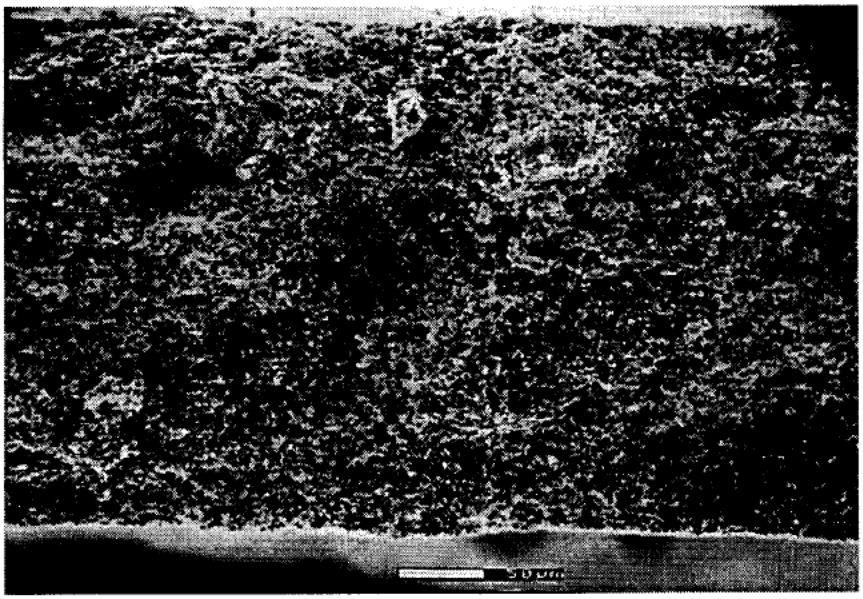

Fig. 12. Calendered Tape #B2B-P-7; sintered 1050°C/1h.

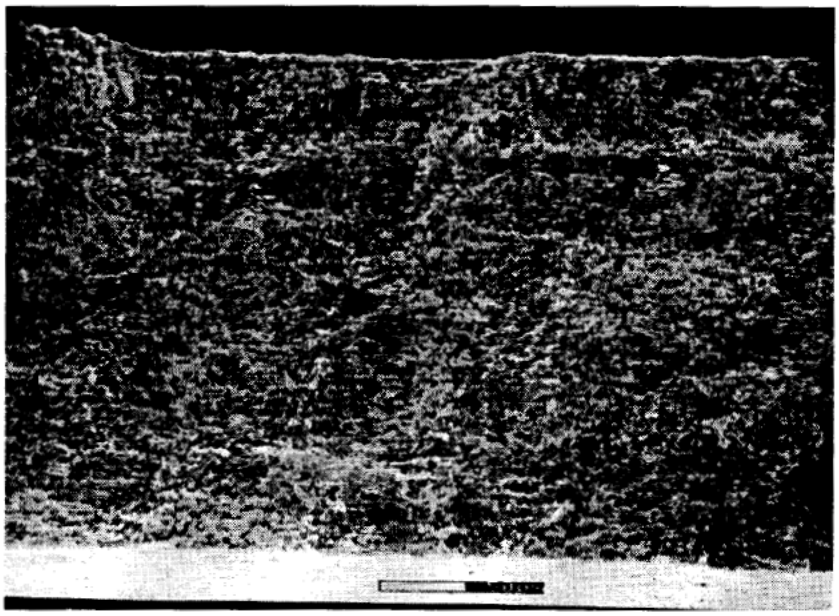

Fig. 13. Calendered Tape #B2B-P-8; sintered 1050°C/1h.

Fig. 14. Calendered Tape #B2B-P-9; sintered 1050°C/1h.

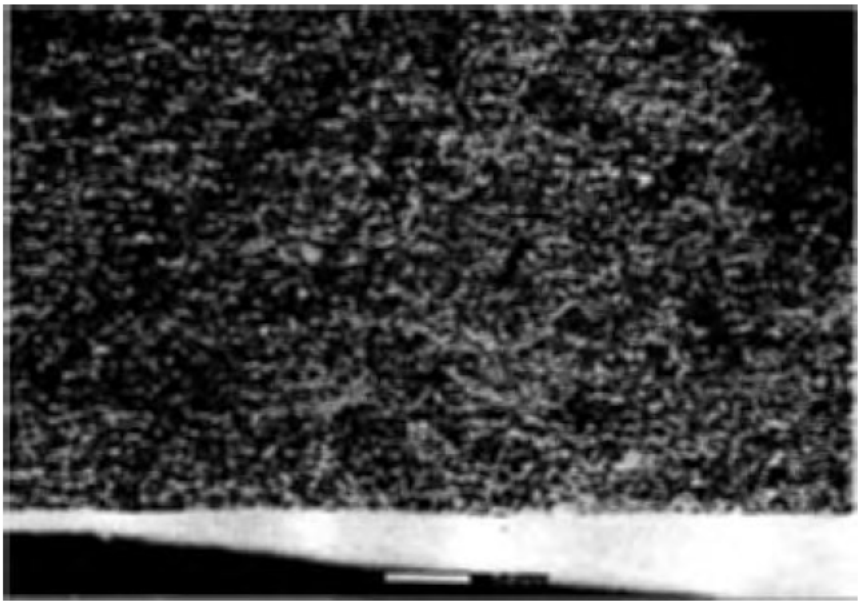

Fig. 15. Calendered Tape #B2B-P-10; sintered 1050°C/1h.

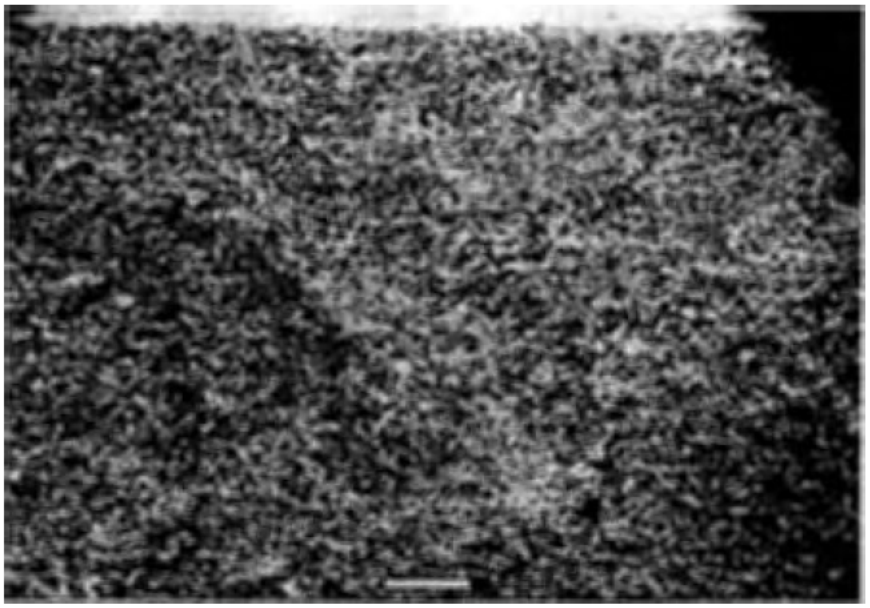

Fig. 16. Calendered Tape#B2B-P-11; sintered 1050°C/1h.

Fig. 17. Calendered Tape #B2B-P-12; sintered 1050°C/1h.

Fig. 18. Calendered Tape #B2B-P-13; sintered 1050°C/1h.

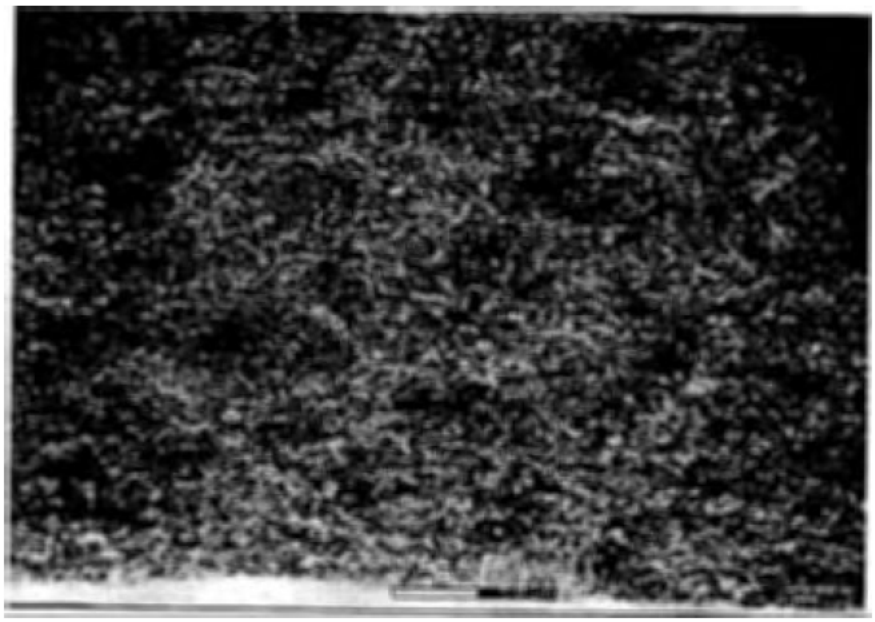

Fig. 19. Calendered Tape #B2B-P-14; sintered 1050°C/1h.

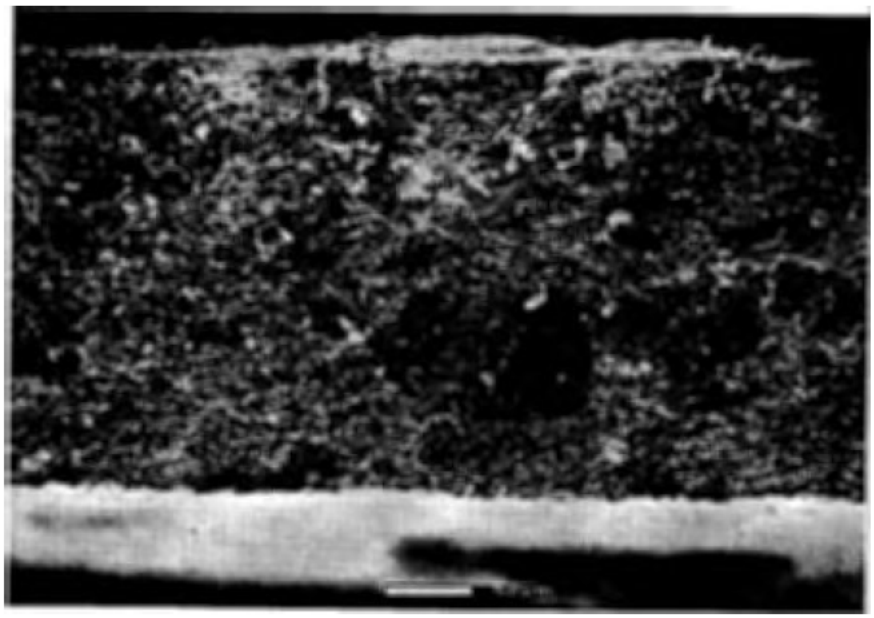

Fig. 20. Calendered Tape #B2B-P-15; sintered 1050°C/1h.

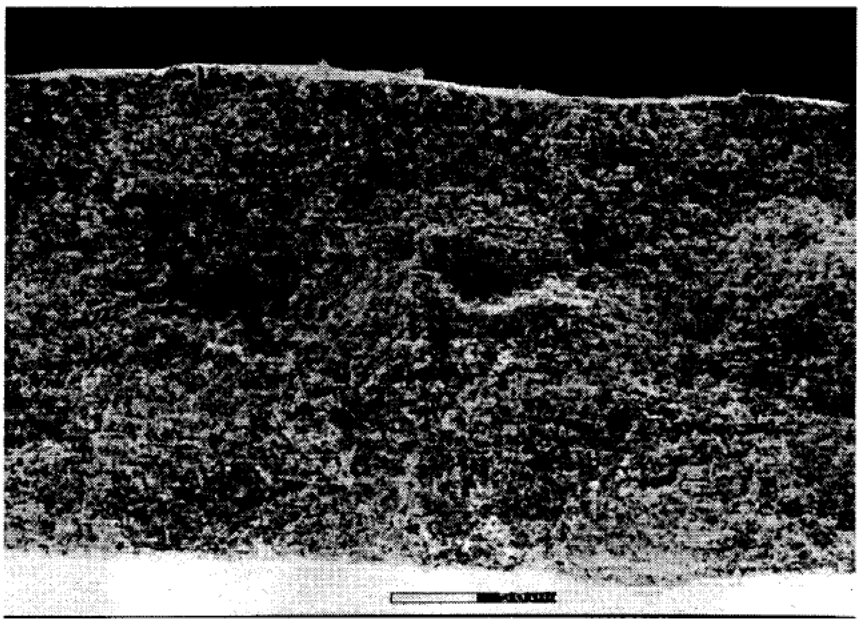

Fig. 21. Calendered Tape #B2B-P-16; sintered 1050°C/1h.

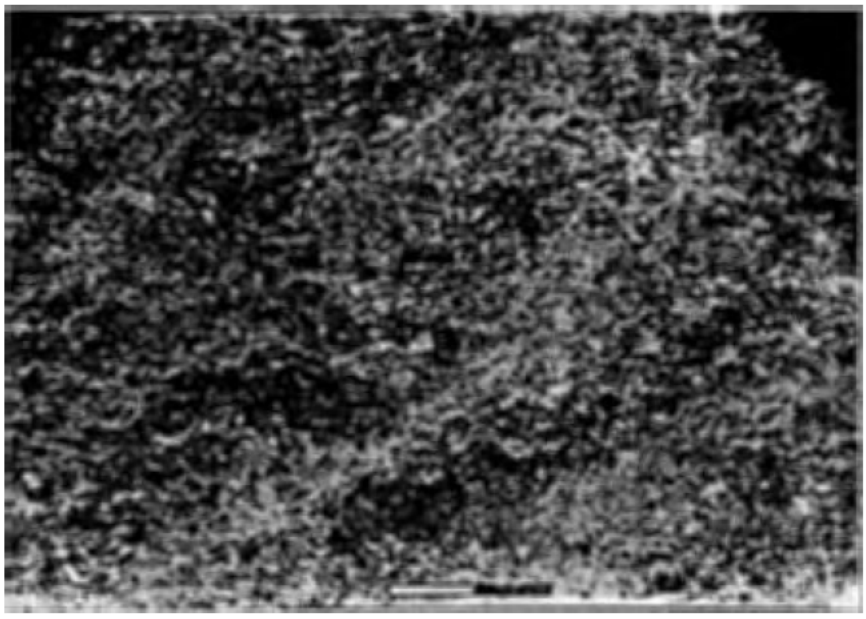

Fig. 22. Calendered Tape #B2B-P-17; sintered 1050°C/1h.

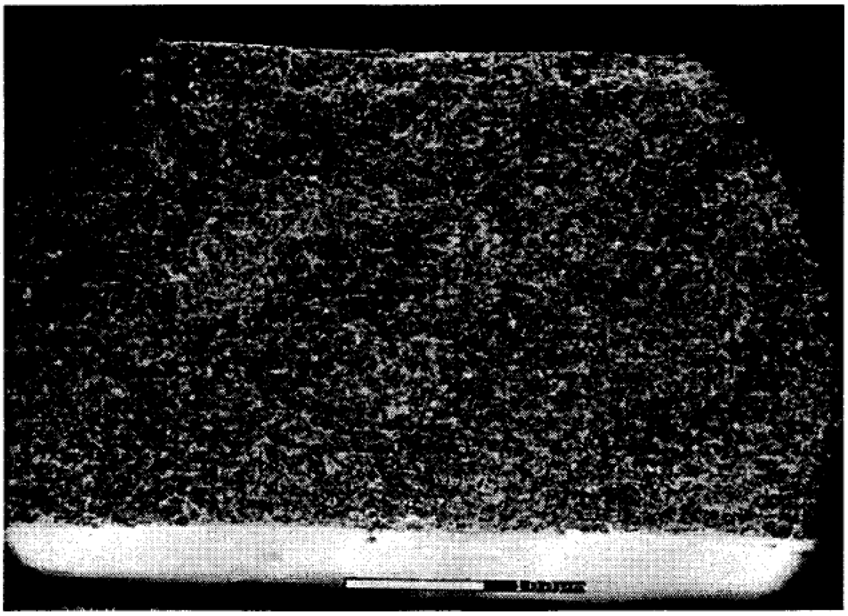

Fig. 23. Calendered Tape #B2B-P-18; sintered 1050°C/1h.

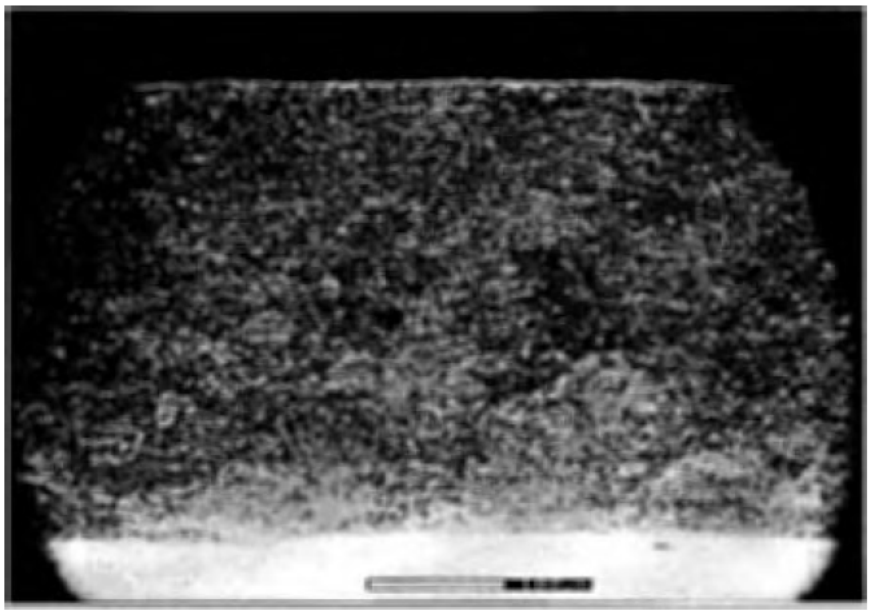

Fig. 24. Calendered Tape #B2B-P-19; sintered 1050°C/1h.

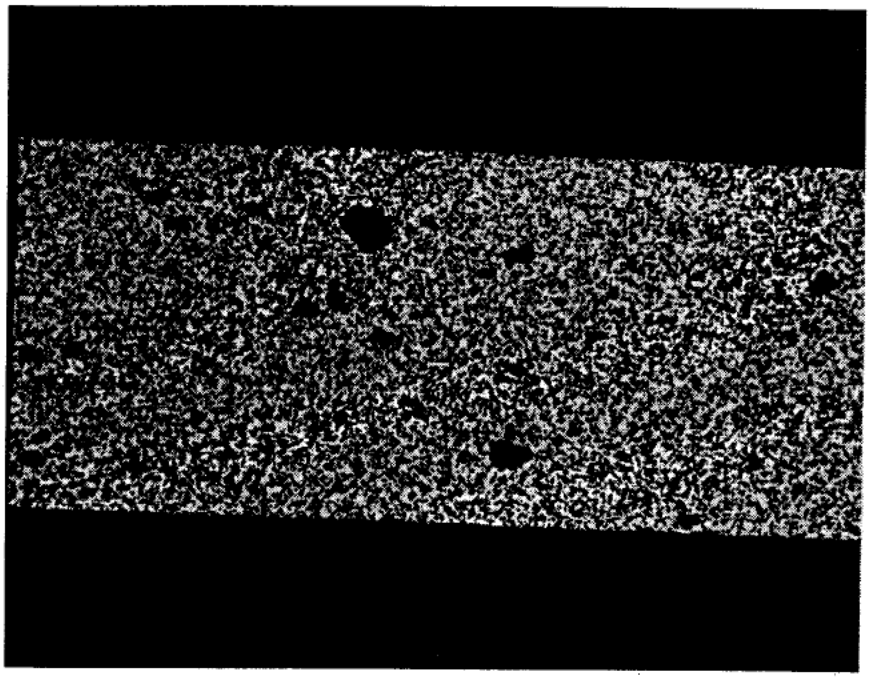

Fig. 25. Calendered Tape #B2B-P-21; sintered 1050°C/1h. Magnification: 100X

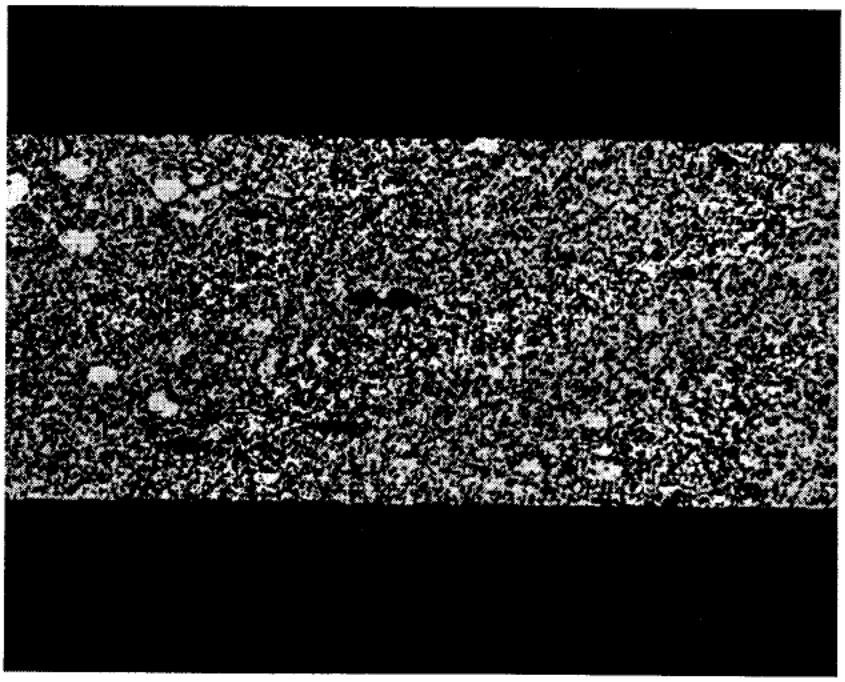

Fig. 26. Calendered Tape #B2B-P-22; sintered 1050°C/1h. Magnification: 100X

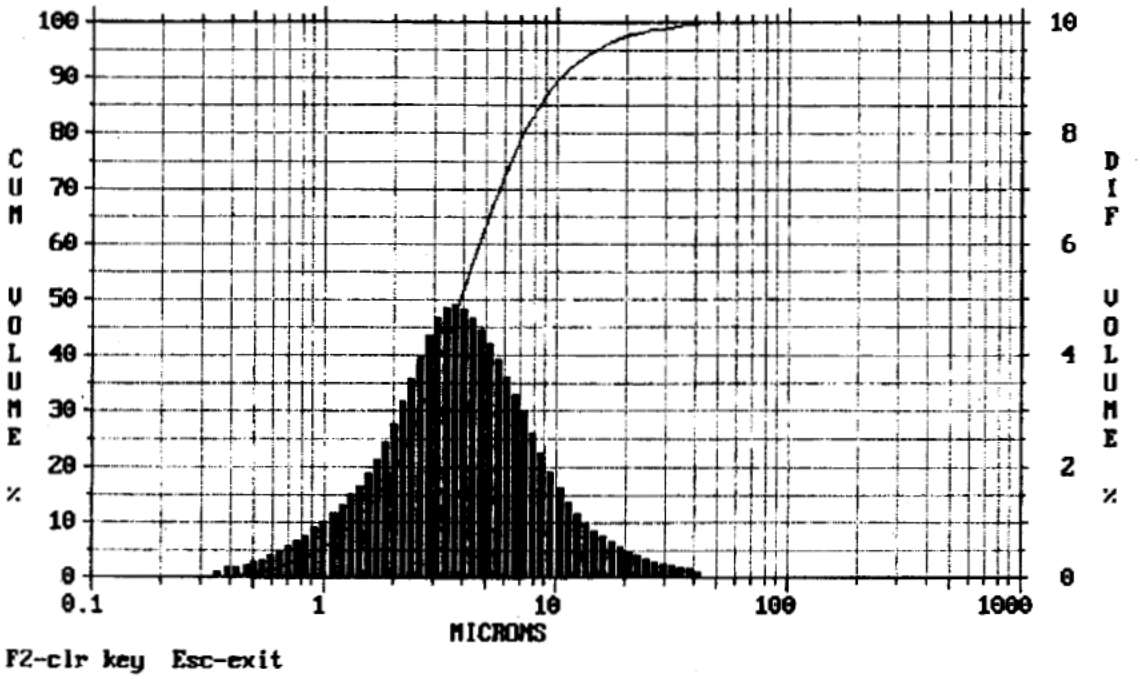

Figure 27. Particle Size Analysis of B2B, wet milled in IPA for 4 hours w/ Darvan; sieved –200 mesh.

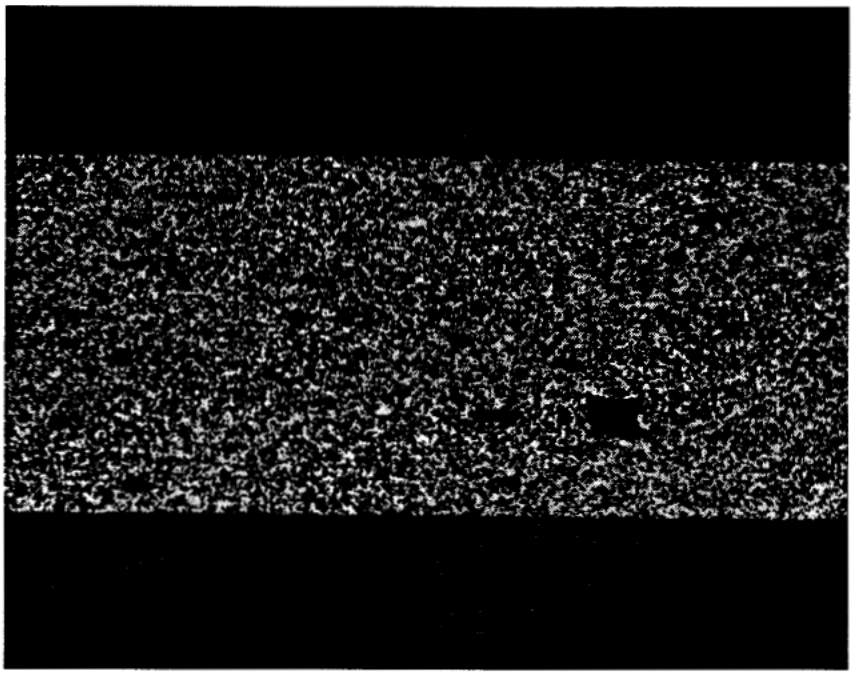

Fig. 28. Calendered Tape #B2B-P-23; sintered 1050°C/1h. Magnification: 100X

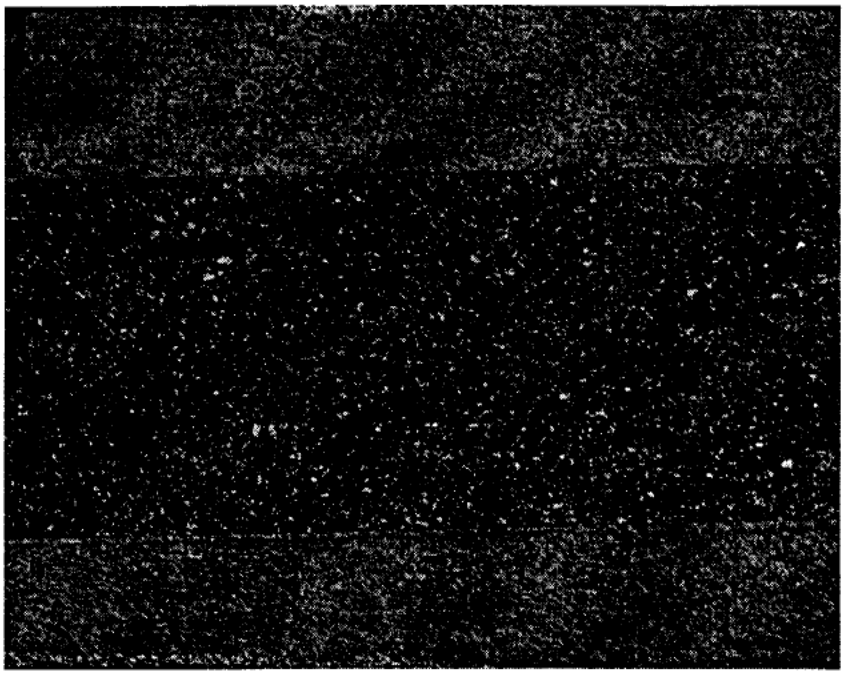

Fig. 29. Calendered Tape #B2B-P-24; sintered 1075°C/1h. Magnification: 100X

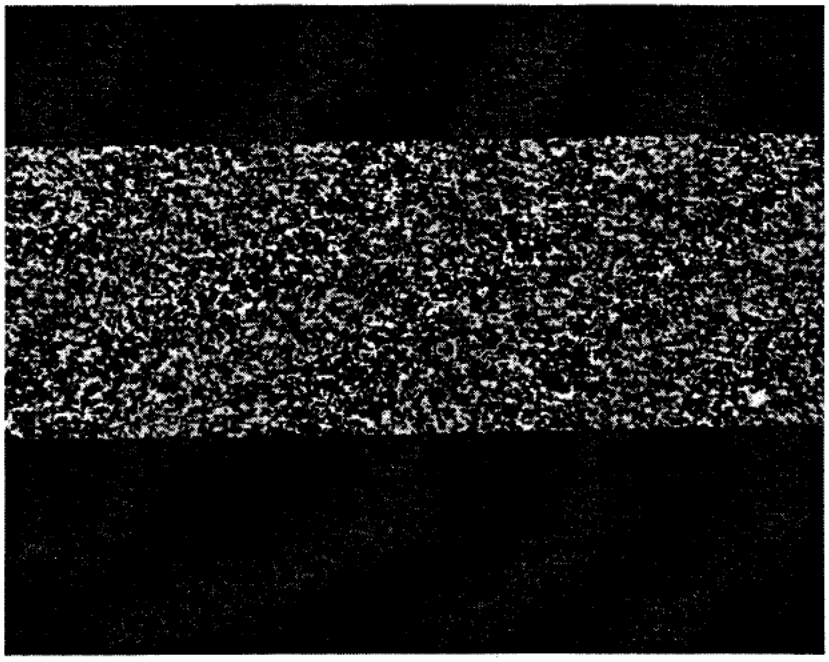

Fig. 30. Calendered Tape #B2B-P-25; sintered 1075°C/1h. Magnification: 100X

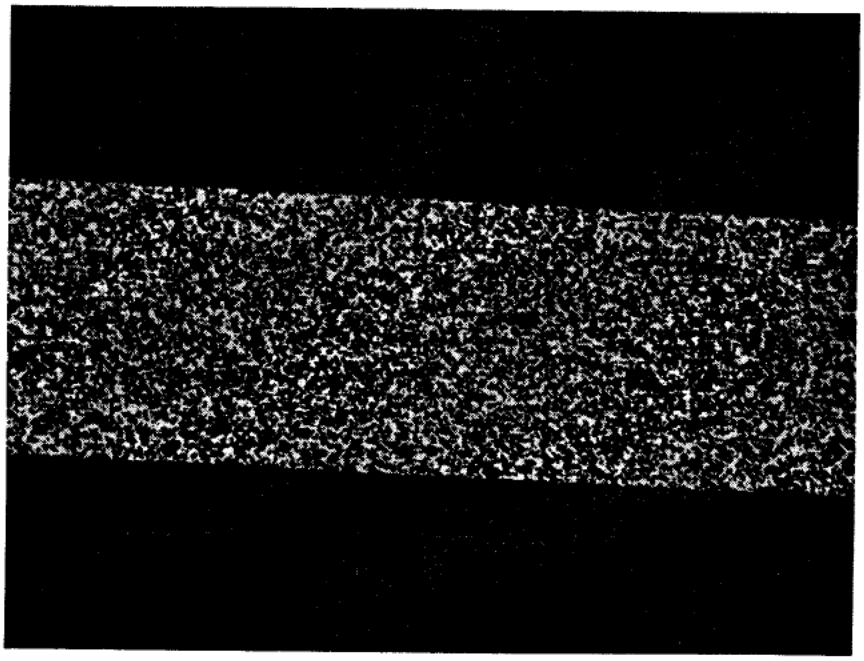

Fig. 31. Calendered Tape #B2B-P-26; sintered 1075°C/1h. Magnification: 100X

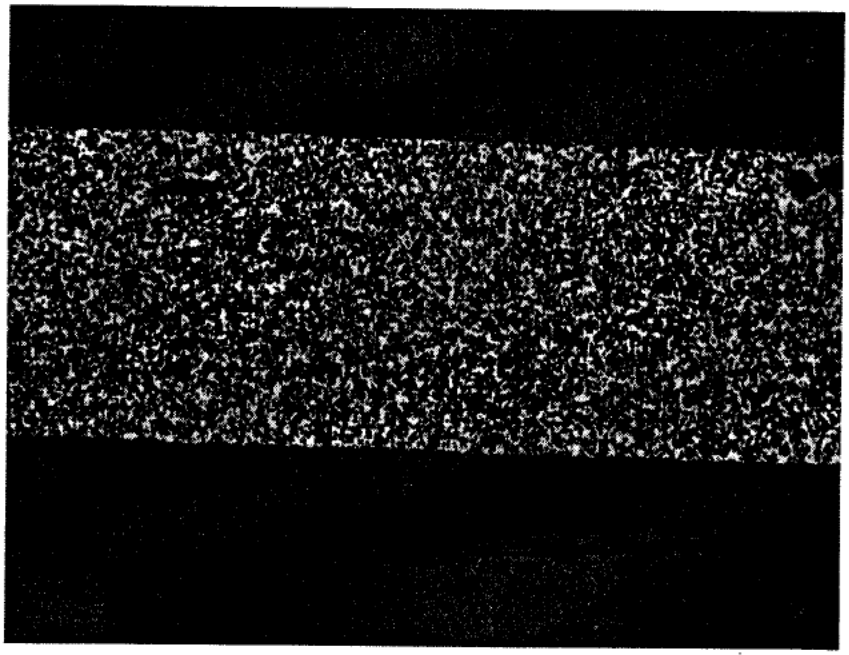

Fig. 32. Calendered Tape #B2B-P-27; sintered 1075°C/1h. Magnification: 100X

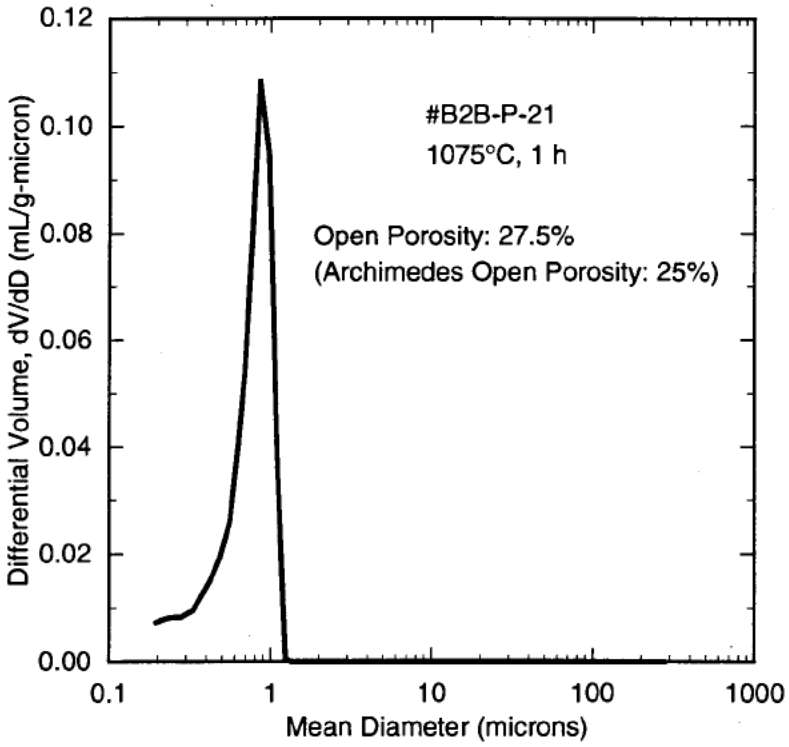

Figure 33. Mercury porosimetry results for tape #B2B-P-21, sintered 1075°C/1h.

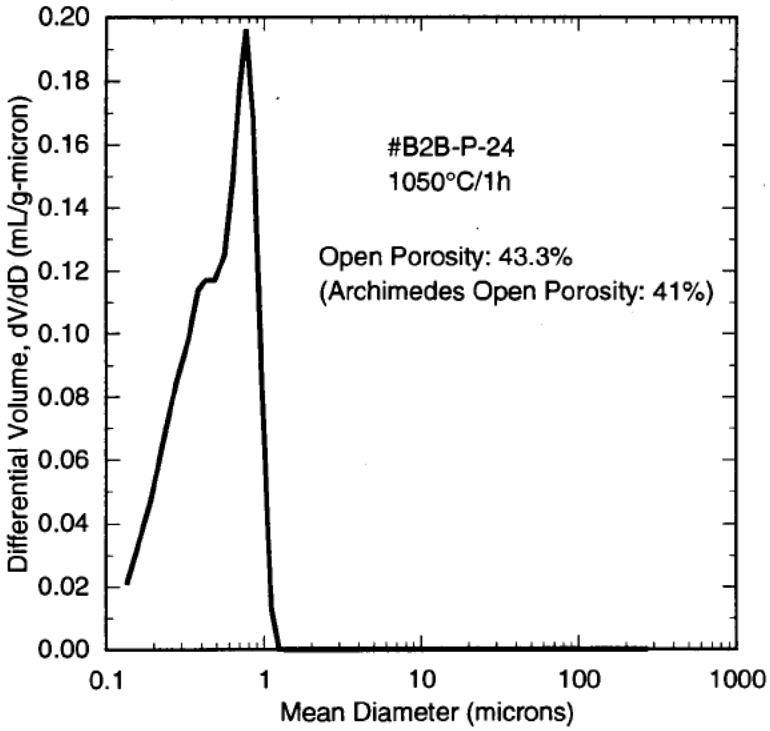

Figure 34. Mercury porosimetry results for tape #B2B-P-24, sintered 1050°C/1h.

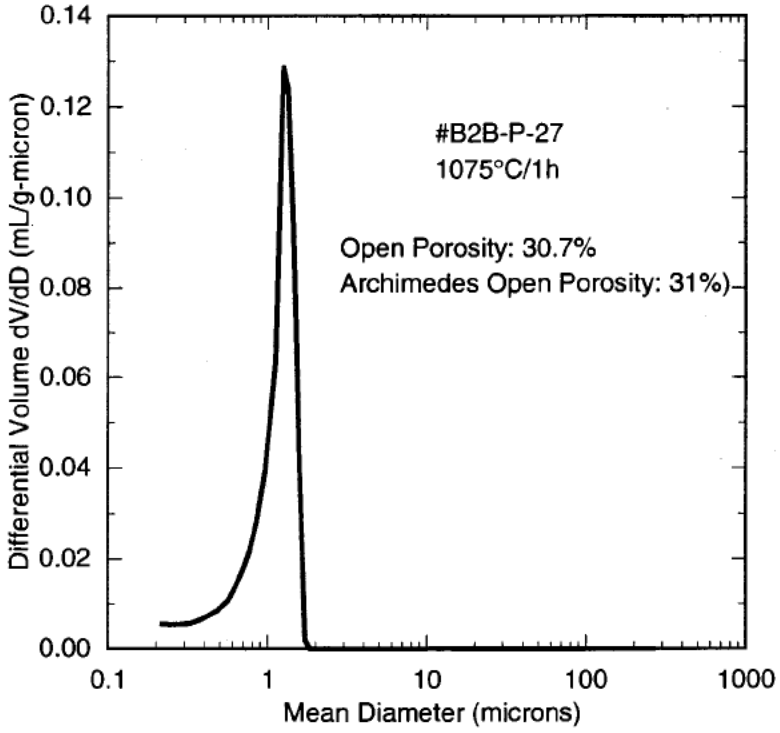

Figure 35. Mercury porosimetry results for tape #B2B-P-27, sintered 1075°C/1h.

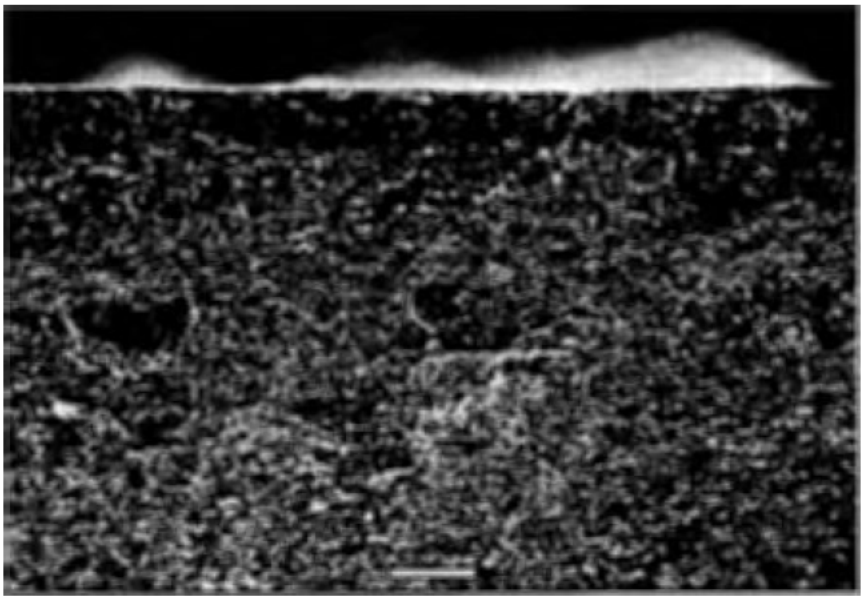

Fig. 36. Calendered Bilayer #B2B-B-1; sintered 1050°C/1h.
Dense layer at top.

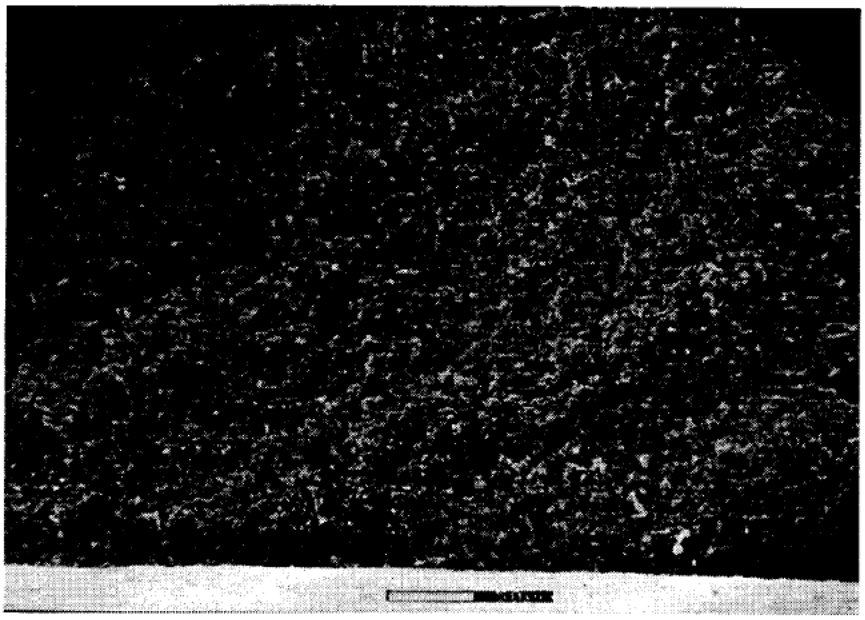

Fig. 37. Calendered Bilayer #B2B-B-1; sintered 1075°C/1h.
Dense layer at bottom.

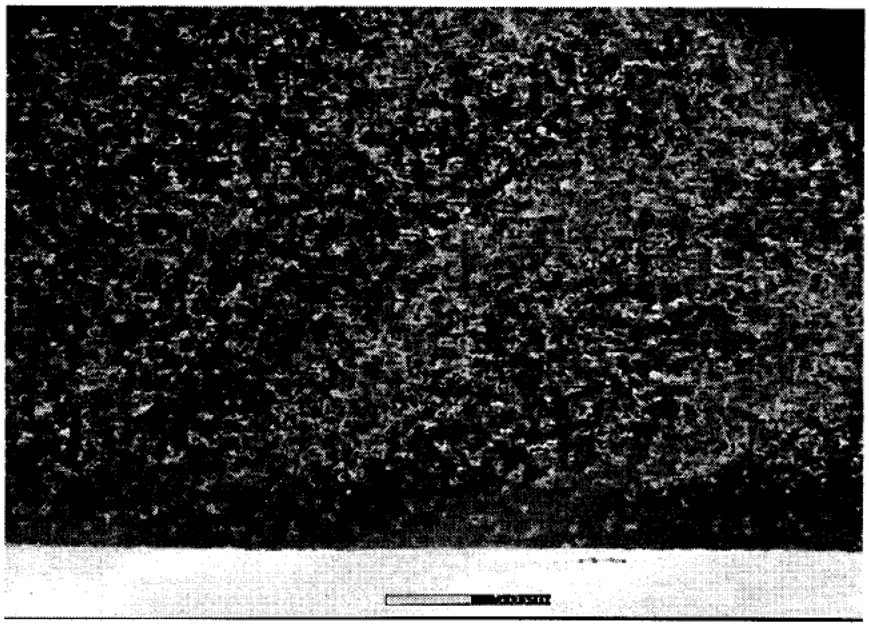

Fig. 38. Calendered Bilayer #B2B-B-1; sintered 1100°C/1h.
Dense layer at bottom.

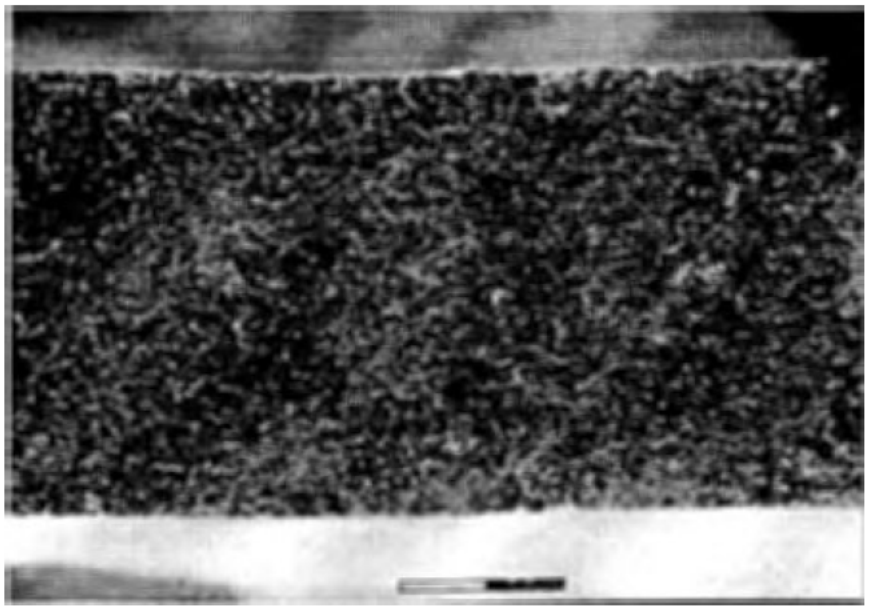

Fig. 39. Calendered Bilayer#B2B-B-2; sintered 1050°C/1h.
Dense layer at bottom.

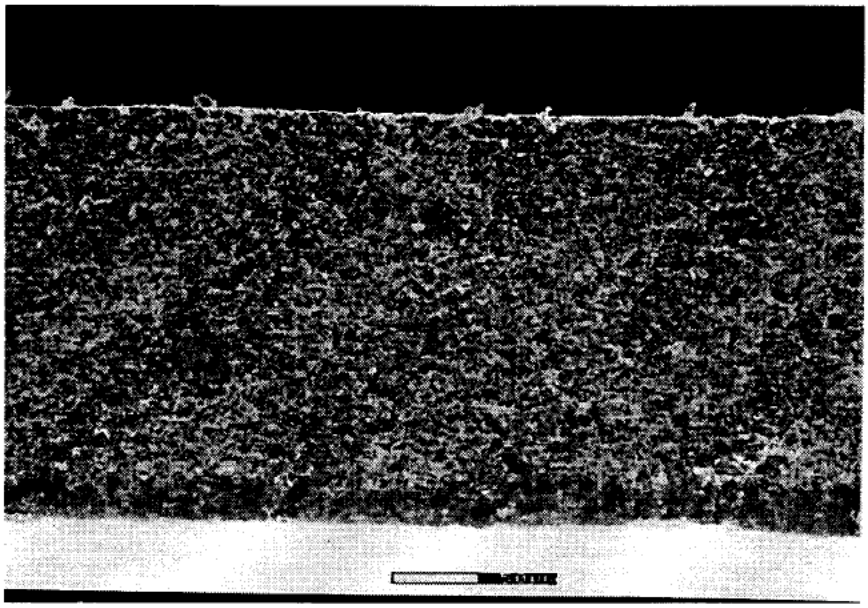

Fig. 40. Calendered Bilayer #B2B-B-2; sintered 1075°C/1h.
Dense layer at bottom.

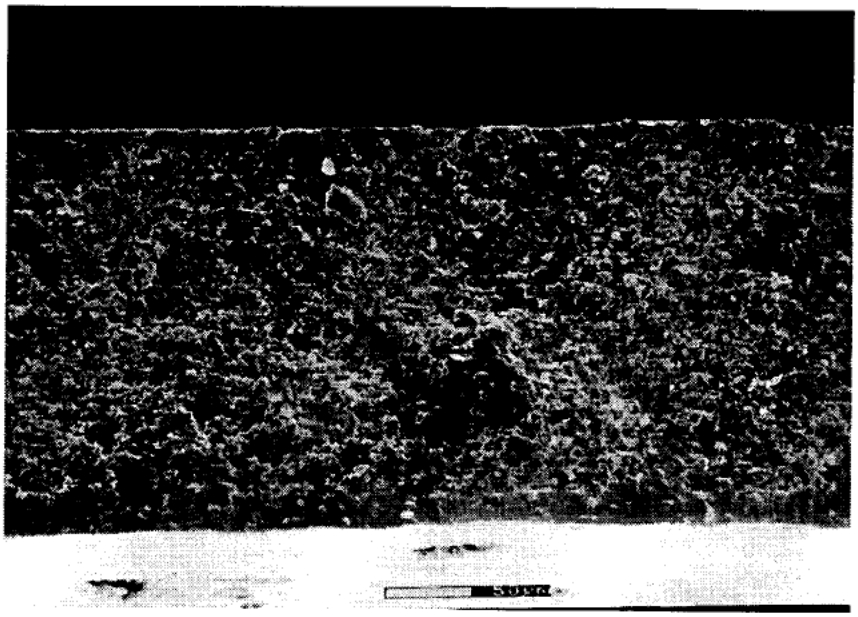

Fig. 41. Calendered Bilayer #B2B-B-2; sintered 1100°C/1h.
Dense layer at bottom.

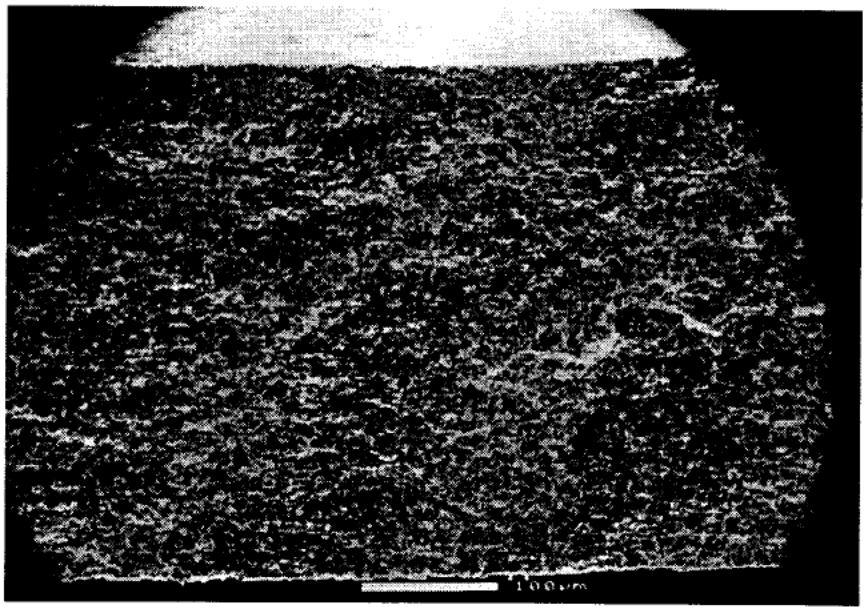

Fig. 42. Calendered Bilayer #B2B-B-3; sintered 1050°C/1h.
Dense layer at top.

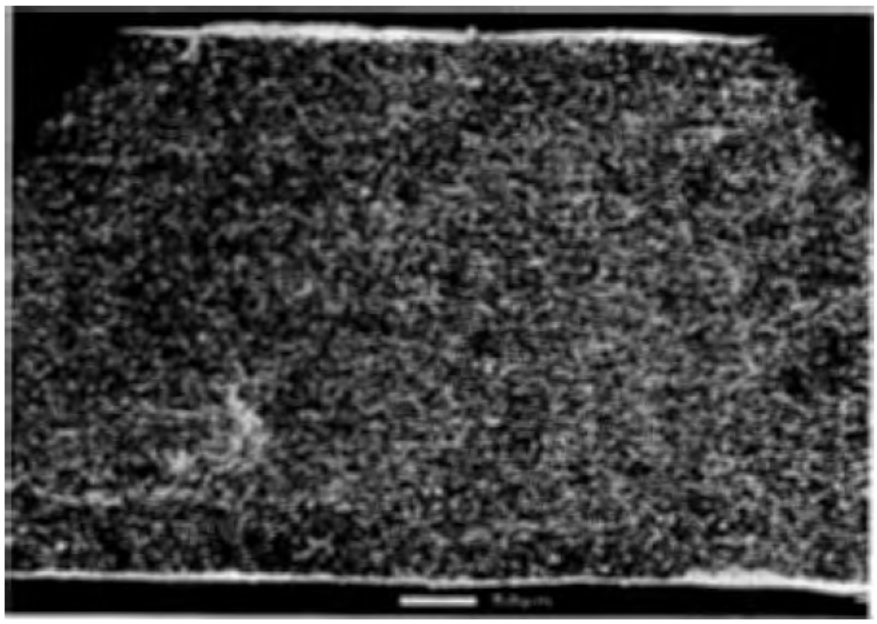

Fig. 43. Calendered Bilayer #B2B-B-3; sintered 1075°C/1h.
Dense layer at bottom.

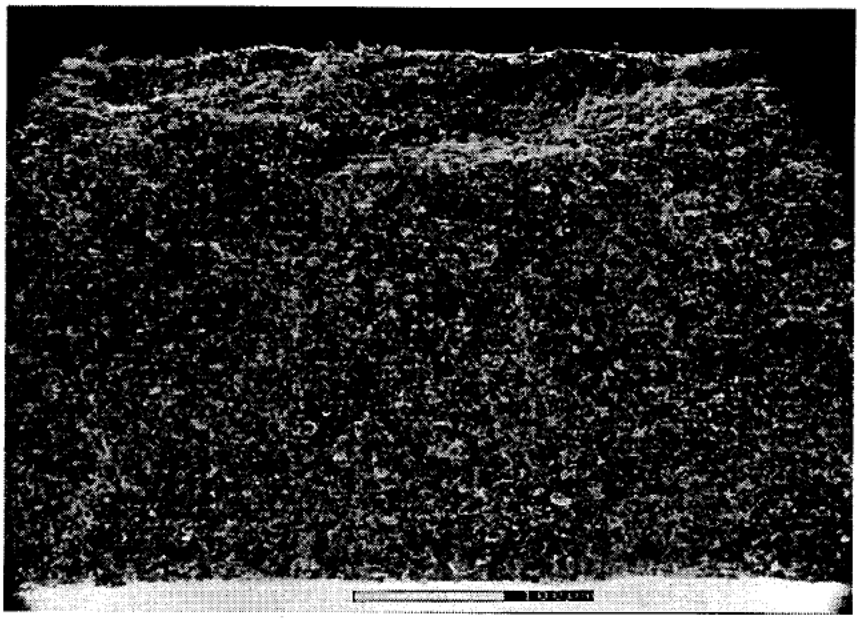

Fig. 44. Calendered Bilayer #B2B-B-3; sintered 1100°C/1h.
Dense layer at bottom.

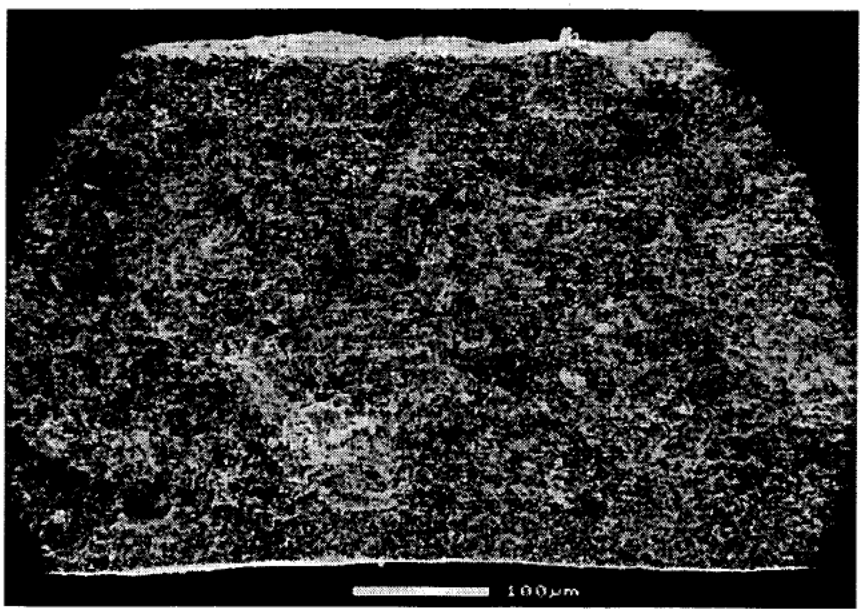

Fig. 45. Calendered Bilayer #B2B-B-4; sintered 1050°C/1h.
Dense layer at bottom.

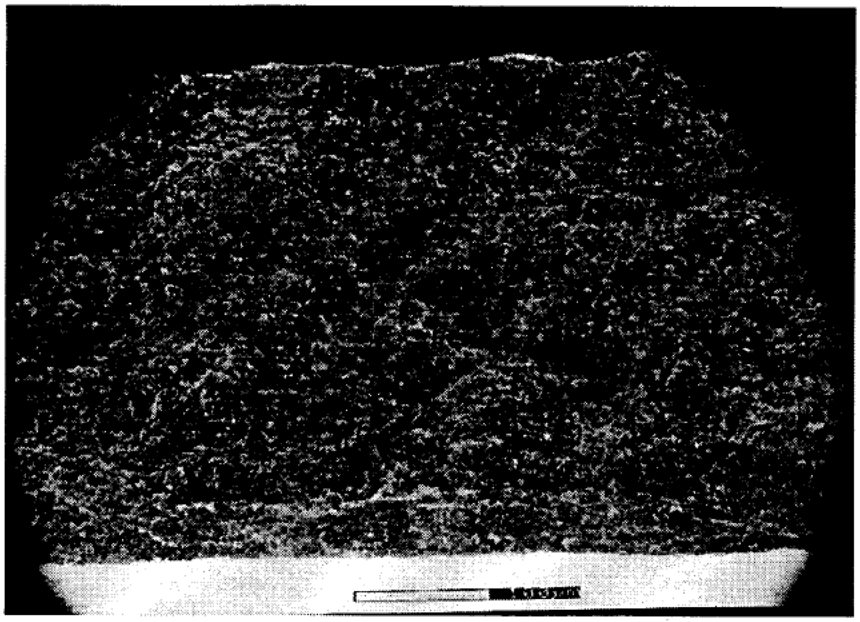

Fig. 46. Calendered Bilayer #B2B-B-4; sintered 1075°C/1h.
Dense layer at bottom.

Fig. 47. Calendered Bilayer #B2B-B-4; sintered 1100°C/1h.
Dense layer at bottom.

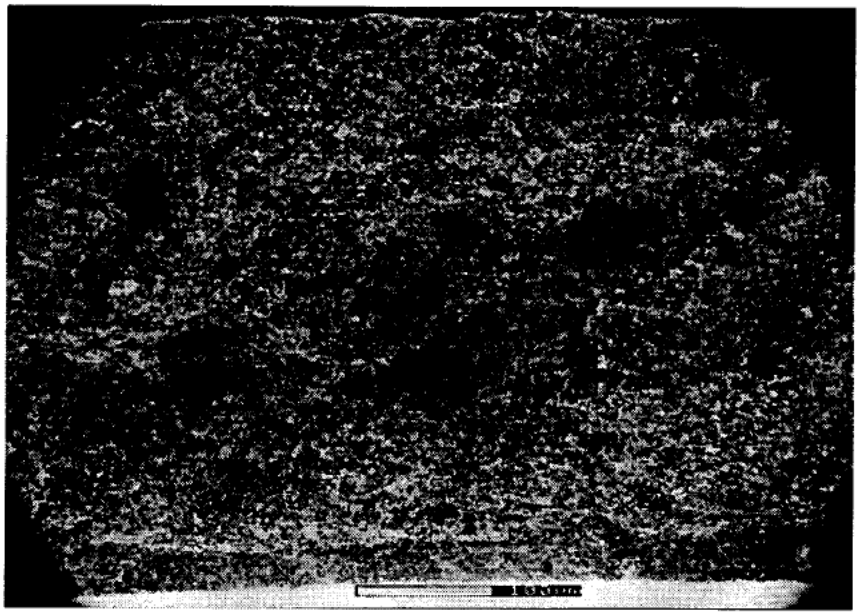

Fig. 48. Calendered Bilayer #B2B-B-5; sintered 1050°C/1h.
Dense layer at bottom.

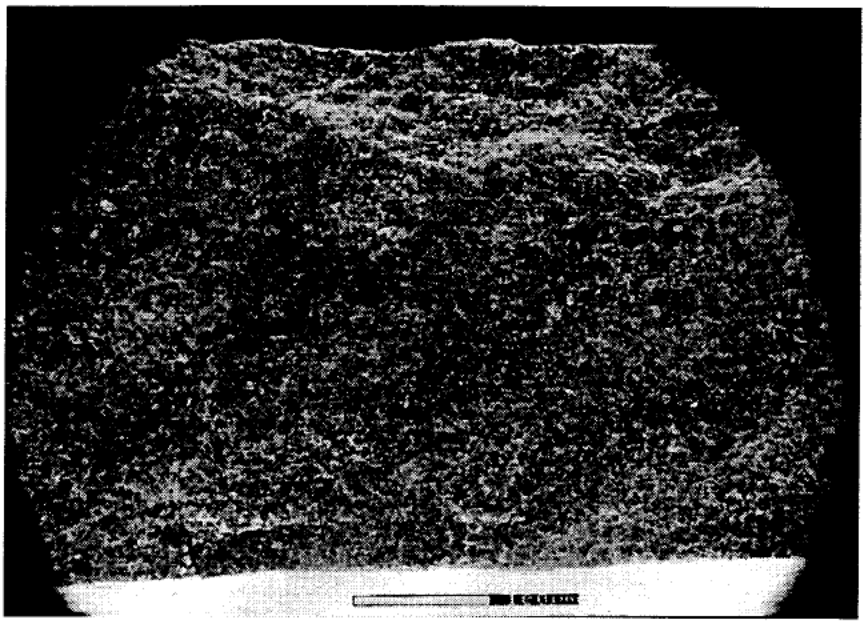

Fig. 49. Calendered Bilayer #B2B-B-5; sintered 1075°C/1h.
Dense layer at bottom.

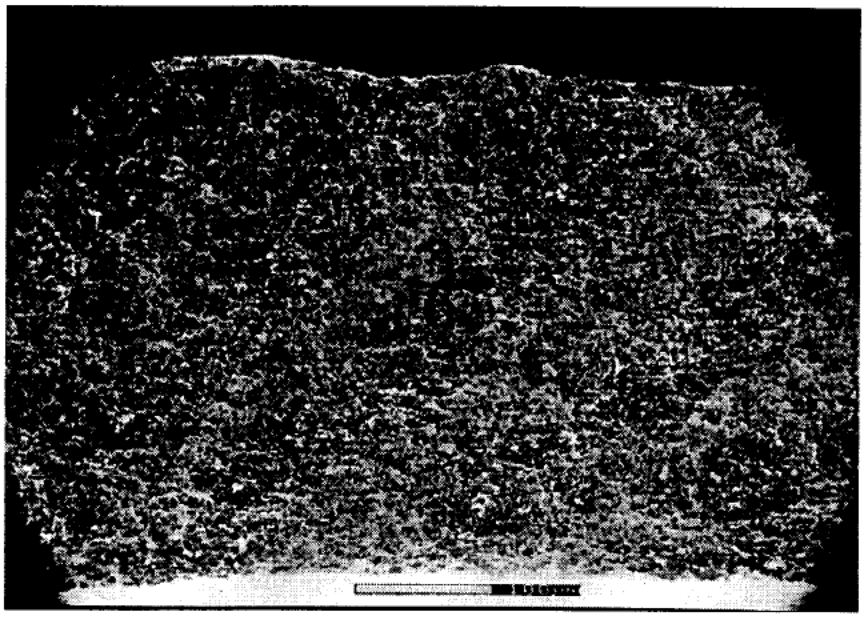

Fig. 50. Calendered Bilayer #B2B-B-5; sintered 1100°C/1h.
Dense layer at bottom.

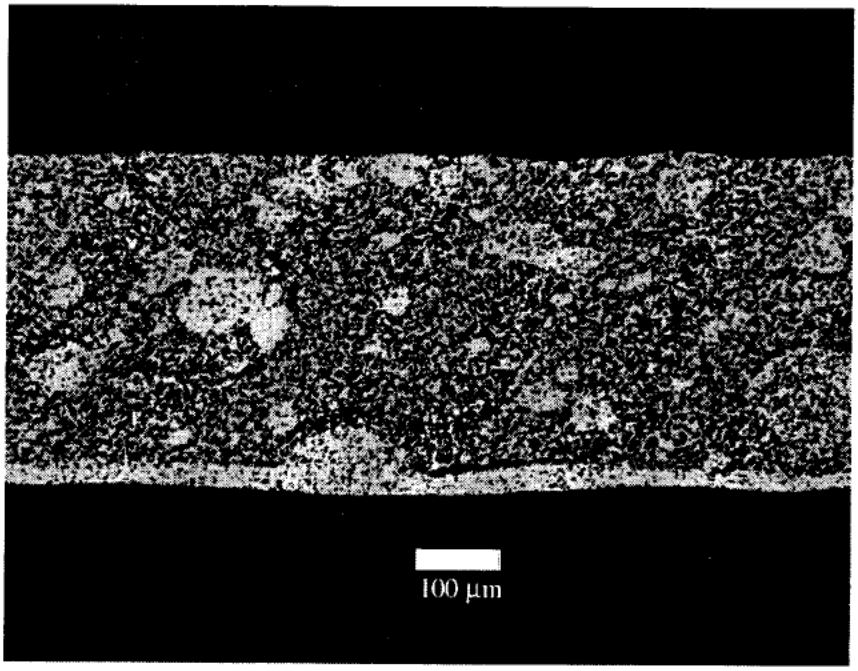

Figure 51. Calendered Bilayer #B2B-B-5; sintered 1050°C/1h. Dense layer at bottom. 100X.

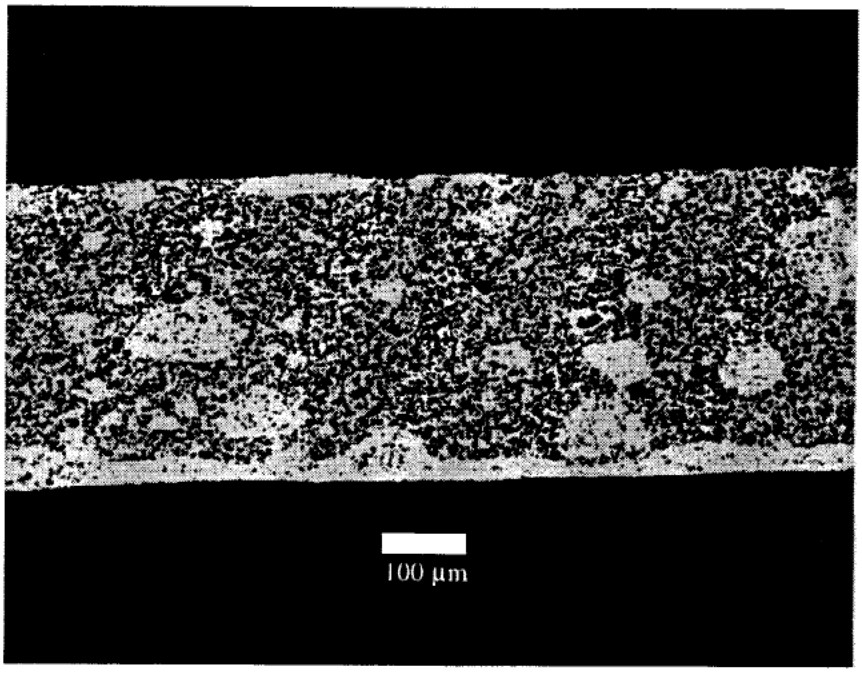

Figure 52. Calendered Bilayer #B2B-B-5; sintered 1075°C/1h. Dense layer at bottom. 100X.

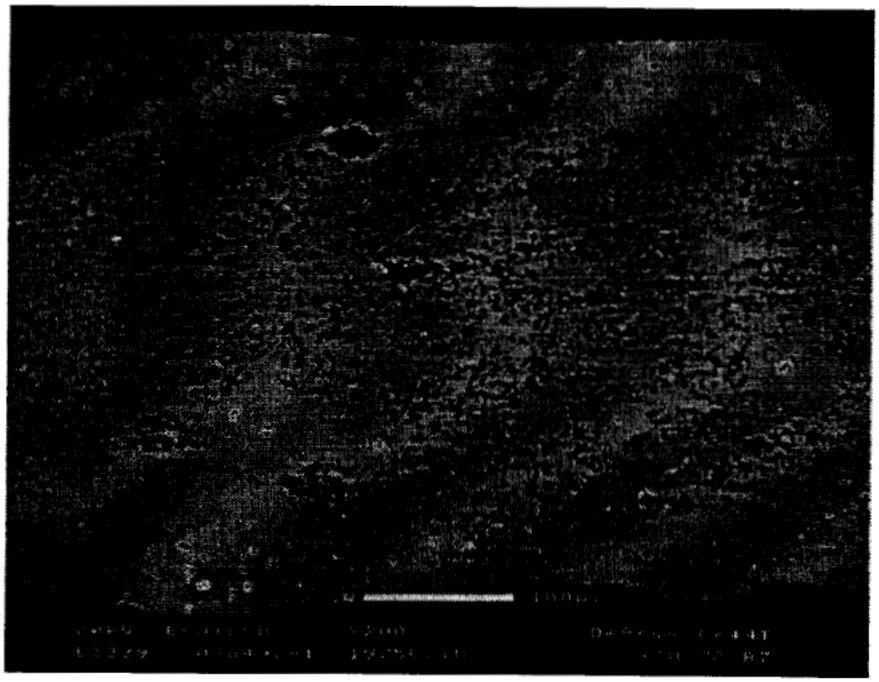

Figure 53. Calendered Bilayer #B2B-B-6; sintered 1075°C/1h.
Dense layer at top.

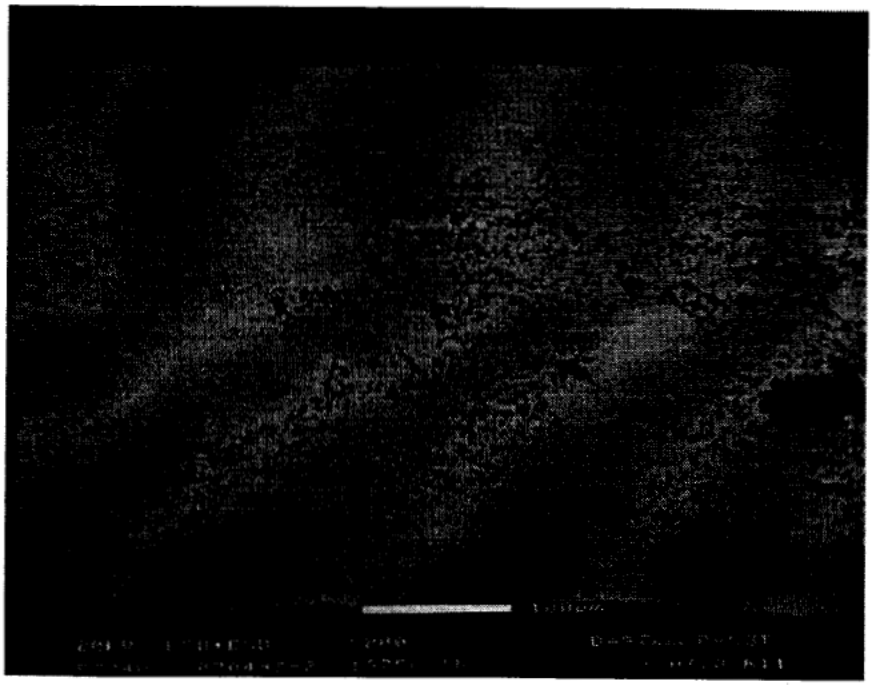

Figure 54. Calendered Bilayer #B2B-B-7; sintered 1075°C/1h.
Dense layer at top.

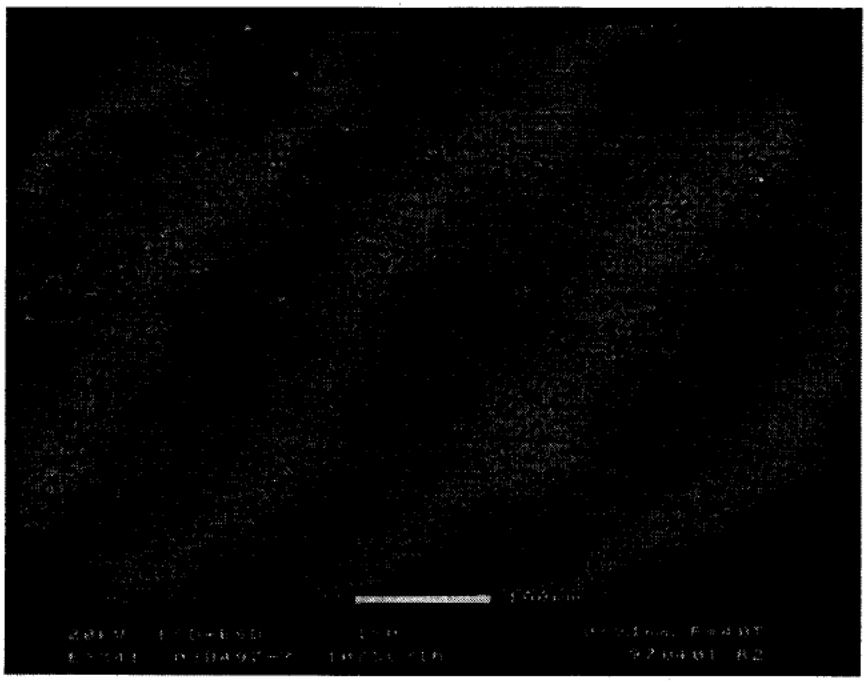

Figure 55. Calendered Bilayer #B2B-B-8; sintered 1075°C/1h.
Dense layer at top.

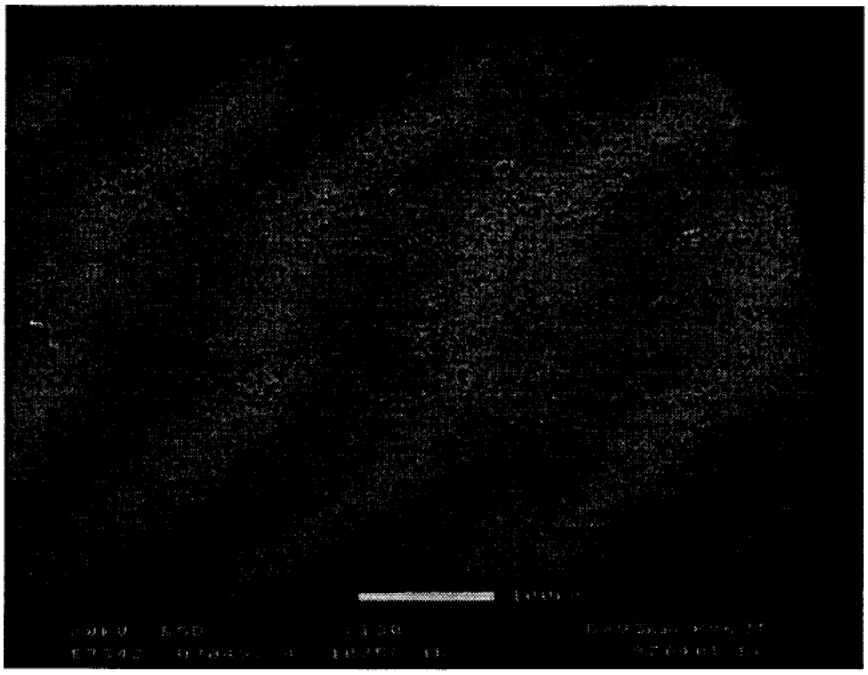

Figure 56. Calendered Bilayer #B2B-B-9; sintered 1075°C/1h.
Dense layer at top.

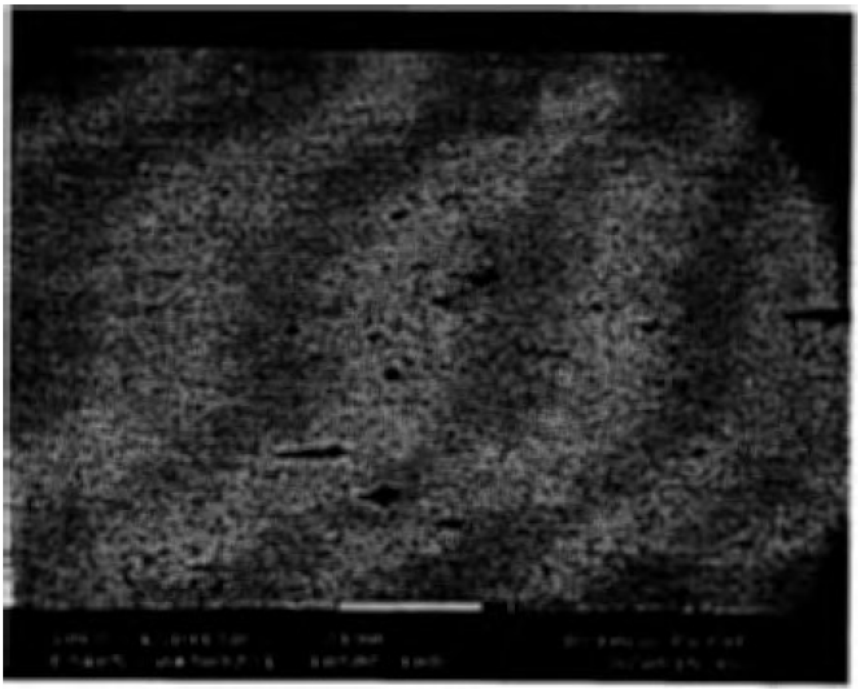

Figure 57. Calendered Bilayer #B2B-B-11; sintered 1050°C/1h.
Dense layer at top.

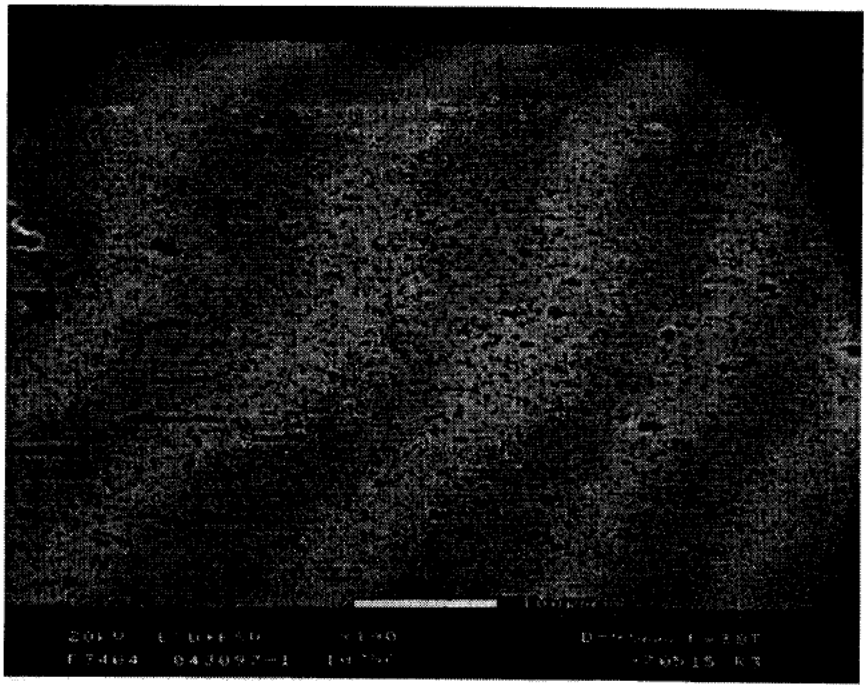

Figure 58. Calendered Bilayer #B2B-B-11; sintered 1075°C/1h.
Dense layer at top.

Figure 59. Calendered Bilayer #B2B-B-11; sintered 1100°C/1h.
Dense layer at top.

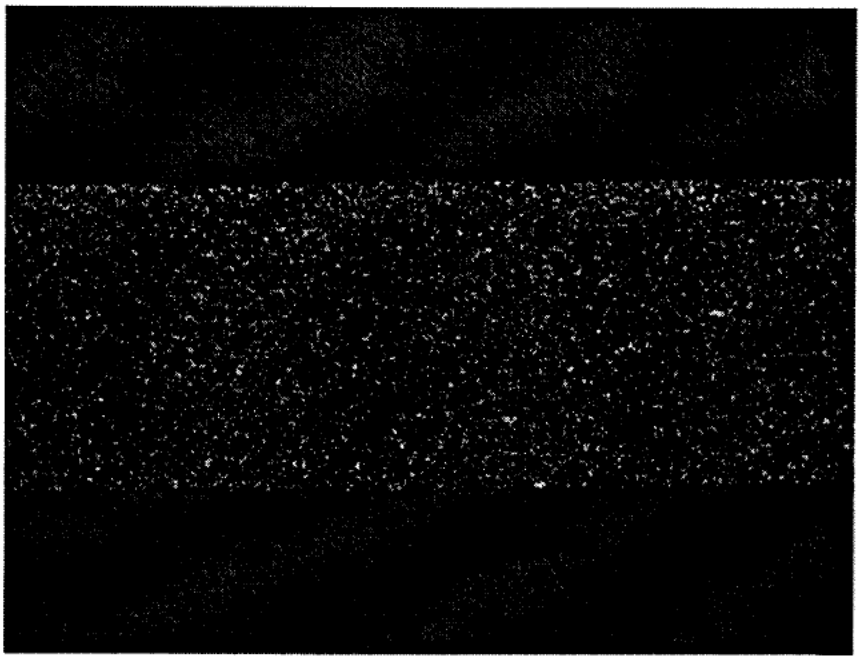

Figure 60. Calendered Bilayer #B2B-B-12; sintered 1050°C/1h.
Dense layer at top. 100X

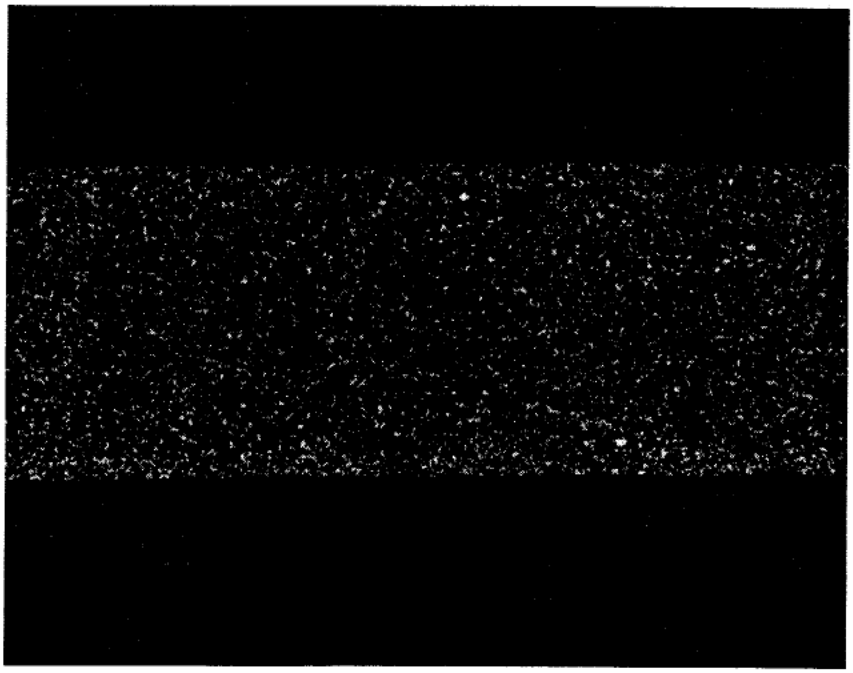

Figure 61. Calendered Bilayer #B2B-B-12; sintered 1075°C/1h.
Dense layer at bottom. 100X

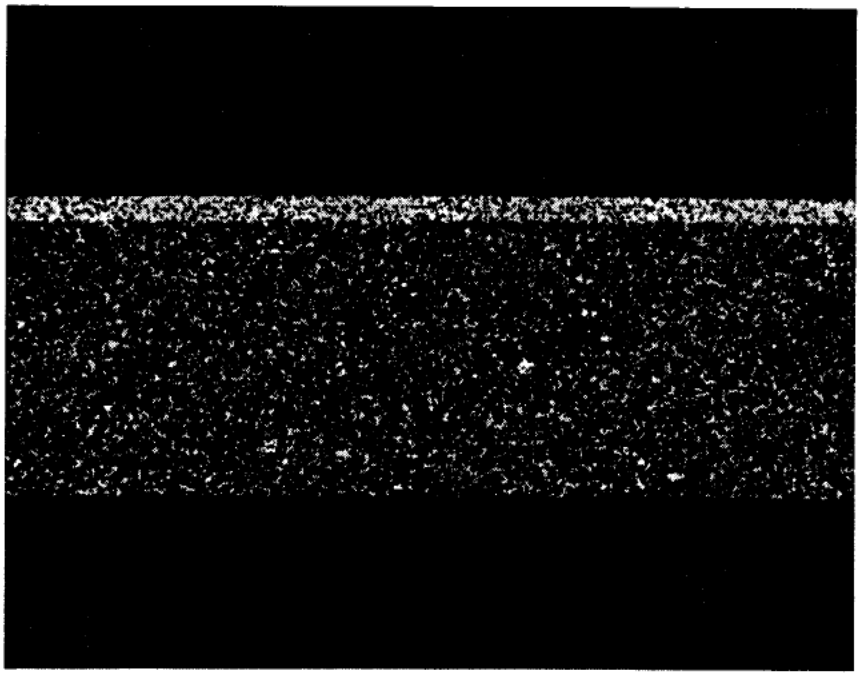

Figure 62. Calendered Bilayer #B2B-B-13; sintered 1050°C/1h.
Dense layer at top. 100X

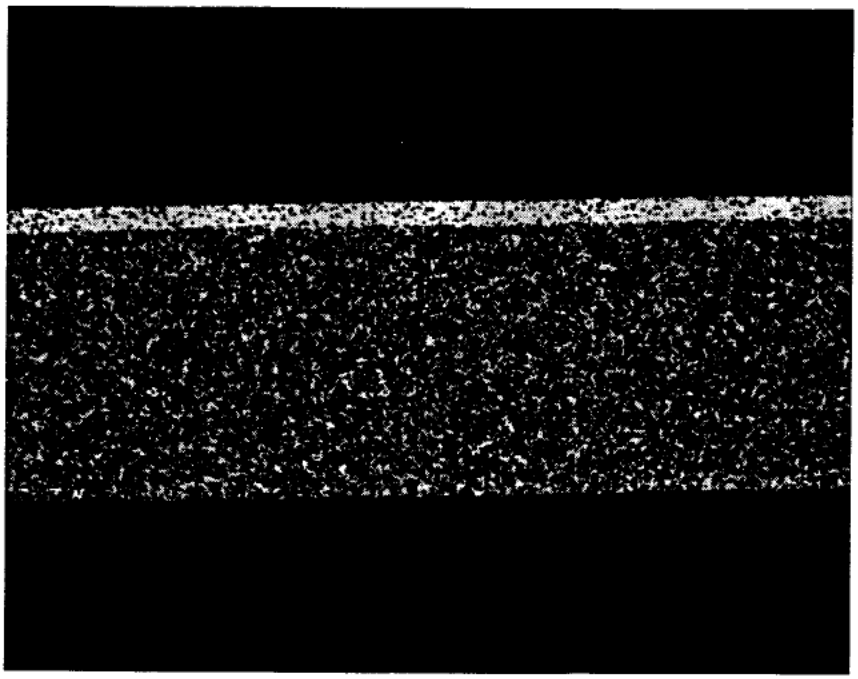

Figure 63. Calendered Bilayer #B2B-B-13; sintered 1075°C/1h.
Dense layer at top. 100X

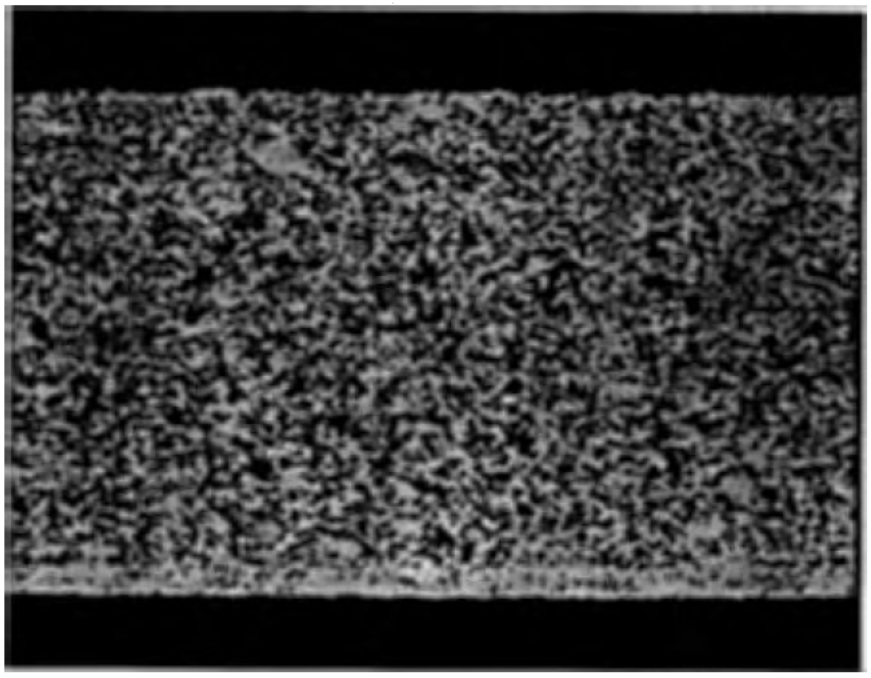

Figure 64. Calendered Bilayer #B2B-B-14; sintered 1050°C/1h.
Dense layer at bottom. 250X

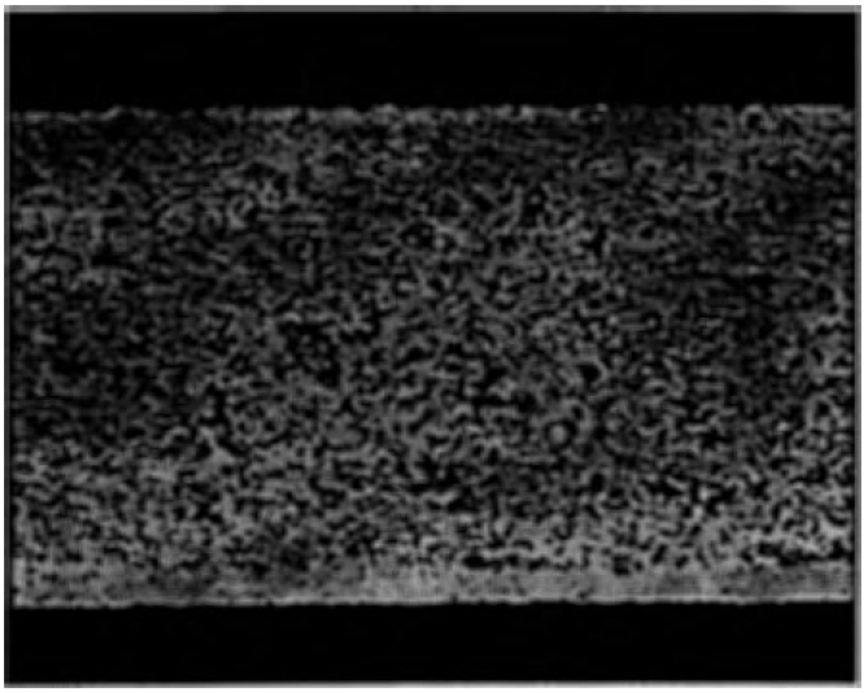

Figure 65. Calendered Bilayer #B2B-B-14; sintered 1075°C/1h.
Dense layer at bottom. 250X

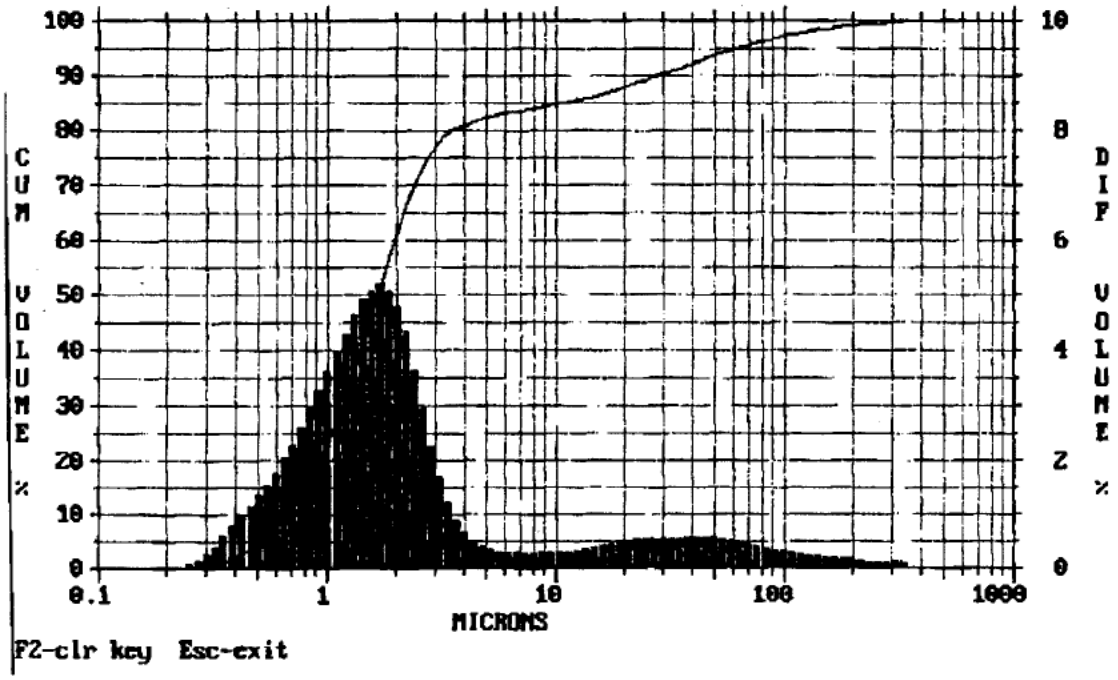

Figure 66. Particle Size Analysis of B2 powder, as-received.

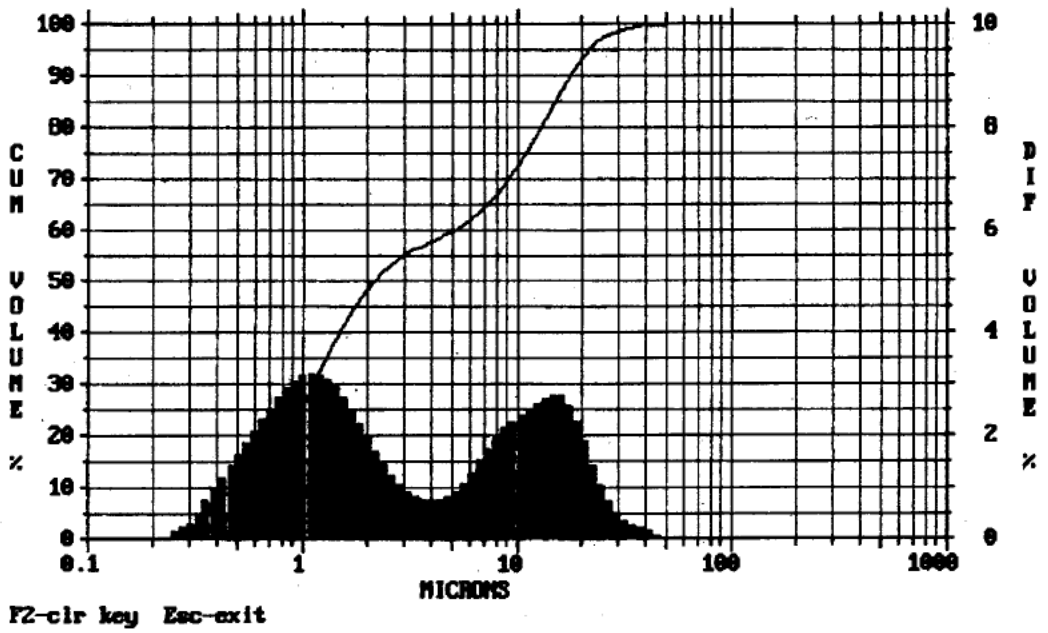

Figure 67. Particle Size Analysis of B2 powder; calcined 900°C/1h, sieved –70 mesh, wet-milled 8 h, sieved –200 mesh.

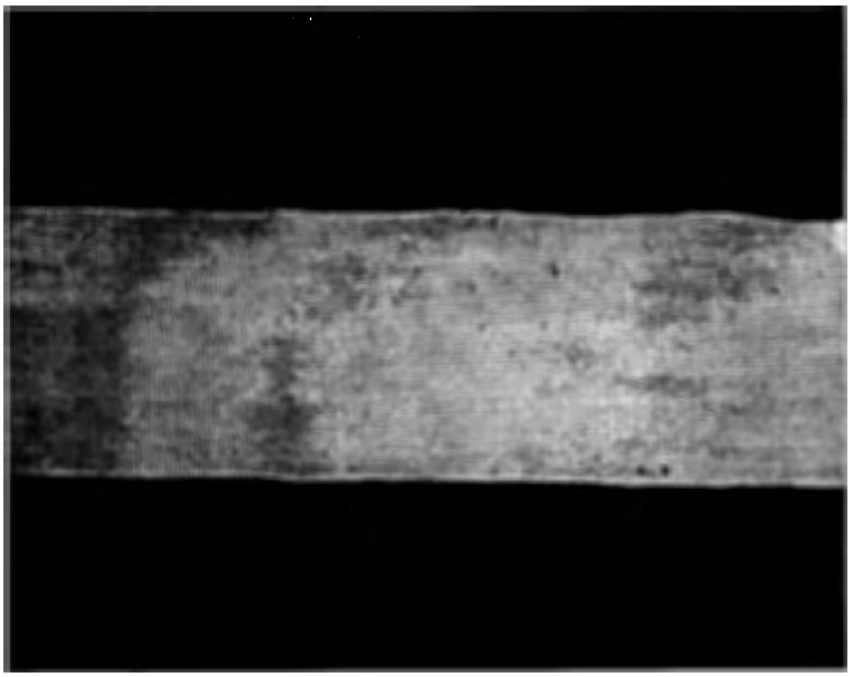

Figure 68. Calendered tape #B2-D-4; sintered 975°C/1h. 100X.

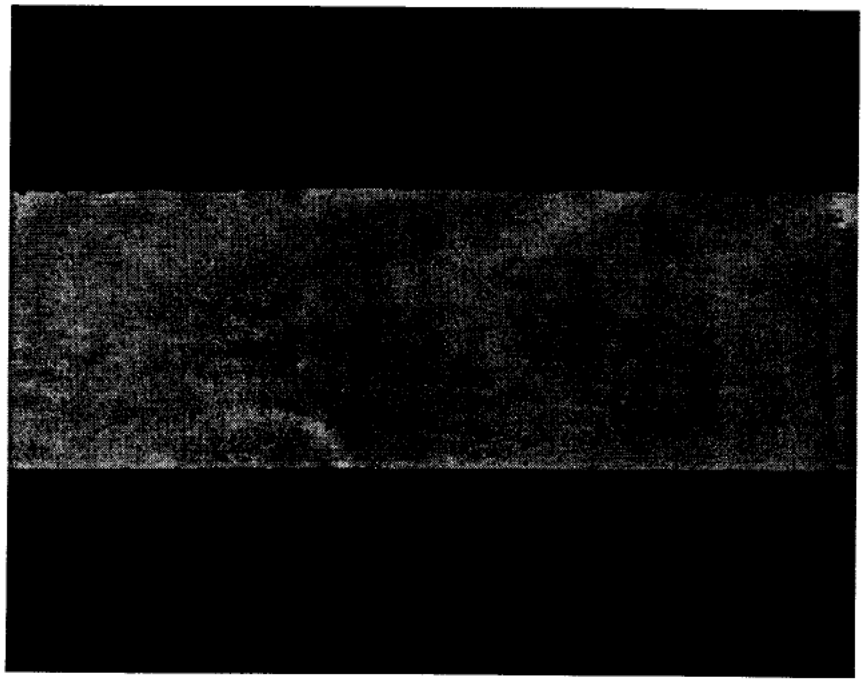

Figure 69. Calendered tape #B2-D-3; sintered 975°C/1h. 100X.

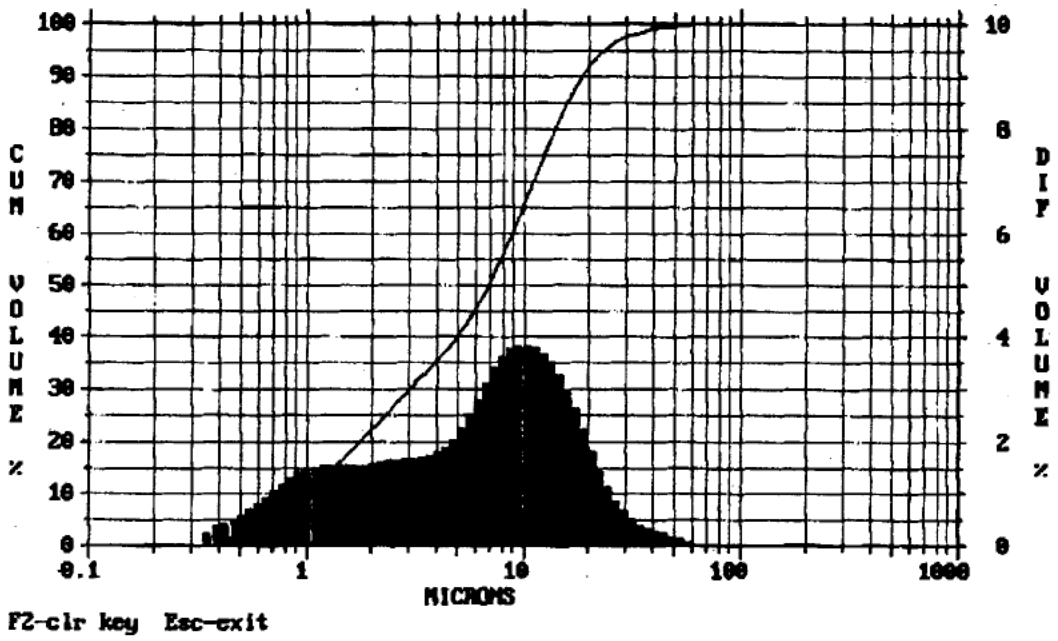

Figure 70. Particle Size Analysis of Alfa/Aesar MgO (-325 mesh as-received).

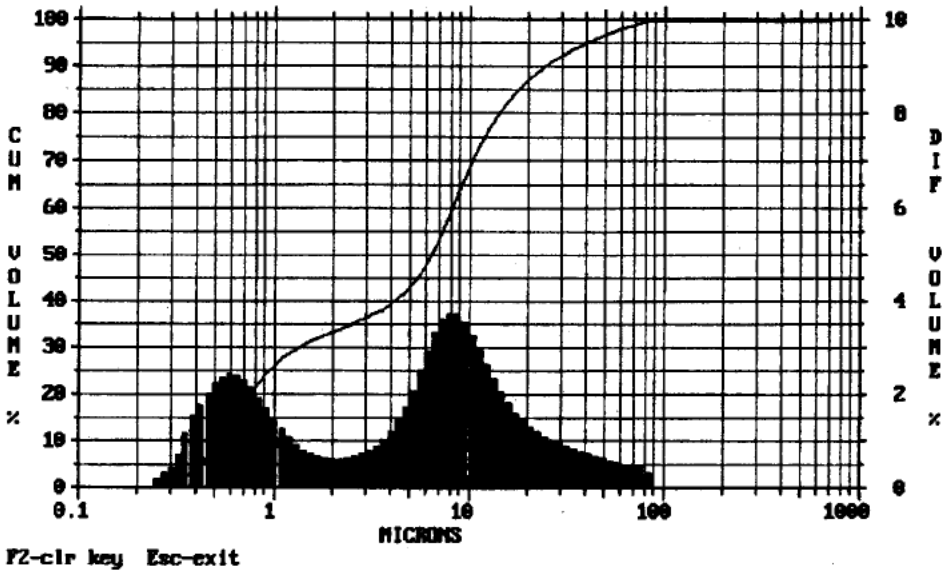

Figure 71. Particle Size Analysis of G/N MgO (Stoich., 650°C, Milled 144 h, -200 mesh).

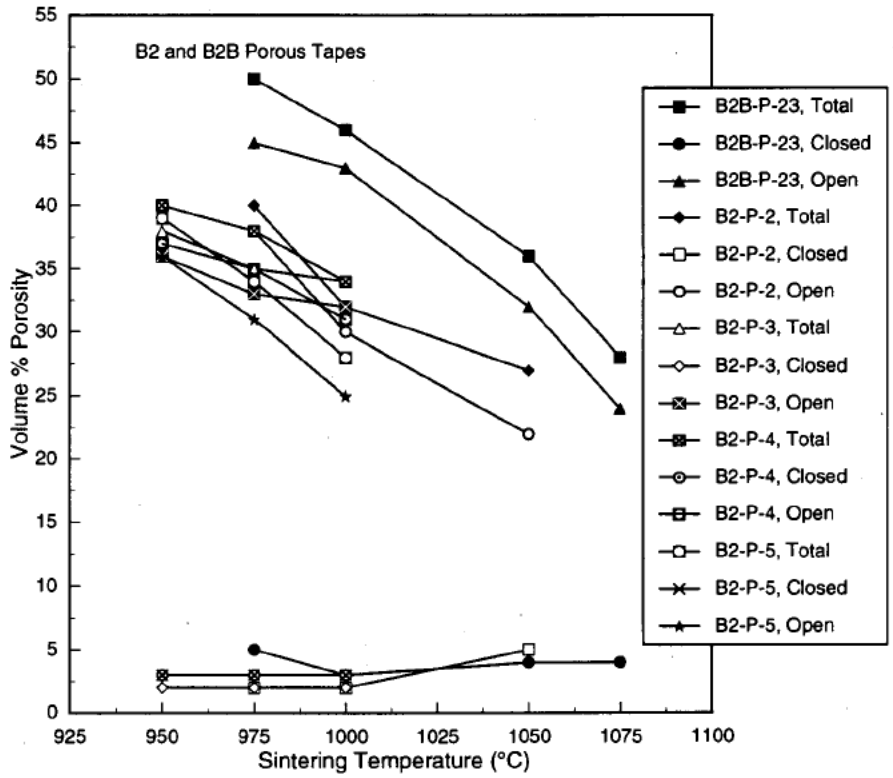

Figure 72. Calculated Porosity (Total, Closed, and Open) of Sintered Porous Tapes.

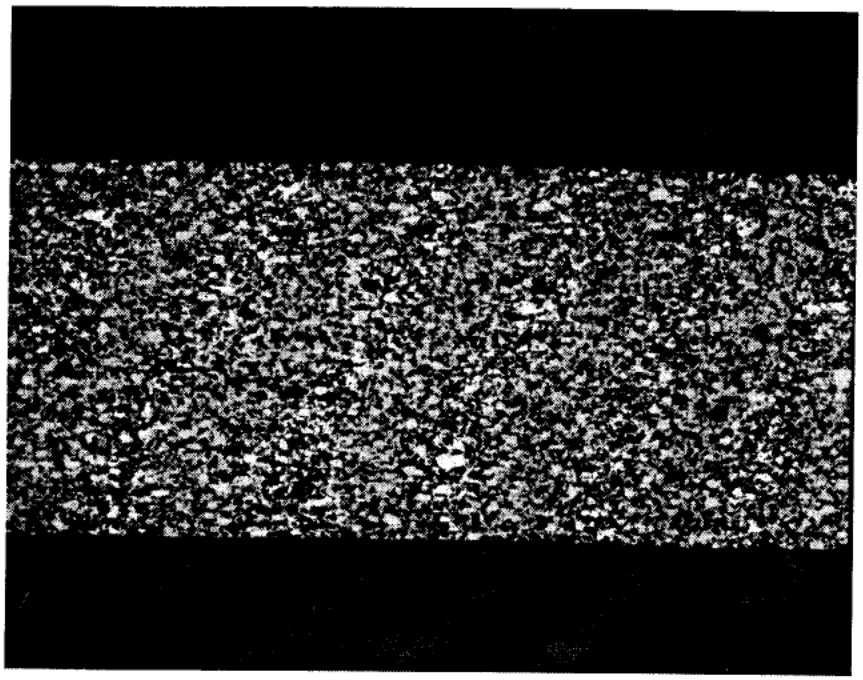

Figure 73. Calendered tape #B2-P-2; sintered 975°C/1h. 100X.

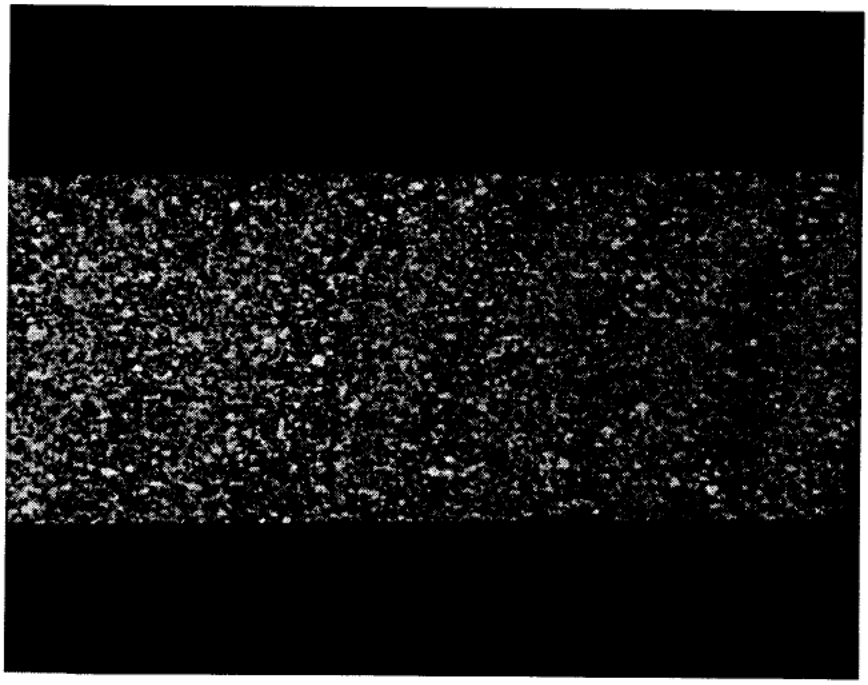

Figure 74. Calendered tape #B2-P-3; sintered 975°C/1h. 100X.

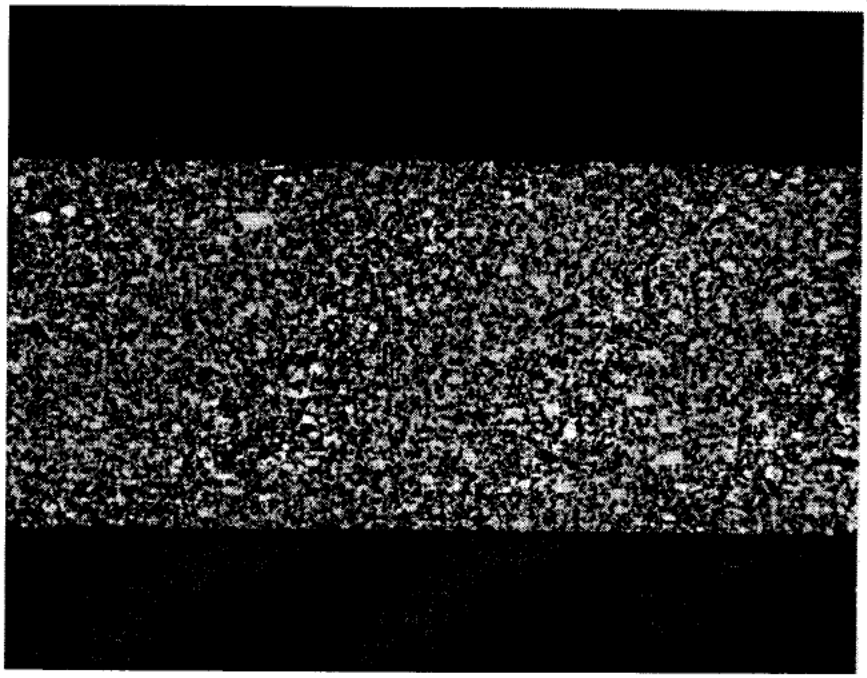

Figure 75. Calendered tape #B2-P-4; sintered 975°C/1h. 100X.

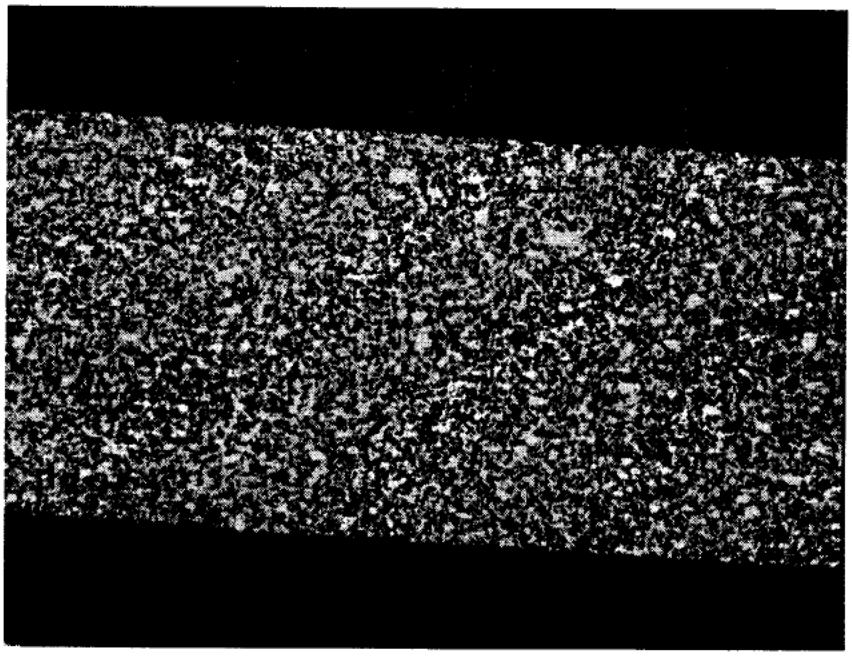

Figure 76. Calendered tape #B2-P-5; sintered 975°C/1h. 100X.

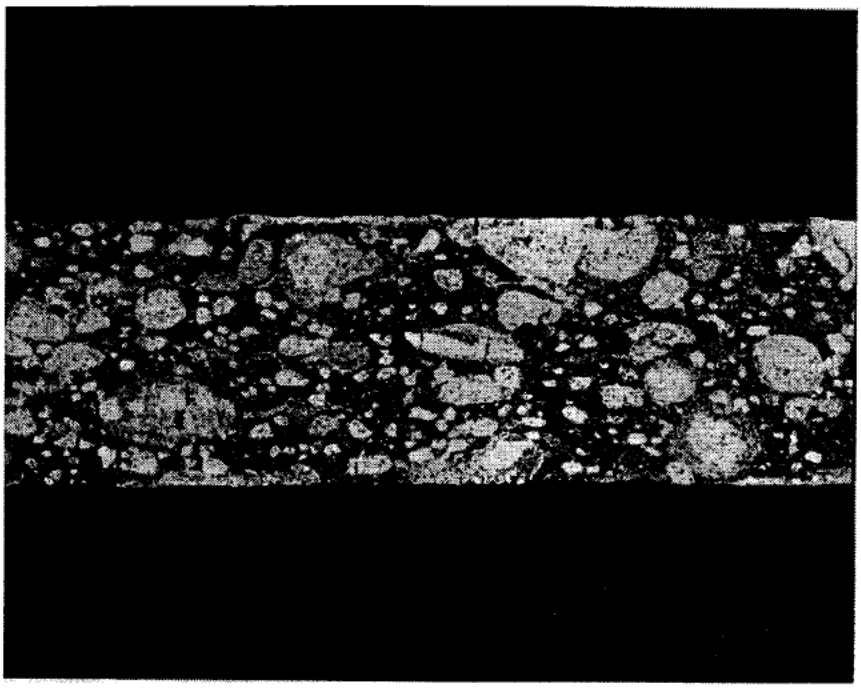

Figure 77. Calendered tape #B2-P-6; sintered 975°C/1h. 100X.

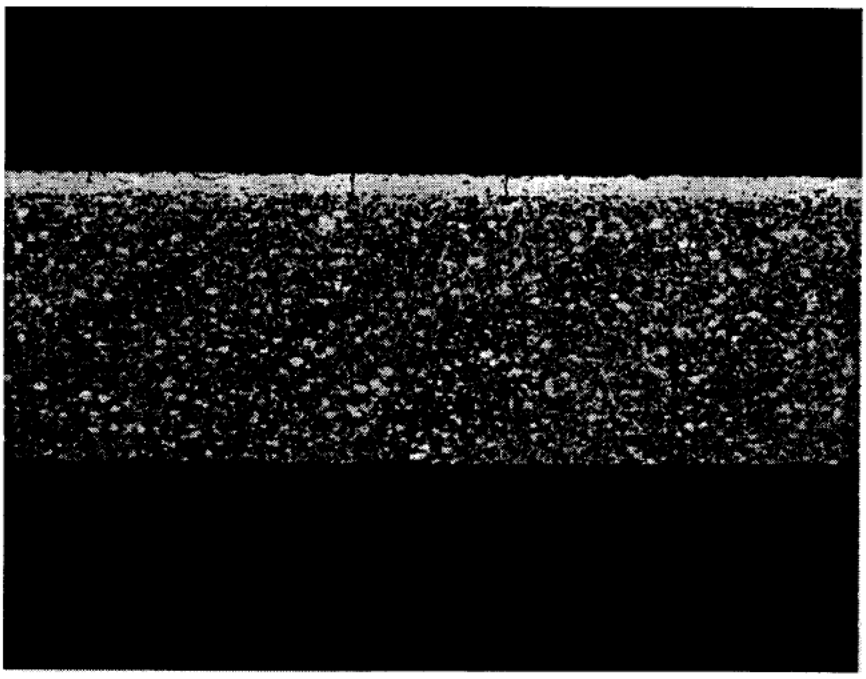

Figure 78. Calendered Bilayer #B2-B-2; sintered 975°C/1h.
Dense layer at top. 100X

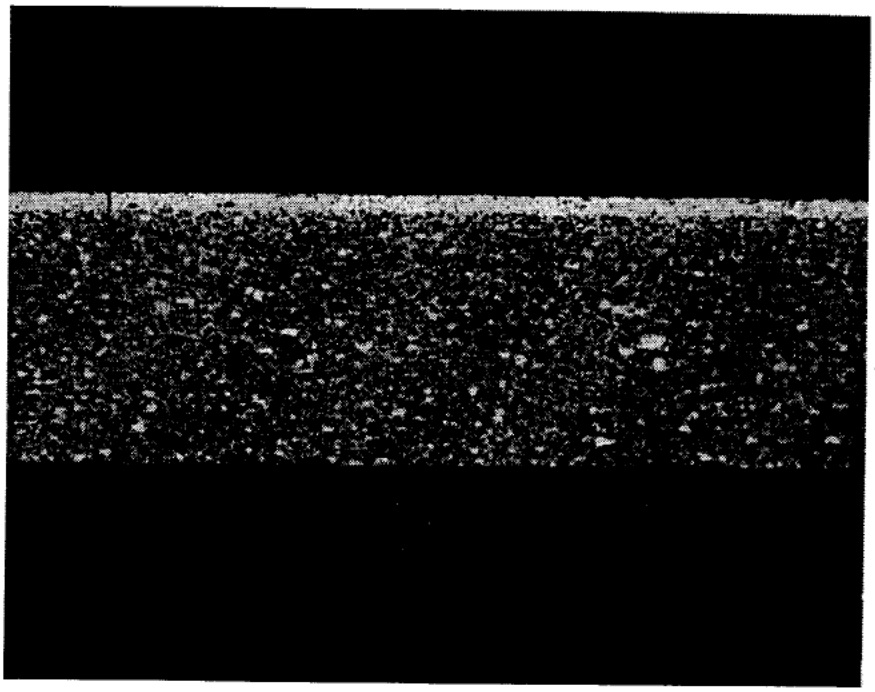

Figure 79. Calendered Bilayer #B2-B-1; sintered 975°C/1h.
Dense layer at top. 100X

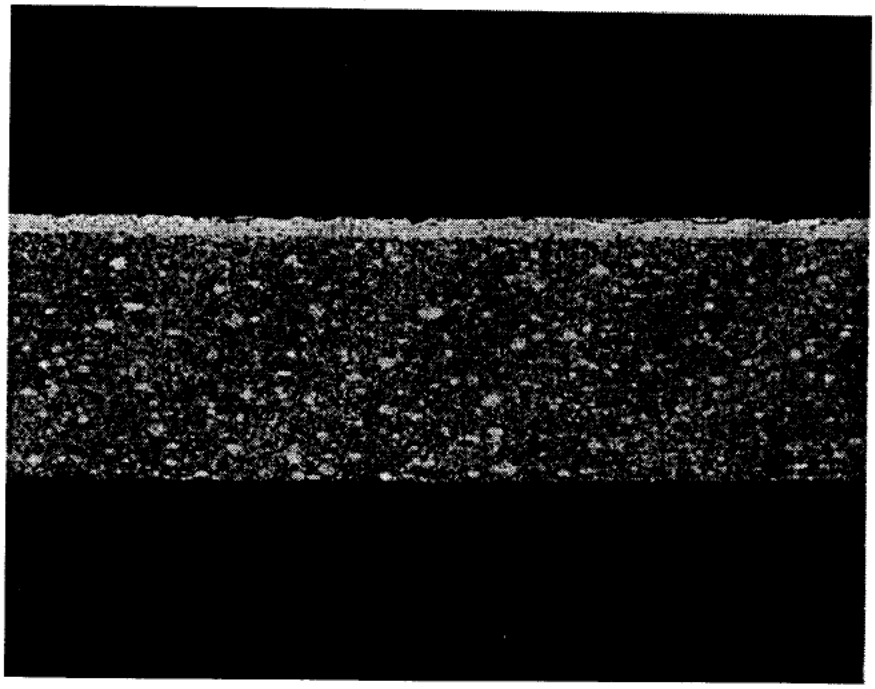

Figure 80. Calendered Bilayer #B2-B-3; sintered 975°C/1h.
Dense layer at top. 100X

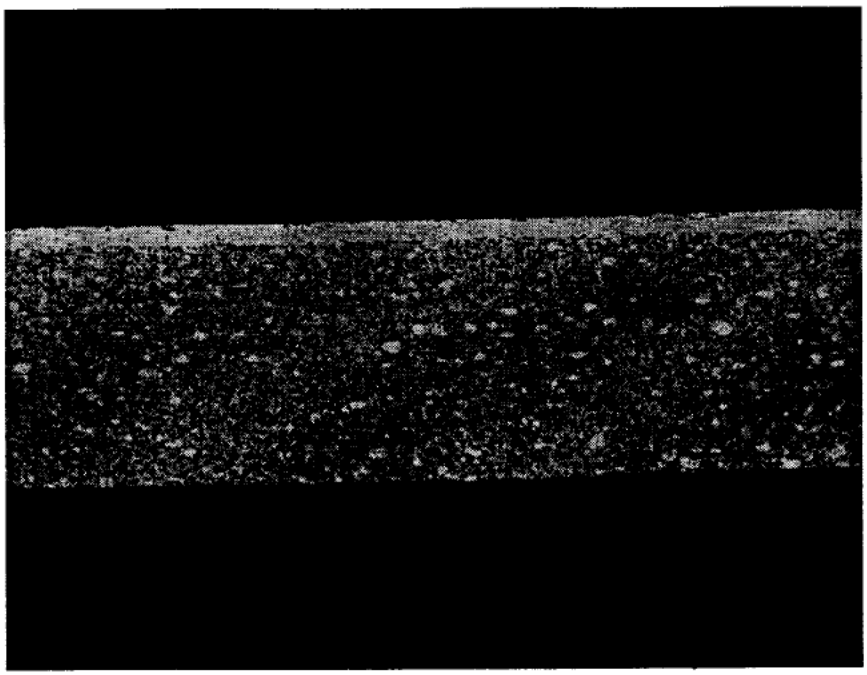

Figure 81. Calendered Bilayer #B2-B-4; sintered 975°C/1h.
Dense layer at top. 100X

Figure 82. Calendered Bilayer #B2-B-3A; sintered 975°C/1h.
Dense layer at top. 250X

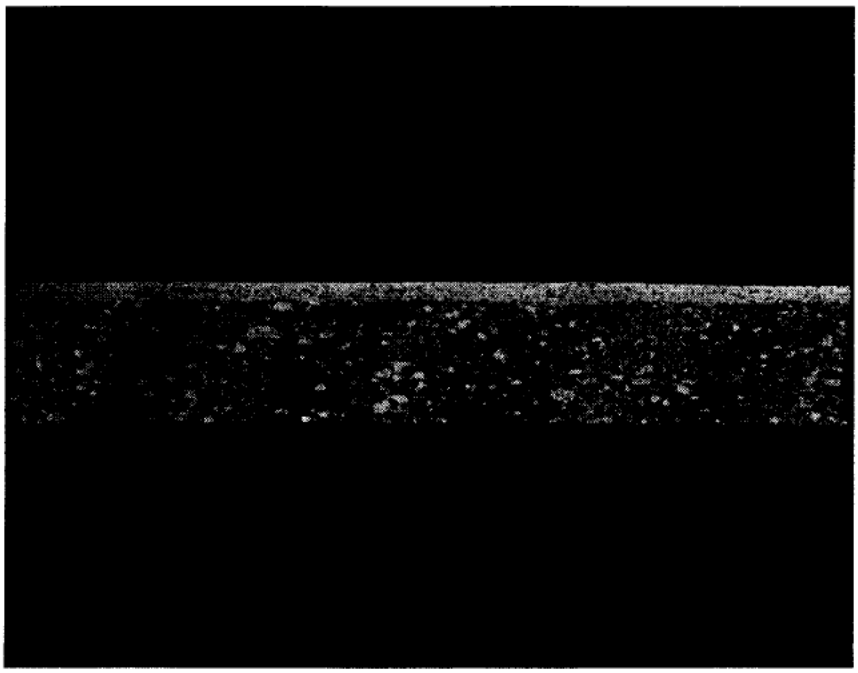

Figure 83. Delivered Bilayer; sintered 975°C/1h.
Dense layer at top. 100X

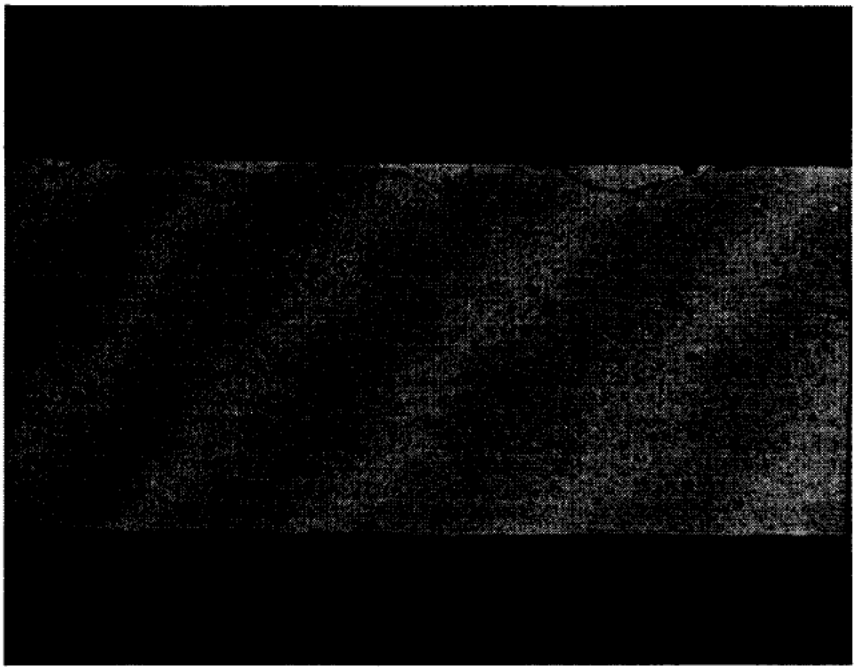

Figure 84. Delivered Thin Dense Tape; sintered 975°C/1h. 250X

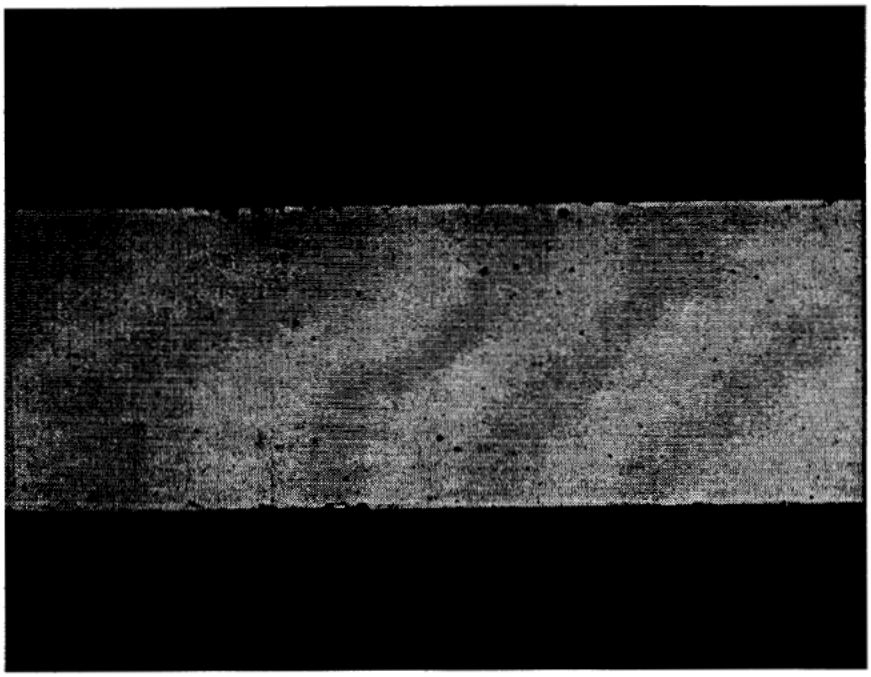

Figure 85. Delivered Thick Dense Tape; sintered 975°C/1h. 100X

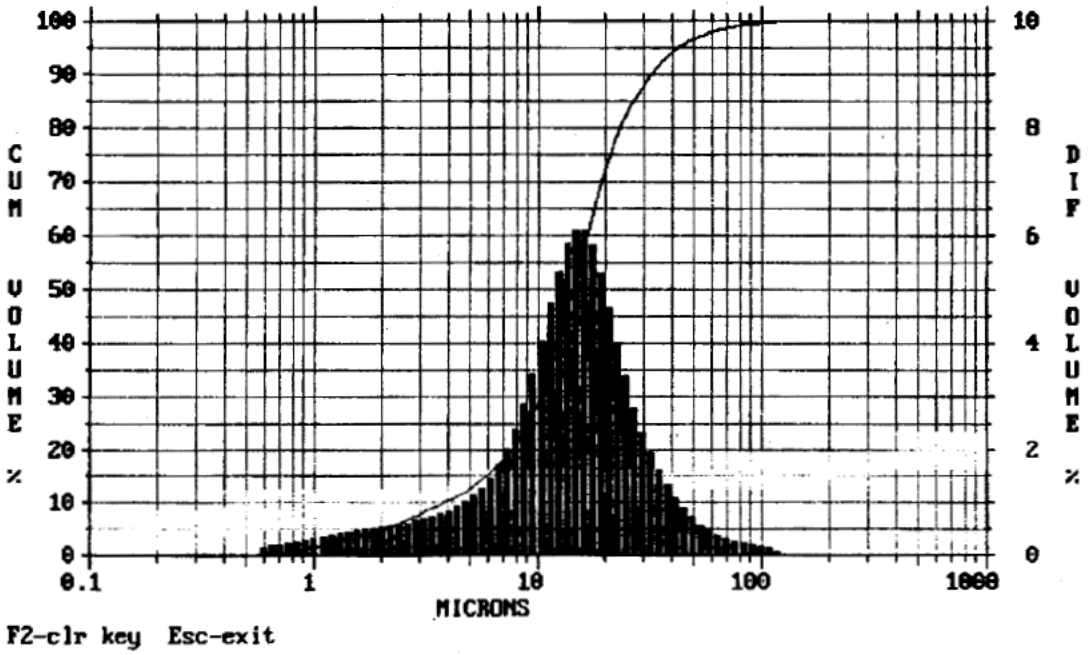

Figure 86. Particle Size Analysis of as-received B2(2) powder.

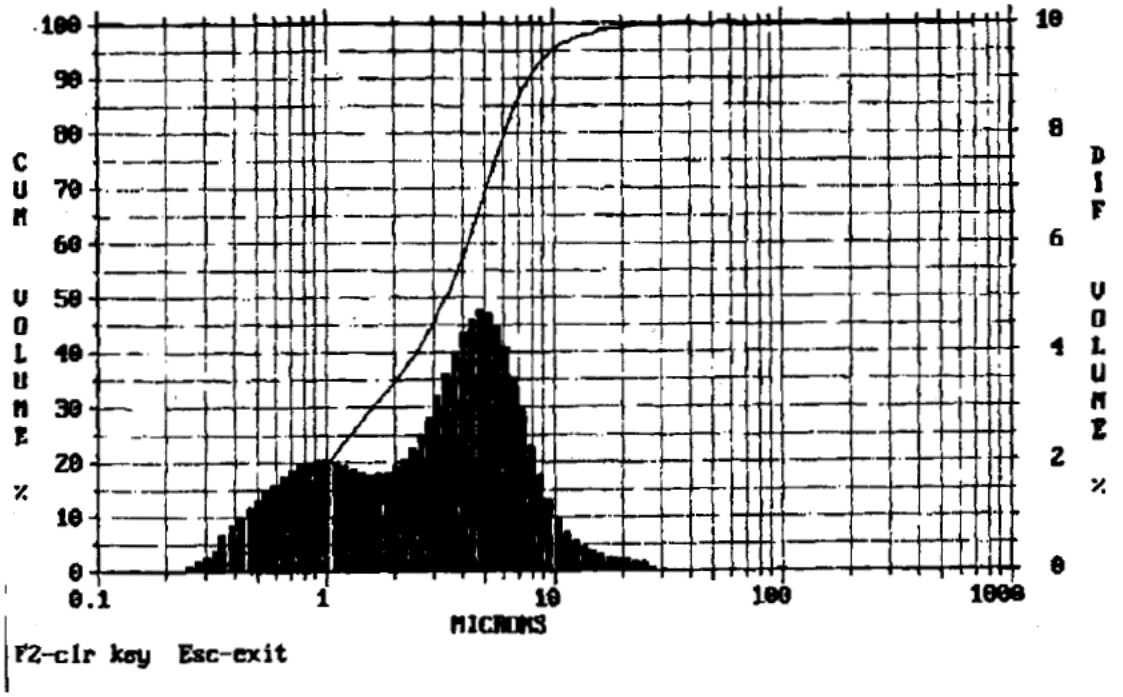

Figure 87. Particle Size Analysis of B2(2) powder; wet-milled 48 hours, sieved –200 mesh.

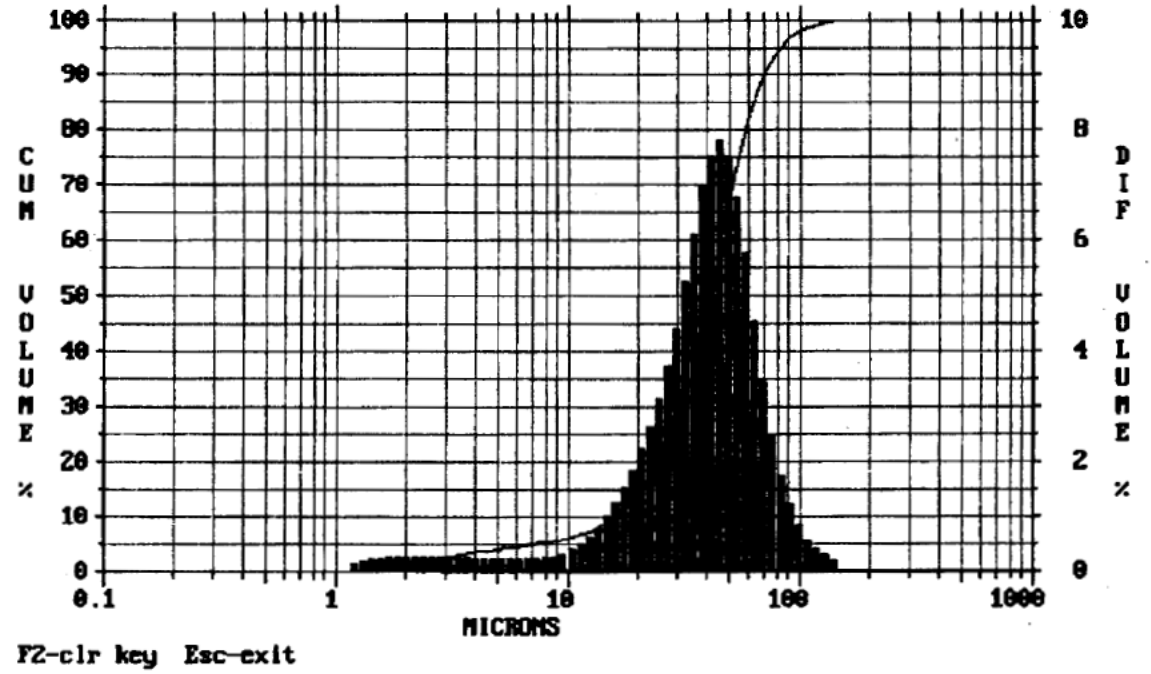

Figure 88. Particle Size Analysis of Sigma potato starch.

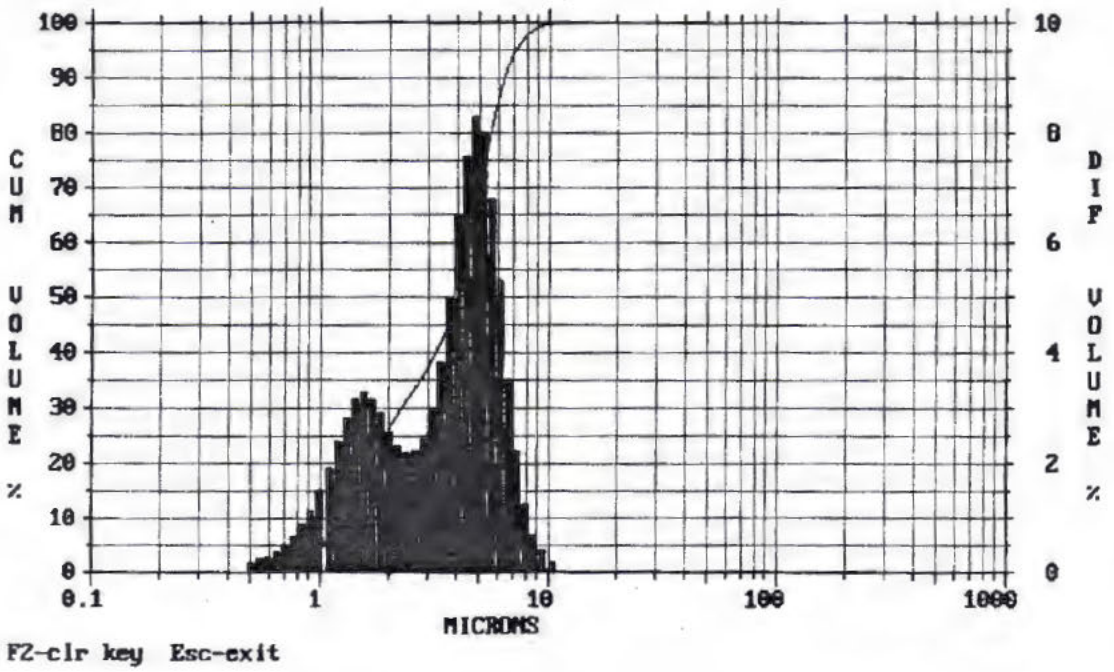

Figure 89. Particle Size Analysis of VWR rice starch.

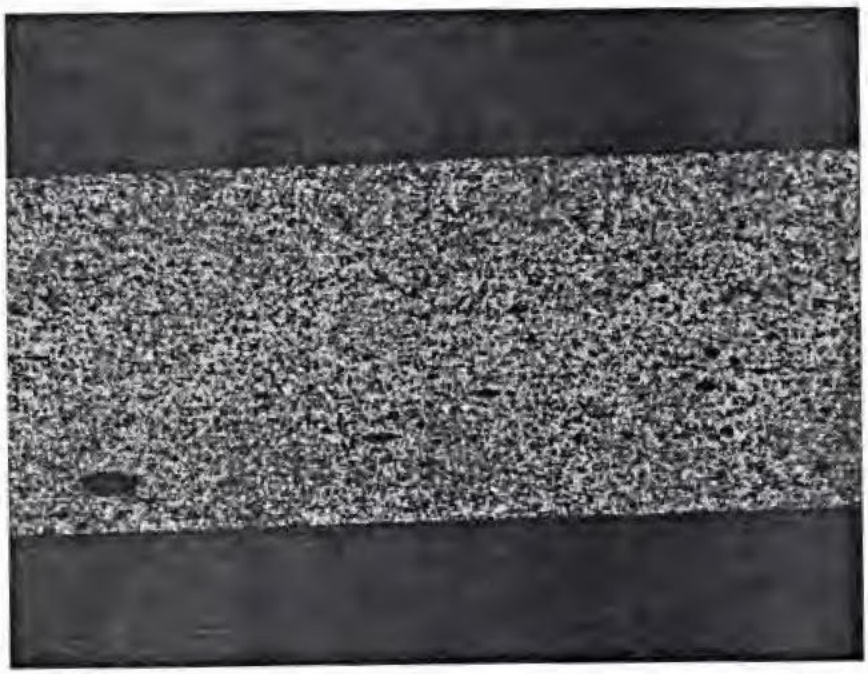

Figure 90. Calendered tape #B2(2)-P-3; sintered 975°C / 1 hour. 100X.

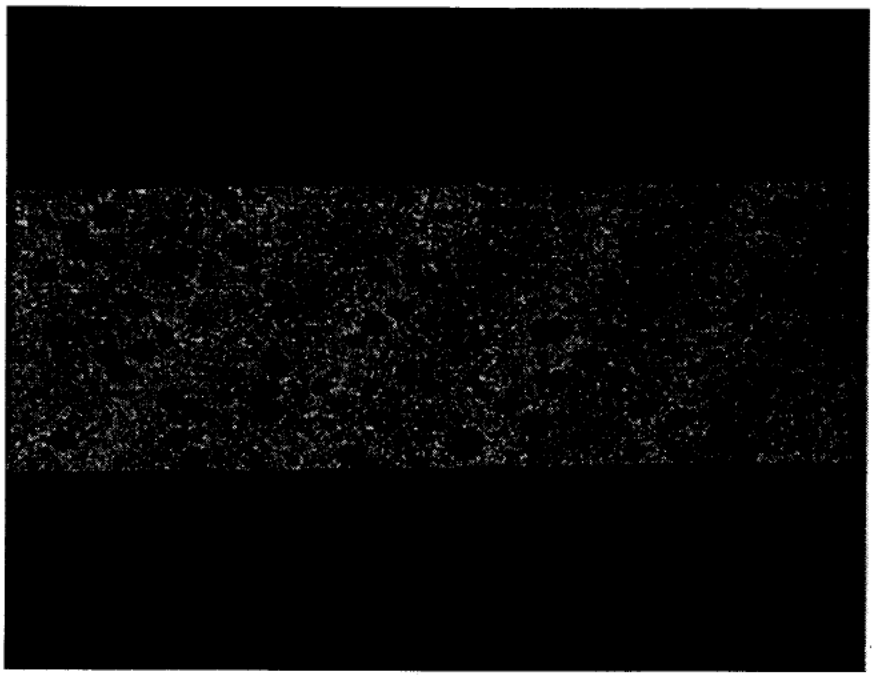

Figure 91. Calendered tape #B2(2)-P-4; sintered 975°C / 1 hour. 100X.

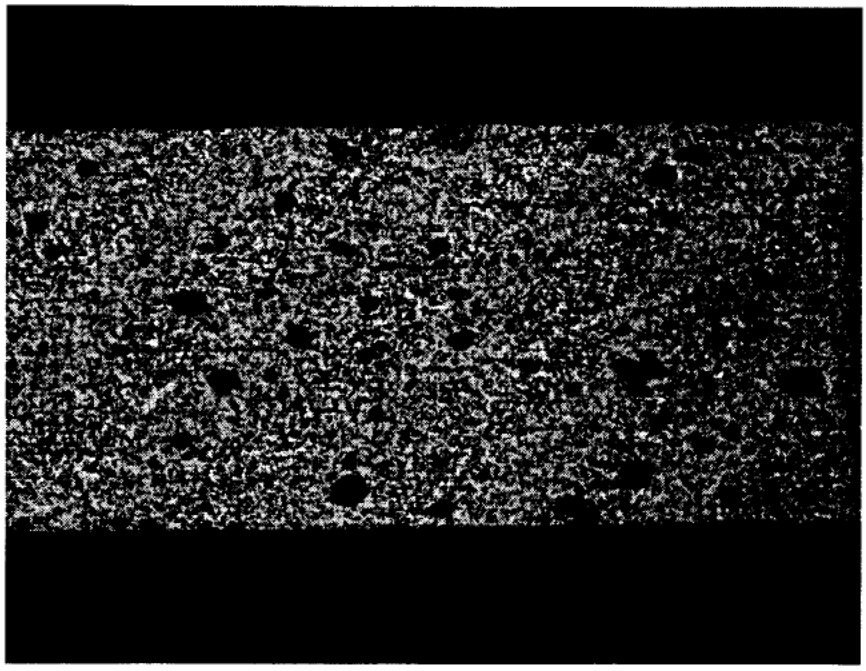

Figure 92. Calendered tape #B2(2)-P-5; sintered 975°C / 1 hour. 100X.

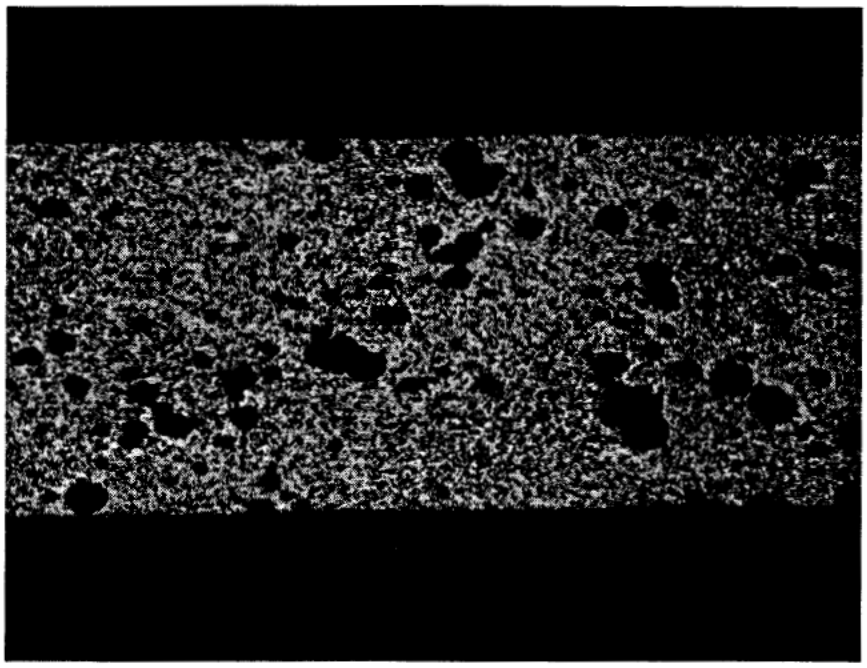

Figure 93. Calendered tape #B2(2)-P-6; sintered 975°C / 1 hour. 100X.

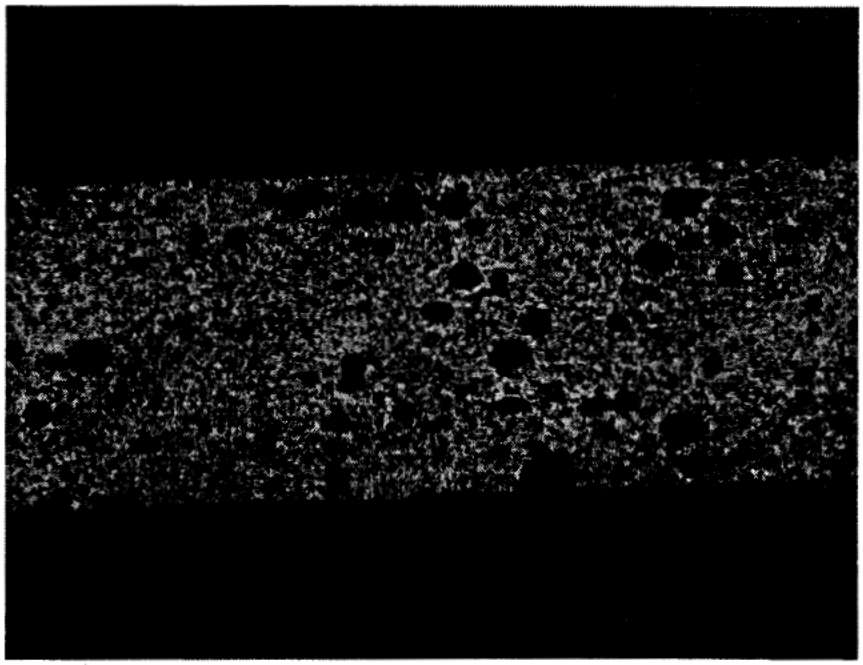

Figure 94. Calendered tape #B2(2)-P-7; sintered 975°C / 1 hour. 100X.

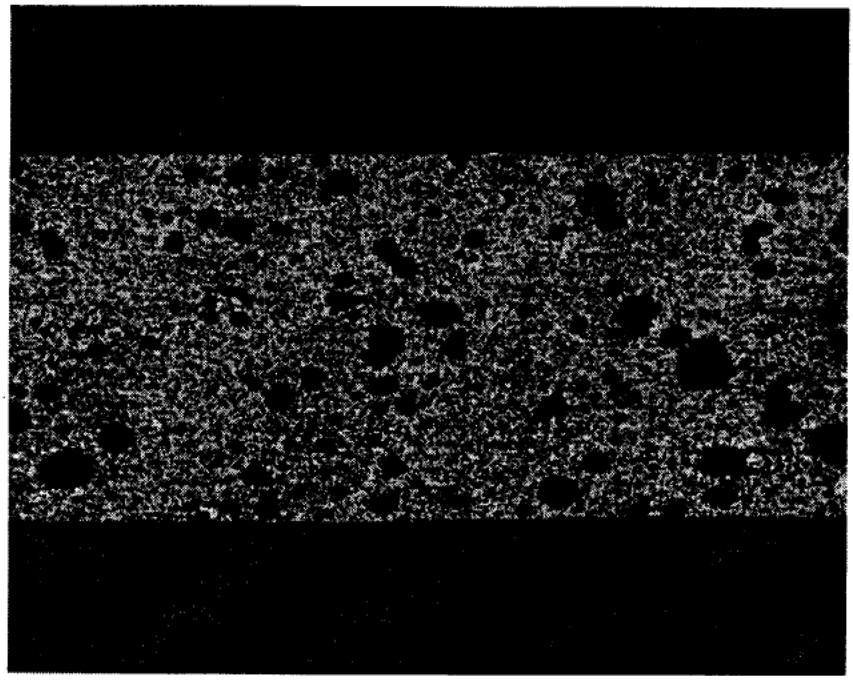

Figure 95. Calendered tape #B2(2)-P-8; sintered 975°C / 1 hour. 100X.

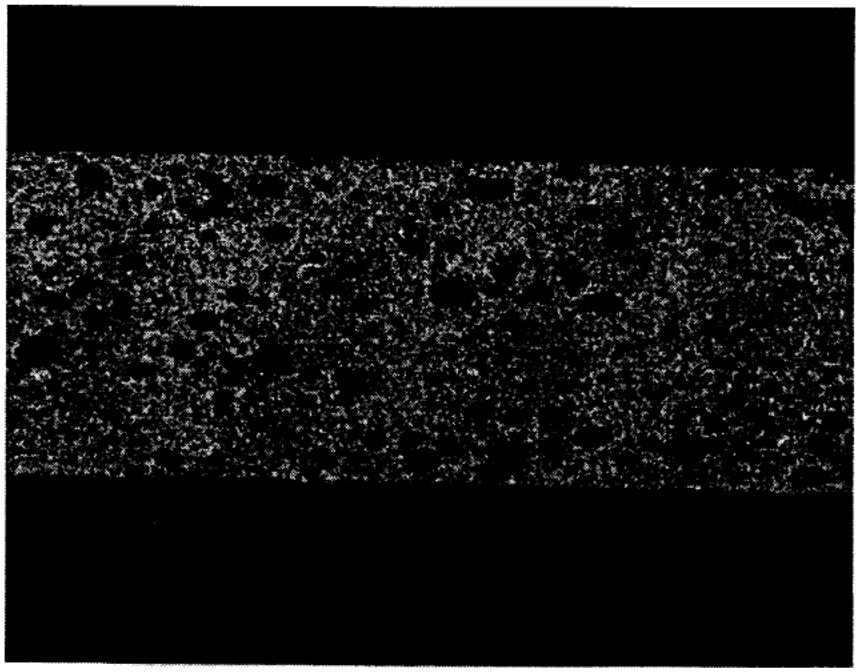

Figure 96. Calendered tape #B2(2)-P-9; sintered 975°C / 1 hour. 100X.

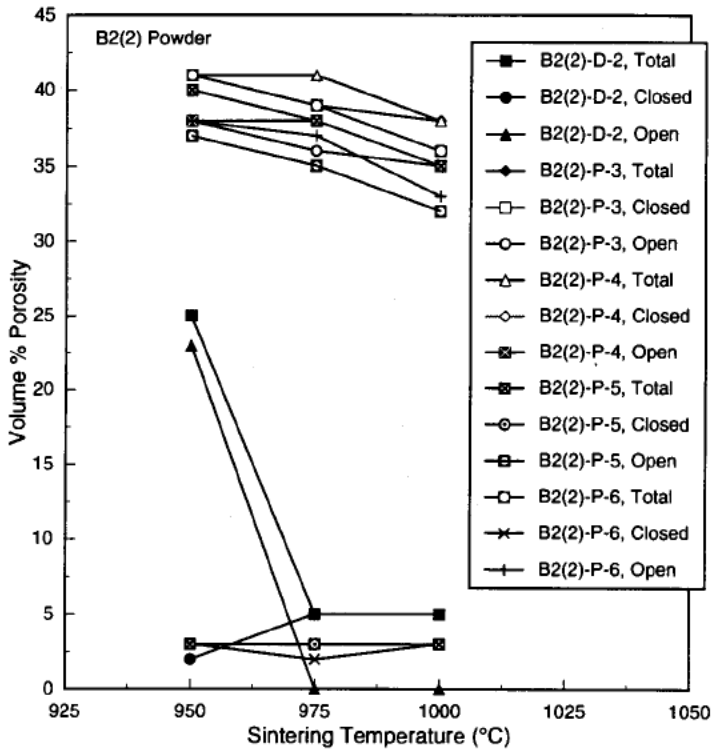

Figure 97. Calculated porosity (total, closed, and open) of tapes containing B2(2) powder.

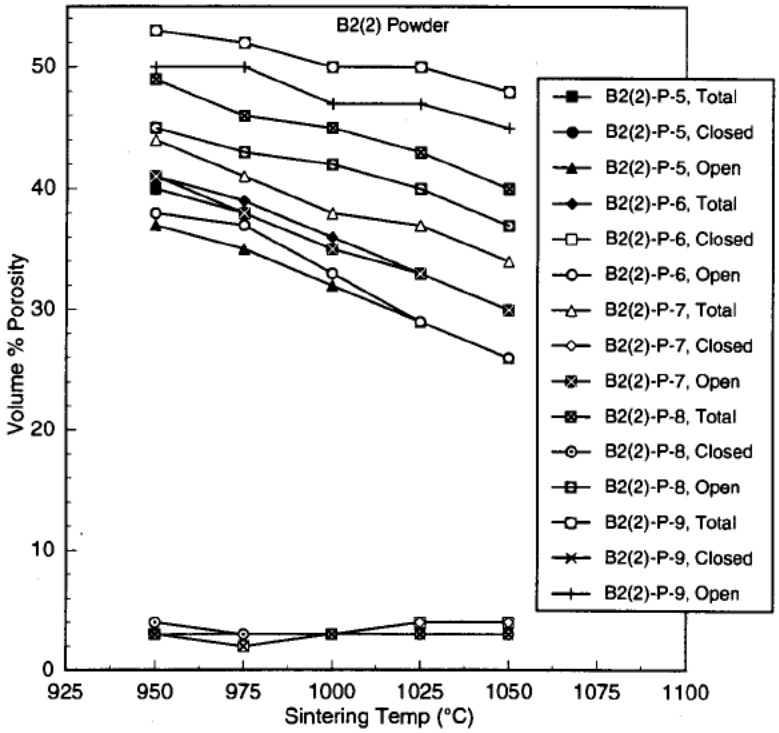

Figure 98. Calculated porosity (total, closed, and open) of tapes containing B2(2) powder.

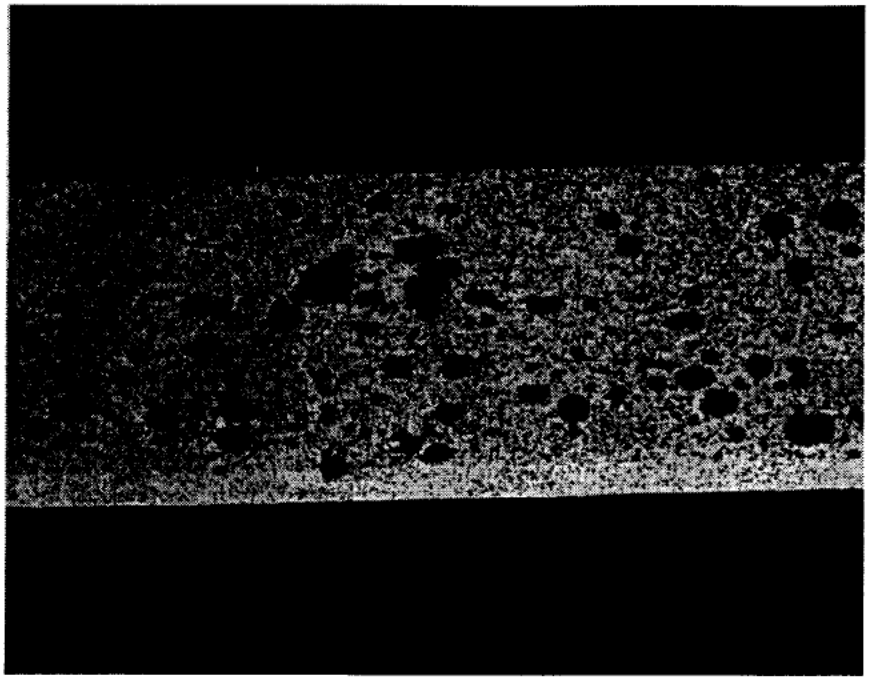

Figure 99. Calendered Bilayer #B2(2)-B-1; sintered 975°C/1h.
Dense layer at bottom. 100X.

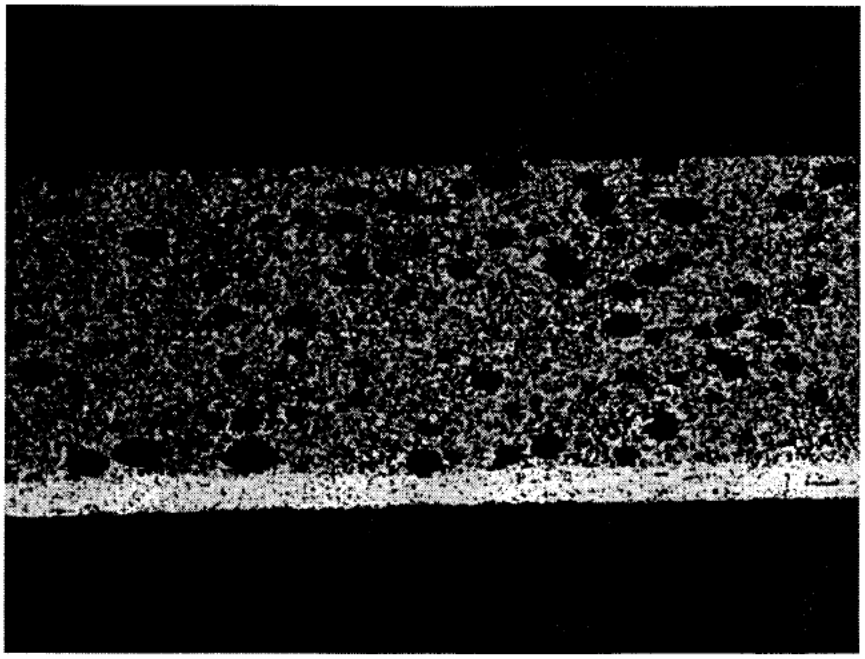

Figure 100. Calendered Bilayer #B2(2)-B-2; sintered 975°C/1h.
Dense layer at bottom. 100X.

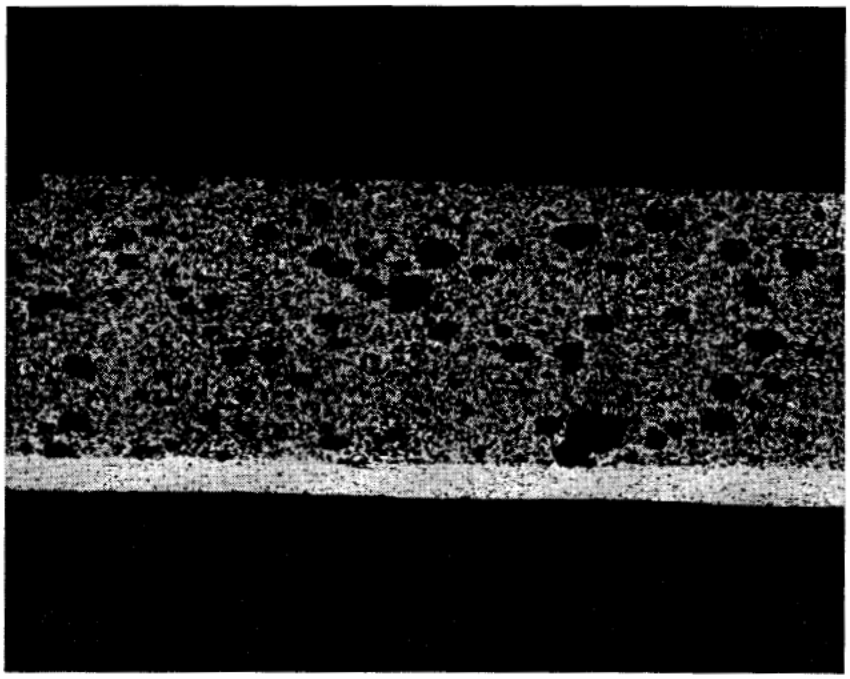

Figure 101. Calendered Bilayer #B2(2)-B-3; sintered 975°C/1h. Dense layer at bottom. 100X.

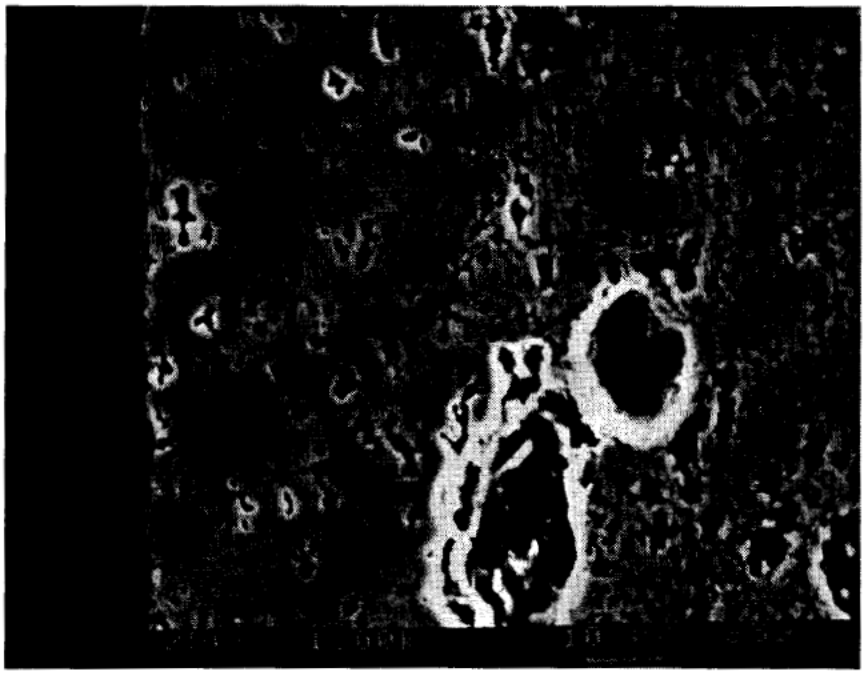

Figure 102. Calendered Bilayer #B2(2)-B-2; sintered 975°C/1h. Dense layer at left.

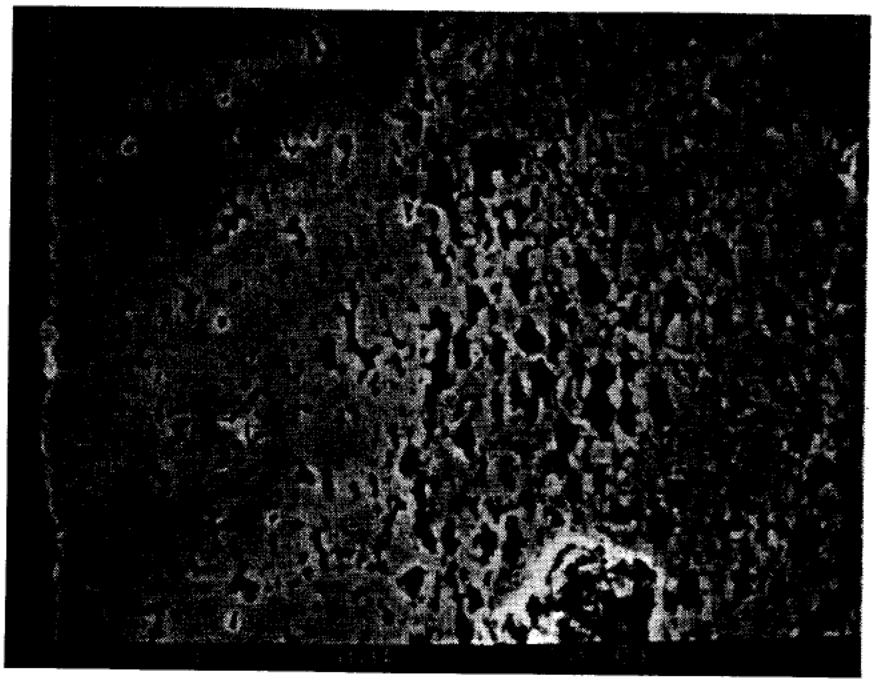

Figure 103. Calendered Bilayer #B2(2)-B-3; sintered 975°C/1h.
Dense layer at left.

Distribution

No. of Copies

Offsite

Ted Vojnovich
Technical Program Manager
Office of Computational and Technology Research
Laboratory Technology Research Division
U.S. Department of Energy
Room G434 (SC-32)
19901 Germantown Road
Germantown, Maryland 20874

No. of Copies

Onsite

DOE/Richland Operations Office

NL Hieb

10 Pacific Northwest National Laboratory

BJ Harrer (2)
Information Release Office (7)
JW Stevenson (1)